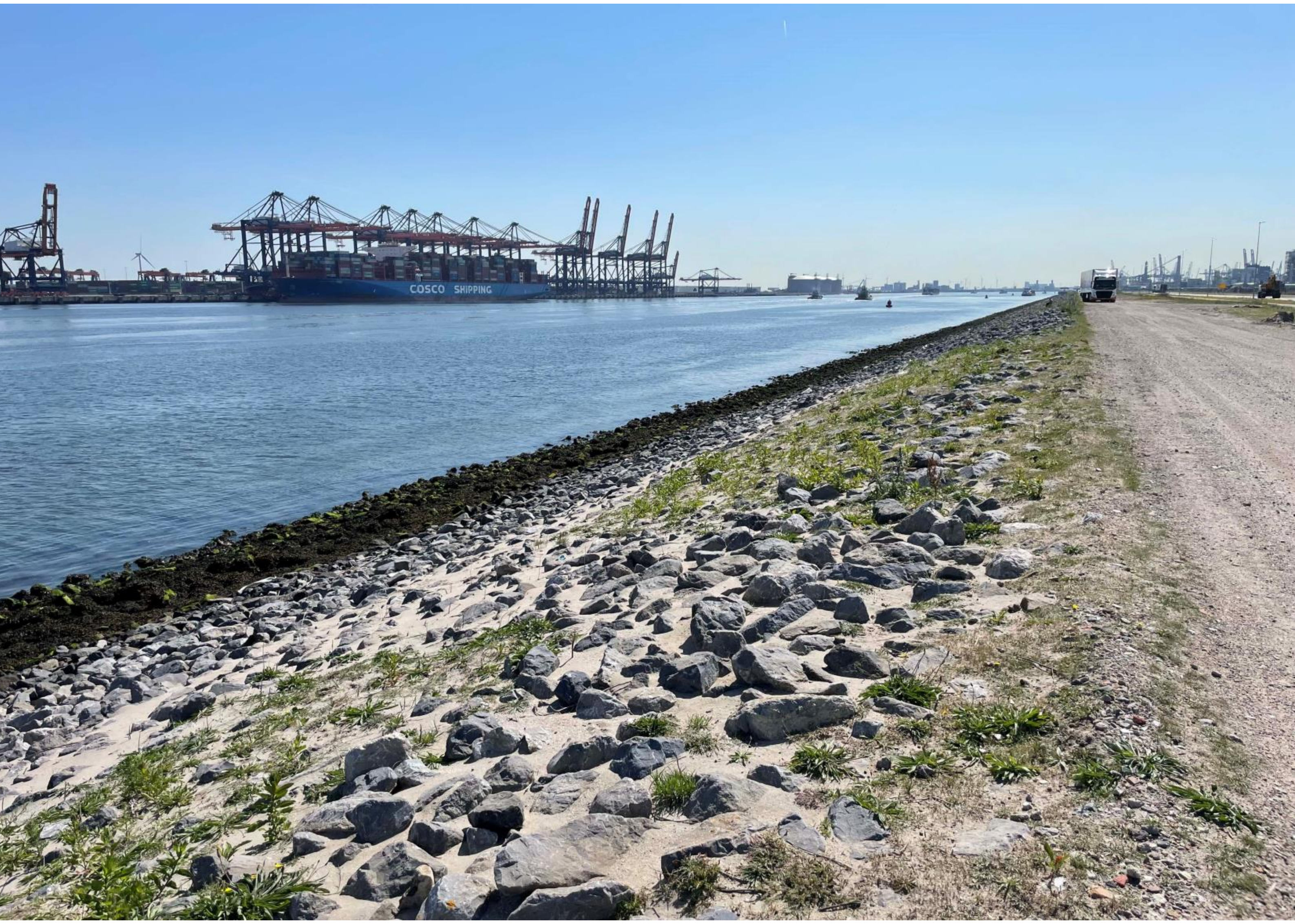

Load Test In Quay Walls

Civil Engineering Bachelor Thesis

Widening Yangtze Canal
(Port of Rotterdam)
Phase B

Andrea Velasco García de la Calera

July 2024

Date: 5th of July 2024

Conducted by:
Andrea Velasco García de la Calera
S2697254
a.velascogarciadelacalera@student.utwente.nl

Supervised by:

University of Twente
Sherrin Joseph
s.joseph@utwente.nl

Witteveen+Bos
Sten Jacobs
sten.jacobs@witteveenbos.com

I. Preface

This document is submitted as my final bachelor thesis for the degree of Civil Engineering at the University of Twente. The research presented was conducted during a 10-week internship, at Witteveen+Bos in Deventer, from the 29th of April 2024, to the 5th of July 2024.
The idea to carry out my thesis within the field of geotechnical engineering, began at the beginning of my 3rd year of study, through several courses and projects offered at the University of Twente. The specific research idea for this thesis, about the prediction of a load test on a quay wall, was proposed by Witteveen+Bos, which aimed to provide insights and predictions regarding the load test of a quay wall at the Port of Rotterdam.
Furthermore, the entire process of research and study at Witteveen+Bos has been remarkably fun and rewarding, filled with a lot of learning and which has boosted my growth both as a student and as a young professional. Over these past 10 weeks, I have dived into a variety of exciting research activities, starting from analyzing soil data and running FEM simulations in PLAXIS, to calculating the strength parameters of the quay wall and even exploring some hydraulics!
This project has reaffirmed my definition of what a civil engineering project looks like, as integrating soil, water and structures into one, and also taking into account nature uncertainties so that they can play in the project's favor, is my opinion the essence of civil engineering. This experience has been my first real life experience, and it has provided me with new and fresh insights all while exceeding my expectations. All of the results and analysis presented in this thesis are the outcome of effort and amazing guidance I received during my internship at Witteveen+Bos.
That is why, I would like to express my deepest gratitude to my external supervisor, Sten Jacobs, whose firm support, inspiring and critical feedback, and continuous encouragement have been crucial in the completion of this thesis.
Additionally, I am very grateful to my internal supervisor, Sherrin Joseph for her essential guidance throughout the proposal and the thesis revisions.

Lastly, this thesis has navigated the complexities of soil mechanics and engineering, which has required the integration of intuitive understanding and scientific theories. To put it in the words of the father of soil mechanics, Karl von Terzaghi (1883 – 1963):

"Soil Mechanics arrived at the borderline between science and art. I use the term 'art' to indicate mental processes leading to satisfactory results without the assistance of step-for-step logical reasoning… To acquire competence in the field of earthwork engineering one must live with the soil. One must love it and observe its performance not only in the laboratory but also in the field, to become familiar with those of its manifold properties that are not disclosed by boring records."

II. Table of Contents

III. Table of Figures

IV. Table of Tables

V. Abstract

Quay walls are critical infrastructures that play an essential role in the functionality, safety and prosperity of ports, canals rivers, inland waterways etc. They are essential structures in retaining the soil but also to serve the berthing and mooring of boats and vessels, and with that the handling of the cargo contained in them. These walls are the essence of a port's functionality as they serve as the main connection between a thriving commerce and economy of the port and the unknown of the ocean. That is why they must be able to withstand during long periods of time, to withstand adversity and remaining future proof.

This research will ensure that the quay wall of the Yangtzecanal of the Port of Rotterdam in phase B is able to resist loads, unexpected conditions and remains future proof. The context of this project will be based on phase B, from which a road passes at only 10 meters behind the quay wall, therefore the predictions and analyses will take into account the physical boundaries of the site and monitor them. Furthermore, in order to cover the most unexpected scenarios, safety factors will be applied for the soil and for the loads.

Therefore, the main objective of this thesis is going to be about analyzing the different responses by the quay wall, when subjected to different load scenarios, particularly when taking the road into account. This way, during the actual load test, the response of the quay wall such as its deformation can be monitored all along, and based on the results obtained from the predictions and modeling, the load can be increased or not. It is important to mention that the load test will be carried out once the quay wall is installed, and it will be a permanent structure, therefore the results from the predictions need to be carefully analyzed so that no failure happens in real life situations.

Furthermore, to conduct this research, data was gathered from the company's resources, such as the soil data, the geometry and parameters from the quay wall, the water levels and other. The type of study will computational, as the main goal is to develop an accurate model that is capable to predict this quay wall's response and behavior under various situations. This way, the results can serve to make informed decisions before and during the actual load test.

The results of this research are obtained by combining different load combinations, and also different values for the soil's strength parameters and for the water levels. To be more precise, a comparison is done between using average soil parameters and 95th percentile soil values also called the characteristic values, based on experimental data. The first would determine more accurately the typical day, therefore in this case a very valuable prediction for the actual load test, and the second takes into account unexpected events such as extreme weather conditions or other uncertainties.

Therefore, this study will give academic context as well as background information in order to analyze the soil and find the weakest location where the load test will be performed. Next the strength parameters of the soil and the structures are calculated, followed by a calculation of load combinations and a maximum load that can be applied during the load test, along with its displacement.

Moreover, the weakest soil location along the entire quay wall is found to be around the CPT point DKM051, which lies around 600 meters from the beginning on the quay wall (from left to right) in Terra+. Furthermore, with the soil layering of that point, the maximum load that can be applied within the first 10 meters behind the quay wall is 31kPa, which creates a horizontal deformation that lies in the range of 71.86 mm to 98.02 mm, without taking into account the road impact and depending on the values used for the water levels, either springtides or average and on the soil parameters, where the average values or the characteristic values are used. When the road is taken into account with its 2 lanes the range is higher, going from 74.04 mm to 101.3 mm, and when considering only 1 lane of the road the range of deformation goes from 72.51 mm to 99.18 mm.

VI. Introduction

Quay walls have an essential role into the functionality and the resilience of port infrastructures. They serve as essential structural barriers which facilitate efficient vessel operations as well as cargo handling. Moreover, port activities are becoming more important, which are leading to extensions of the ports and dealing with bigger vessel containers. Therefore, the resilience and integrity of the quay walls have become more critical than ever before. Moreover, the challenges that quay walls face, also include aging infrastructure, the evolving maritime dynamics, and new environmental demands, therefore a proper understanding of how quay walls perform is essential. Besides, there is an increasing need to develop new methodologies to assess the tolerance limit and load testing of the quay walls and hence enhance the efficiency and resilience of the design.

The aim of this report is to explore the structural complexities of combi quay walls, focusing on understanding their dynamics, and identifying the loads that act on these walls and their points of impact.

Furthermore, the vessel's transfer operation takes place at the quay wall, and they need to be as efficient as possible for the commercial success of the port. Therefore, especially when dealing with larger ships, the quay walls need to be adjusted to be able to withstand the higher external forces. And in order to withstand those forces, the wall needs to ensure sufficient stability and strength.

And in order to ensure that the quay wall is stable, a load test must be performed in to verify that the wall is able to behave as predicted and has enough capacity to handle loads in every scenario, and can be considered a resilient structure. Therefore, insights and predictions for the values of the actual load test need to be developed. Hence, the ultimate goal of this report is to find those predictions, by finding the weakest soil point along the quay wall, the different strength parameters of the soil and of the wall's structure, and the different loads that act on the wall, and their combinations. Most importantly, this study aims to research the maximum load that can be applied during the load test, as well as the horizontal deformations that are created by it. Furthermore, the study will take into account different factors impacting the predictions, such as safety factors, different water level scenarios, and different strength parameters for the soil. Furthermore, it will also take into account a use phase, and a ultimate phase, which is the worst case scenario.

A. Study Area

For this project, the main focus will be the quay walls located in the Port of Rotterdam. This port has an area which exceeds the 12 600 hectares, and it is the largest port of Europe. This port is also known for accommodating the largest vessels, as it has a great depth with extensive basins. Furthermore, the port is renowned globally, as it has been recognized on multiple occasions as the premier port infrastructure by the World Economic Forum [23]. Moreover, the port of Rotterdam has a strong position as the market leader in dry bulk, liquid bulk and handling of containers. The Port of Rotterdam has in fact around 80 kilometers of quay walls. It is also important to point out, that the Port of Rotterdam, has been constantly growing for the past 150 years and for that growth to continue, it is primordial to continue to adapt the design of the port´s infrastructure like quay walls, to the newest requirements [18].

In fact, in order to keep its position among Europe´s largest container port, the Port of Rotterdam is investing the expansion of the Prinses Amaliahaven located on Maasvlakte II, more precisely at the water passage called the Yangtze canal, where quay walls will be constructed with the main focus being, safety, and resilience. This expansion will be able to attract an extra flow of containers of around 4 million TEUs (Twenty-foot equivalent unit) per year [17].

Furthermore, the specific location for this project is situated in the Maasvlakte Rotterdam, more specifically at the Antarcticaweg. The study section is divided into two: phase A and phase B. This project is therefore called the widening of the Yangtzecanal. Figure 1 shows the Yangtzecanal as well as the two locations A and B.

Figure 1: Sections A and B of study area

1. Quay Wall Phase A and B

Phase A has a length of 500 meters and phase B has a length of 1500 meters. In both sections quay walls are placed all along the length. In this situation, quay walls have a structure of combined wall with steel tubes and a sheet pile between them, which will be explained more in detail in section VII.C.
The first design that was developed by the company Witteveen+Bos was phase A. The installment method was to install the steel tubes into the ground by vibration, which resulted in the creation of settlement around the tubes and the installment had to be put on hold. And the problem was that in this case, the settlements were larger and in a broader area than predicted in the design. This was a problem as in phase A, industries are present in the area, therefore, another installment method must be proposed a solution. The cement-bentonite installation method is the solution that was proposed, and the construction with this method for phase A has started during the duration of this thesis. This method consists on placing the tubes into the ground without vibration. The ideas is that a trench is dug with a depth equal to the length of the combined wall, and by the use of cement-bentonite slurry which prevents the collapse of the soil during excavation. Figure 2 shows an actual picture of the construction of the cement-bentonite wall in phase A. So, phase A has a section of the quay wall being installed by vibration and a section of the quay wall being installed by the cement-bentonite slurry trench excavation. However, the problem with load testing for this section, is that the installment methods have a direct impact on the stability of the wall which can therefore affect the results for load testing in phase A. Hence phase B is the primary area of interest for the study of this thesis.
The objectives of the study are the following: the identification of the optimal location for load testing in phase B along the 1500 meters, and the development of a method for conducting the load test and the analysis of its results, which will provide the prediction values for the actual load test.


Figure 2: construction of cement-bentonite wall phase A Yangtzecanal

B. Problem statement

The quay walls in the Port of Rotterdam, especially those in Prinses Amaliahaven which are in expansion, located on the Yangtzecanal, are essential assets in supporting the port´s infrastructure, and keeping its global status. Because the container volumes are expected to rise, there is an urgent need to ensure the safety of these quay walls.

However, challenges already arise in the design and in the construction process as explained in section VI.A.1. Due to the use of different installment methods for phase A, which can cause different degree of soil disturbance which can affect the quay wall stability and the reliability of the load tests, the execution of a load test is preferred in an area which does not have 2 different installment methods. Therefore, the focus is shifted to phase B, which is still in the design phase, and where the challenge is to identify the optimal location for load testing, and frame a methodology to conduct these tests effectively. Moreover, factors such as soil characteristics, soil layering, water levels and the proximity to a nearby road, are factors that add complexity to the testing process, and need to be taken into account, and the development of appropriate measures is essential to mitigate the potential impacts of the road on the load testing accuracy, as the soil layering and its characteristics affect the stability of foundation, and the roads in the vicinity add to the vibrational loads.

C. Research Objective

The ultimate research objective of this study is to determine the optimal location and method to conduct the load testing on phase B on the quay wall in Yangtzecanal, through modeling, to get insights into the wall's stability, and conclude on a reliable assessment of it. Furthermore, this study aims to identify factors that can have an impact on the load testing results, and to address them. This is the case of soil characteristics, water levels, material strength parameters, the proximity of the traffic infrastructure, and therefore contribute to having an improved design and a more resilient port infrastructure.

D. Research Questions

- What is the optimal location for load testing in phase B?
  - What criteria should be considered when selecting the optimal location for load testing along phase B?
  - How do factors such as soil stability, proximity to a road, different loads and pressures, impact the decision-making process for the load testing location?
  - Are there specific areas within phase B that are more prone to settlement or other stability issues, and how does this influence load testing site selection?
- What is impact of different soil characteristics on load testing?
  - How does the layering of soil beneath phase B affect the distribution of loads and potential failure mechanisms?
  - Is there a correlations between soil properties and deformation behavior of the quay wall, or potential settlements?
  - What is the impact of different soil characteristics on the stability and load bearing capacity of the wall?
  - What methods and instrumentation are necessary to validate predictions, and how can strain, pore pressure, and settlement be accurately measured during testing?
- What is impact of the infrastructure near phase B on the load testing?
  - How does the road passing near phase B affect the accuracy of the load testing?
  - What mitigating methods can be put in place to mitigate this potential impact?
- Can the results obtained be extrapolated?
  - Can the results obtained from the load testing methodology developed for phase B be used for other quay walls in the Port of Rotterdam?
  - What are the insights gained from this research that can be applied elsewhere?
- How will the calculations be carried out?
  - What is the selection of parameters of a suitable constitutive model in PLAXIS?
  - What methods are used in PLAXIS?

E. Research Methods

The main themes regarding the research methods, in order to answer the research questions are the following.

1. <u>Preliminary Data Analysis</u>: First, in order to gather data on soil characteristics and assess the impact of the infrastructure near the quay wall in phase B, a site investigation would need to be carried out. To find the soil´s characteristics geotechnical tests, such as cone penetration tests need to be done, to characterize the soil. Other tests, such as triaxial compressions tests, shear tests, and the behavior of soil under different load conditions can also be done for the testing and the analysis. Nevertheless, for this case, the data has

already been gathered by the company Witteveen+Bos, so no additional field study will be needed. Furthermore, the data was analyzed during this study, in order to implement it into the model.

2. Quay Wall Design Specification: In second place, the quay wall´s design from phase B needs to be specified regarding its geometry, material components and their properties and quay its wall type needs to be known. This will also be provided by the company Witteveen+Bos.
3. PLAXIS Model Set Up: with the previous information and data, a numerical model, in this case PLAXIS will need to be developed, by use of finite element modeling in order to simulate the quay wall´s behavior under different scenarios. To set up the model properly, boundary conditions will need to be defined as well as the constitutive model which needs to be selected.
4. Simulation of Load Tests: With the model set up, the simulation of various load tests needs to be performed, by taking into account different loads, such as water pressure, soil pressure, the weight of the wall, the load caused by the quay wall´s activity and others. This enables to evaluate the wall´s behavior under different load scenarios.
5. Analysis of Simulation Results: the next step is to analyze the results obtained by the modeling and simulation in order to evaluate the different deformations of the wall, its stress distributions, the safety factor and also the optimization, all under different load situations. Furthermore, some other case studies, such as similar project which also involve the load testing on quay walls, can be researched to compare, and adapt the model if needed
6. Report writing and documentation: The last step is then to document the entire research carried out, in the form of a report. This will include the assumptions made, the numerical values obtained in terms of the wall´s properties, the results obtained from the simulation, its analysis and a final location for the load test on the quay wall.

All of these research methods are visualized in a flowchart (see Figure 3).

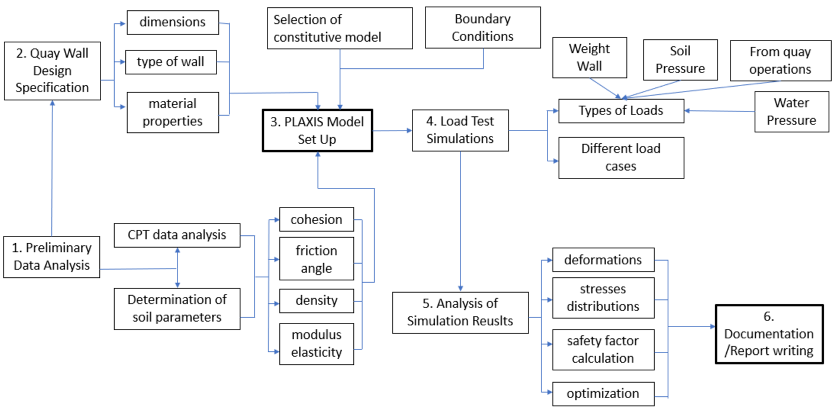

Figure 3: Flowchart research methods

VII. Academic Context

A. Importance of quay walls

A quay wall is more than just a wall submerged into the water, they are in fact essential to ensure not only the functionality but also the safety of a port, canals, rivers, inland waterways etc. They need to be able to withstand during long periods of time, while subjected to loads from the water, from the soil and from other loads coming from the ships. Yet, the quay infrastructure faces additional challenges such as corrosion, sea level rise and extreme weather conditions. Thus, in order to ensure longevity and safety, the quay walls must be designed very carefully, so that they are able to withstand adversity while remaining future proof.

Moreover, the maintenance of a quay wall is a significant expense for the port or the city in question. A strategic combination of inspection, monitoring and modeling is imperative to judge a quay´s wall functionality.

Researching methodologies for load testing is essential to encourage the development of more efficient and more environmentally friendly quay wall designs, which is the aim of this project for the load test on phase B. Moreover, innovative technologies such as sensors, and drones, can be used for the monitoring of the quay walls, along with wise selection of materials, and techniques for reinforcement of the walls.

B. Involved parties

For this project there are several stakeholders involved and they are explained as follows, and from which a power interest grid will be made. Furthermore, by considering the different interests, an effective plan to execute the load test can be done. A visual representation in the form of a power interest grid is shown in Figure 4.

1. Port Authority

The port authority for this project is the Port of Rotterdam, which is the key stakeholder, and client from Witteveen+Bos for this project. They are the owners of the port and are in charge of its management. They have a high interest in this project as they aim to ensure that their quay walls are structurally stable and that they can handle safely the larger vessels and handle their cargo. They can also provide their own requirements and demands on the load testing. Therefore they have a high interest and a high power.

2. Engineering Firm

The construction company responsible for the construction and testing of the quay walls is Witteveen+Bos. Their primary role is to design the quay wall and carry out the load test. It needs to ensure that it meets the safety standards and also to perform the necessary tests to verify the wall's load bearing capacity and its integrity. Therefore they also have high power and high interest, however a bit less than the port authority which will have the last word.

3. Maritime Traders

Many stakeholders in the maritime industry, such as shipping companies, cargo owners, have a really high interest in the safety and efficiency of the port they are arriving to. Therefore they highly rely as well on quay walls for their operations. They have high interest but low power.

4. Local Community

The local community which surrounds the port can also be considered an involved party, as they can be affected by the construction and testing of the quay walls because of the traffic, the potential deviated roads, noise, or other potential disruptions. They have both low interest and power.

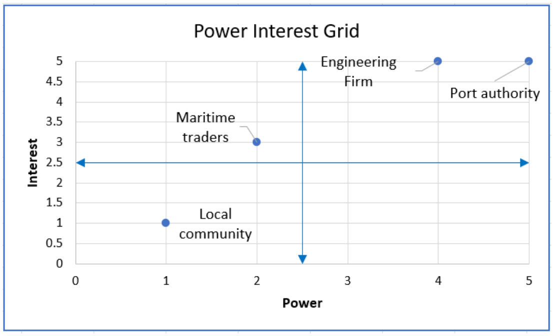

Figure 4: Power Interest Grid

C. Combi Quay Wall

The type of quay wall for this project is a combi quay wall, which is an earth retaining structure built using different profiles, so by the combination of steel tubes and sheet piles. The tubes are put in place to provide strength to the wall, and the sheet piles are used for earth retainers.

The tubes are provided with interlocking points into which the sheet piles fit. To stabilize the combi wall, anchors can be used, in case the wall is not auto stable. These anchors are placed in the ground and they are attached behind the wall. They are steel tension elements, with a pipe shape, from which the forces form the wall are transferred to the soil behind the wall. Furthermore, anchors provide an additional horizontal force acting against a potential overturning of the wall.

In other cases, different types of retaining walls might be more favorable, however in this case, the combi walls are also the preferred technique for quay walls [5]. Furthermore, combi quay walls are used instead of just regular sheet piles, which are not strong enough to support the load. Some advantages of this structure is that it can resist heavy loads as it has a strong bending stiffness, with a relatively low weight. Furthermore, they have a mix of load-bearing elements for the vertical and horizontal loads, along with other elements which facilitate the transfer of the loads to the load bearing elements. Lastly, the combi quay walls also are more cost effective than a contiguous sheet pile wall while providing more load bearing capacity, and one reason for this is that steel elements can easily be removed and reused is the structure is no longer needed [4]. In fact, "combined steel sheet piling is often economical for larger section moduli" from Committee for Waterfront Structures of the Society for Harbour Engineering and the German Society for Soil Mechanics and Foundation Engineering, [12]. A top view representation of a combi quay wall can be seen in Figure 5.

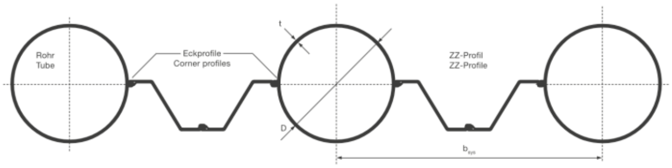

Figure 5: Combined tubular sheet pile wall-top view [22]

D. Forces and loads

The primary forces that a quay wall must withstand are outlined below:

1. Soil Pressure

Granular materials like soil and rock generate horizontal and vertical pressures, where the horizontal pressure increases linearly with depth, and the quay walls need to be able to resist these pressures. Soil pressure is the lateral pressure exerted by the soil on the quay wall, which is separated into the active and the passive soil pressure. Furthermore, the effective stress of the soil will be considered, which is the total stress minus the pore water pressure.

a) Active Pressure

The active pressure happens when the wall has the freedom to move outward, and the soil applies force on the quay wall. As the wall shifts away from the soil the active condition develops, and the lateral pressure against the wall diminishes with its movement until reaching the minimum active earth pressure force (Pa). Furthermore, the soil behind the wall is in tension.

b) Passive Pressure

On the other hand, if the wall moves inward into the soil, then the soil mass behind the wall is compressed, which also mobilizes its shear strength and the passive pressure develops. This situation might occur along the section on the opposite side of the retained soil. Furthermore, passive pressure is much larger than active pressure.

c) Earth Pressure Coefficients

The theory commonly employed when discussing the active and passive lateral soil pressures is the Rankine Earth Pressure Theory, which has the following assumptions: no friction between the wall and the soil, lateral pressure is applicable solely to vertical walls, failure within the backfill material occurs as a sliding wedge along a potential failure plane defined by the effective angle of friction, lateral pressure increases linearly with depth, and the resultant pressure is positioned one-third of the total height of the quay wall above the base of the wall. The following equations ((1) and (2)) determine the active and passive soil coefficients where φ is the effective angle of friction. Furthermore, these coefficients are different for each soil layer.

$$Ka = \frac{1 - \sin(\varphi)}{1 + \sin(\varphi)} \tag{1}$$

$$Kp = \frac{1 + \sin(\varphi)}{1 - \sin(\varphi)} \tag{2}$$

As the soil friction angle (φ) increases, and the soil becomes stronger, the active pressure coefficient decreases, resulting in a decrease in the active force while the passive pressure coefficient increases, resulting in an increase in the passive force.

d) Total Lateral Soil Pressure Force

To calculate the total lateral soil pressure force, it can be calculated by finding the total area of the pressure distribution along the quay wall. This distribution varies linearly, and therefore its area is the area of a triangle. The base of the triangle is the horizontal pressure, which can be found by multiplying the horizontal's soil pressure coefficients Ka and Kp, which depend on the type of horizontal loading, by the vertical effective stress ($\sigma' v$). It is defined by the following equation, where γ is the specific weight of soil, and H the height of the wall. Also γ*H is the effective stress ($\sigma' v$) at depth H, only if all the soil is above the groundwater level, see equations (3) and (4) :

$$\sigma' h = Ka \times \sigma' v \tag{3}$$

$$p\ (bottom) = Ka \times (\gamma \times H) \tag{4}$$

Otherwise, the vertical effective stress $\sigma' v$ is the total stress σ minus the pore water pressure u, see equations (5), (6), (7):

$$total\ stress: \sigma = \gamma \times \mathrm{H} \tag{5}$$

$$pore\ water\ pressure: u = \gamma\ (\mathrm{water}) \times \mathrm{H} \tag{6}$$

$$effective\ stress: \sigma' \mathrm{v} = \sigma - u \tag{7}$$

So, if the soil is not all above groundwater level, then taking into account different layers, the total stress is shown in equation (8) :

$$\sigma = (\gamma_{unsat} \times \mathrm{H}) + (\gamma_{sat} \times \mathrm{z}) \tag{8}$$

Where H is height above water level, and z is the height below water level. Also γ_{unsat} is the unsaturated volumetric weight of the soil above water level (also depending on the different layers), and γ_{sat} is the saturated volumetric weigh of the soil below water level.

As the force is the pressure times the area, the total force acting on the wall due to the soil's pressure is calculated in equation (9):

$$Fsoil = p(bottom) \times area\ triangle = (Ka \times \gamma \times H) \times (0.5 \times b \times H) \tag{9}$$

When assuming the force per unit span, b=1, which results in equation (10):

$$Fsoil = \frac{Ka \times \gamma \times H^2}{2} \quad (per\ unit\ span) \tag{10}$$

The location where this force acts is at H/3 from the bottom of the wall and is presented in Figure 6.

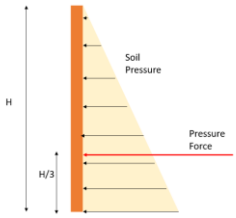

Figure 6: Visualization soil pressure (active)

2. Water Pressure

The water pressure also increases linearly with depth, based on the hydrostatic equation which refers to the change in pressure with respect to the change in depth. It is the pressure that the water exerts on the wall when standing still. With ρ as the density of water, g is the gravitational constant and dh the change in height, this equation is represented with the hydrostatic equation (see equation (11)) :

$$\Delta P = -\rho \times g \times \Delta h \tag{11}$$

Following the same logic as for the soil pressure, the area formed by the water pressure will also be a triangle, from which the total force can be found by the following formula where b =1 as well (see equation (12)):

$$F_{water} = P(H_w) \times Areatriangle = -\rho \times g \times H_w \times 0.5 \times b \times H_w \tag{12}$$

$$= \frac{-\rho \times g \times {H_w}^2}{2}$$

The location of the resultant water force is also at H/3 from the bottom of the wall, of course taking into account only the height that the water is touching. This is shown in Figure 7.

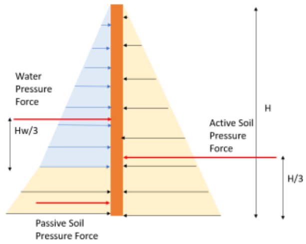

Figure 7: Visualization soil and water pressures

Moreover, if water is accumulated behind the wall, the total pressure and the force resulting from this extra pressure will also increase on the backside of the wall. Furthermore, the rise of excess pore water pressure, can lead to the degradation of effective stress, potentially causing liquefaction, where the soil loses its strength and behaves more like a fluid. This is not a desired situation, therefore quay also need to be designed with adequate drainage systems, to prevent the water from accumulating behind the wall. Some examples of drainage systems are weepholes or lateral drains.

3. Surcharge loads

Surcharge loads acting on the quay walls are additional vertical loads normally at the top of the soil, and above the wall as well. These loads can be dead or live loads, which would be the case of the movement of cranes on the rails. These loads are considered to be spread in the downward direction, and will be considered to be uniform loads, such that they are applied uniformly over the soil's surface. They will therefore cause a uniform pressure distribution. Therefore, for soil in active and passive conditions, the formulas for the force resulting from the surcharge loads and exerted on the wall are see in equations (13) and (14):

$$F_{load,active} = Ka \times q \times H \tag{13}$$

$$F_{load,passive} = Kp \times q \times H \tag{14}$$

Furthermore, the location of this force is at H/2 from the bottom of the wall, as visualized in Figure 8.

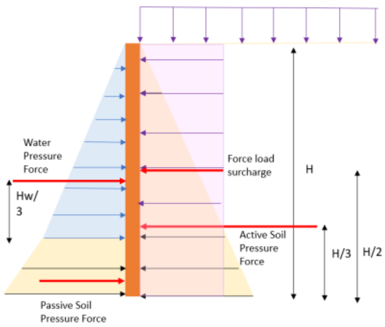

Figure 8: Visualization loads on wall with surcharge loads

4. Wave variations

Finally, the wave variations can play an important role, since they determine different water levels on the wall. This results in an increase of the total water pressure that the wall needs to resist. For this, information from the site needs to be analyzed, to see the ranges in the worst case scenarios registered.

E. Load resistance of combi walls

As previously introduced, the tube piles, are the primary structural elements of the combi quay wall, and the sheet piles act as secondary elements. Therefore, the primary elements guarantee the horizontal stability and they are responsible for transmitting the forces downward into the subsoil. The sheet piles are responsible for managing the

soil and water seal between the tubes. Moreover, the bigger the diameter of the tubes, increases the moment of inertia, which is the main component determining the stiffness of the combi wall. Moreover, also an increase of diameter results in the increase of the modulus, which is the main parameter for the strength of the wall.
Furthermore, the tube piles are responsible for resisting the overturning forces, and the sheet piles are responsible for filling the gaps between the tubes. Moreover, in some cases, ground anchors can be installed to prevent overturning or sliding.

F. Calculation methods

1. BLUM method

The BLUM method is introduced as a way to justify why the FEM is used instead. The model of Blum if a simple calculation method, which can be done by hand. It assumes that the soil behaves either active of passive, as can be seen in Figure 9. However, in reality the soil does not behave like the red line, but rather like the black curve, which is a big limitation of this method. Furthermore, the Blum method assumes that the sheet pile is fully clamped at some point in the soil, and at that point the moments are equal to 0. This way, a fast calculation as a first approximation can be carried out of required depth of the sheet pile. However, the deformations can be not be accurately predicted, that is why for design purposes, a finite element model is used.

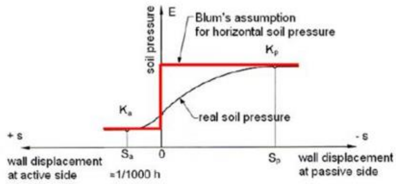

Figure 9: Stress strain relation BLUM method

2. FEM

A finite element method is based on a computerized model, in which the soil's behavior and structure are integrated. An example of the models where this method is used is the model PLAXIS which will be explained in section VII.H.3. In this model, the internal forces of a structure, the soil's stresses and the deformations can be modelled, which is an enormous advantage of using these type of models. In the PLAXIS model, one can introduce the load and material factors to do the calculations, and also characteristic values of the soil. And to find these values, to plug into the model, some field data is needed, for example for soil characteristics, water levels, geometry of the wall, the materials used for the wall etc. Therefore, the most robust approach is to use finite element analysis (FEM), which is a method that enables to minimize simplifications, and provides reliable predictions for both the forces and the deformation of the quay wall. FEM models allow for the consideration of for example, the interactions between different structural components, and the interplay of foundation piles and sheet piles. Nevertheless, to use a FEM analysis a great number of input parameters are needed which are mentioned in as follows. Furthermore, the accuracy of these calculations relies on the soil model employed, and for the quay walls there are 4 typical models used, which can also be used in PLAXIS [15]. These are the linear elastic model, the Mohr coulomb model, the Hardening soil model, and the soft soil creep model. However as only the hardening soil model will be used for the PLAXIS model of this project, only that model is explained in more detail.

a) Hardening Soil Model

This model will be used in this case for the PLAXIS model. This model is the most suitable for retaining structures, such as quay walls. The reason for this is that it describes the soil strength based on the Mohr-Coulomb failure criteria, but by providing a more realistic estimation of the soil's stiffness. The hardening soil model uses a hyperbolic stress strain relation (while Mohr Coulomb uses a linear relation). This model is therefore more advanced, and simulates the soil behavior more accurately. Also, in this model, the calculated stiffness increases with pressure. Therefore, all input stiffnesses are related to a reference stress. In this case, the initial stress generation can also be taken into account by including other parameters such as pre-consolidation, which plays a role as well in the soil deformation. Furthermore, for this model, three types of stiffness are defined: the loading stiffness based on the results from a triaxial pressure test, the unloading stiffness based on the results of triaxial unloading pressure test, and the stiffness loading, based on the results of a one dimensional consolidation test. This hyperbolic stress strain relation is visualized in Figure 10.

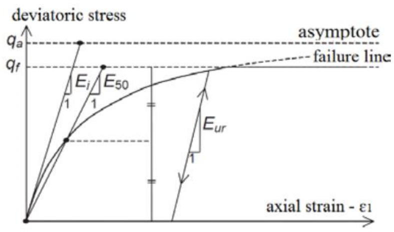

Figure 10: Hyperbolic stress strain relationship [3]

G. Installment methods

1. Vibration into the ground

One way of installing the combi walls, the steel tubes can be vibrated into the soil, with the use of a vibratory hammer. The tubes have the possibility of being filled with concrete/steel, depending on the use. What is needed for this method, is a pilling/guiding frame, so that the piles are secured in an accurate position. This can be visualized in Figure 11. The sheet piles are also driven into their position by using a vibratory hammer, and are aligned with the tubes by the use of welded interlocking points [5]. Also, if the load test of phase B is to be compared to the load test of phase A, then the cement-bentonite installment method will also need to be looked at.

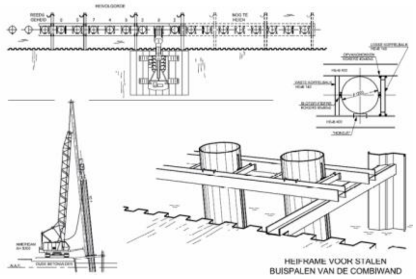

Figure 11: Guiding frame for the installation of combi wall [8]

2. Cement-bentonite slurry trench excavation

Another method for inserting the tube piles into the soil, is by digging a trench using a slurry mixture, which comprises water, bentonite cement, and in some cases, additional additives. The idea, is that the slurry solidifies and forms the ultimate barrier wall. The viscosity of the slurry is designed so that it is maintained in a fluid state during the excavation. The goal behind this is to prevent the collapse of the wall, and the tubes can be placed into the ground accurately. At the end, the wall created is transformed into a permanent underground structure.

H. Load Testing

Building up on the concepts introduced about the load test, it is important to understand why and how a load test is carried out. A load test is carried out to serve the structural assessment of a structure, in this case of the quay wall. The goal of a load test on a quay wall is to ensure that the wall is able to withstand the expected loads without failure. Therefore the load test is carried out by applying controlled loads in increment to evaluate whether the wall can withstand the calculated loads. Load tests aim to simulate real life load scenarios, to evaluate the wall´s safety and also identify possible weaknesses that the wall might have, such as deformations or settlements in the soil. This way, the design of the wall can be updated and optimized. Moreover, the load test aims to validate the assumptions made during the initial design, with respect to the load bearing capacity of the wall. On top of that, load tests are also carried out on existing quay walls in order to reassess their bearing capacity, which can be challenging due to uncertainties section VII.H.4. Overall, the main goal of load testing is to reduce the gap between the theoretical design and reality.

a) Dynamic Load test

The dynamic load test method, involves assessing the wall´s ability to withstand dynamic forces such as ship impacts, for example the generated stress by the waves on the wall or also seismic forces. These are recorded and analyzed to evaluate the wall´s response under those dynamic conditions.

b) Static Load test

On the other hand, the static test method is focused on the quay wall´s response to static loads. This method implies using finite element method, in order to predict the wall´s behavior under these static conditions or also can be done through a physical test. For example, it can be analyzed the effects of increasing the depth of the water or any sustained loading such as earth or water pressure. For this research, the static load test will be prioritized.

2. Sensors

To record the measurements during a load test sensors need to be strategically placed on the quay wall. The sensors must be able to record deformation measurements, water level measurements, and crack width measurements in case they are some. Furthermore, these sensors are also helpful to apply safety measures during the load testing. In order to avoid complete failure of the quay wall during the testing, some maximum allowed displacements need to be set and limited, so that if that value is reached, no more load will be applied, as it will risk the collapse of the wall.

3. PLAXIS

Moreover, for this project a numerical simulation will be prioritized for the load testing rather than a full scale load test. And in order to conduct this simulation, the modeling software PLAXIS will be used. PLAXIS is a geotechnical finite element analysis software to model, simulate, and analyze structures. The software can model deformation, stability, and water flow in the soil. The software can assess the deformation under different load scenarios and within some boundary conditions. Moreover, it can also evaluate the stability of the quay wall structures, and include the impact of groundwater flow on stability. The way that it works is through FEM, to divide the entire structure into smaller elements to analyze, and data and technical details regarding the structure can be included such as soil data, geometric parameters, loads etc., all to evaluate the deformation and stability of the quay wall.

4. Uncertainty

A main topic of this research is to reduce the uncertainty in the prediction. There is uncertainty in soil parameters, soil behavior, traffic data, surcharge loads, and structure response. Therefore in order to reduce these uncertainties, it is first important to define the two types of uncertainty, based on Van Gelder (2000): inherent uncertainty and epistemic uncertainty. Inherent uncertainty is the variability inherent in natural phenomena, which can´t be eliminated. For example, the inability to forecast accurately the maximum water levels for the years to come even based on extensive historical data. The epistemic uncertainty comes from insufficient knowledge or data. This uncertainty can be controlled and diminished, by gaining more data, or by doing more analyses [24].

VIII. Soil Investigation

A. Context about soil data

A study of the soil characteristics is essential across the entire section, to study of all types of soil present in various layers. The goal is to identify the soil types, their strength, and other properties which will be essential to make informed decisions on the location of the load testing.

This study is carried out by performing cone penetration tests (CPT) and getting data from the soil´s characteristics in the zone. The CPT is a in situ geotechnical testing method to assess soil properties, by providing continuous data along a vertical profile. The idea is that a cone-shaped penetrometer is pushed into the ground at a constant rate, and the resistance from the ground is what determines the soil´s behavior. Some key parameters and outcomes from the CPT tests are: the cone resistance which indicates the soil´s strength, the friction sleeve resistance which shows the soil´s friction along the cone, and the pore pressure, which indicates the soil´s compressibility.

Furthermore, the idea is to choose the weakest soil location across the entire section. The reason for this is that the load tests are carried out to validate the quay wall´s stability, therefore if at the weakest location the wall resists the load tests at critical point, then it will perform successfully as well in the rest of the section, where the soil is stronger.

Moreover, the main criteria to find the weakest point is by looking at the thicknesses of the clay layers, at the values of friction ration and angle of friction, which are parameters that give indications on the soil's strength. Concerning for example the clay layers, its location along the stratigraphy of the wall plays a big role, for example if the weaker soil is found at the water bottom on the passive side of the wall, that will be more decisive compared to having a weak layer anywhere else along the wall. This is because that location will contribute more to the overturning of the wall, and lead to failure.

For this project, the data will be found on Terra+, a software developed by W+B where soil CPT data of the area can be found.

When conducting a load test along a quay wall, it is important to identify the critical points, especially the points where the soil is the most weak in order to ensure the entire structures' stability. Therefore, as the load test can not be carried out all along the wall, the objective is to find strategic locations where to conduct the load test and then interpolate the results in order to assess the performance of the quay wall. The weaker points are therefore where the soil has the lower strength characteristics. And for this reason, the identification for weak layers is going to be directed towards areas where clay layers predominate.

The reason is that clay layers have fine particle sizes with cohesive properties, which results in lower strength compared to sand layers. And in order to identify those layers, the strength of the material will first be looked by evaluating the different values for friction ratio and cone resistance of each layer, as well as a visual inspection of the soil's layering.

Moreover, the main criteria to find the weakest point is by looking at the thicknesses of the clay layers, at the values of friction ration and angle of friction, which are parameters that give indications on the soil's strength. Concerning for example the clay layers, its location along the stratigraphy of the wall plays a big role, for example if the weaker soil is found at the water bottom on the passive side of the wall, that will be more decisive compared to having a weak layer anywhere else along the wall. This is because that location will contribute more to the overturning of the wall, and lead to failure.

<u>The friction ratio</u> denoted Rf, is the friction ratio defined as the percentage of sleeve friction, fs, to cone resistance, qc, at the same depth. Therefore, the soil type and therefore the resistance to liquefaction can be deduced from these measurements, as it quantifies the relative contribution of frictional resistance to the total resistance encountered during the CPT. A lower Rf value suggests a relatively higher contribution from the cone resistance, as they are inversely proportional which indicates m or denser soil. The formula for the friction ration is defined in equation (15):

$$Rf = (fs/qc) \cdot 100\% \tag{15}$$

- Fs: sleeve friction
- Qc: cone resistance

Furthermore, the cone resistance, Qc, is the resistance subjected by the soil to the penetration of a cone during cone penetration testing (CPT). It is an indication of the soil's strength and its stiffness. The values of Qc are crucial to understand the soil's bearing capacity as well as its ability to support the loads from the quay wall and its anchor. Therefore, higher values of Qc are an indication of stronger soil, which is what is looked for, as it is beneficial for the support of structures. If the values of Qc are lower, that's an indication of weaker soil. Figure 12 shows the visualization of a cone penetration test [13].

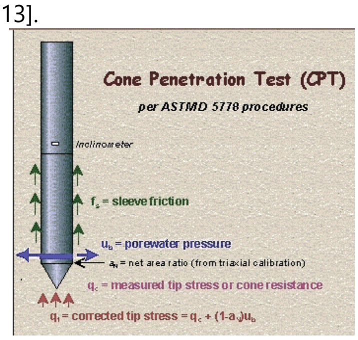

Figure 12: Cone Penetration Test

Besides, in order to obtain the material type of soil based on the friction ratio and the cone resistance, there are some standard values that qualify these values. The following Table 1 shows the classification of soils based off the friction ratio from the Eurocode 7, NEN 9997-1 [14].

Table 1: characteristic values of soil properties [14]

Grondsoort			Karakteristieke waarde [a] van grondeigenschap											
Hoofd-naam	Bijmengsel	Consis-tentie [b]	γ [c] kN/m³	γ_{sat} kN/m³	q_c [d g] MPa	C'_p [g]	C'_s	$C_c/(1+e_0)$ [g] [-]	C_α [f] [-]	$C_{sw}/(1+e_0)$ [g] [-]	E_{100} [g h] MPa	φ' [g] Graden	c' kPa	c_u kPa
Grind	Zwak siltig	Los	17	19	15	500	∞	0,004 6	0	0,001 5	45	32,5	0	
		Matig	18	20	25	1 000	∞	0,002 3	0	0,000 8	75	35,0	0	N.v.t.
		Vast	19 20	21 22	30	1 200 1 400	∞	0,001 9 0,001 6	0	0,000 6 0,000 5	90 105	37,5 40,0	0	
	Sterk siltig	Los	18	20	10	400	∞	0,005 8	0	0,001 9	30	30,0	0	
		Matig	19	21	15	600	∞	0,003 8	0	0,001 3	45	32,5	0	N.v.t.
		Vast	20 21	22 22,5	25	1 000 1 500	∞	0,002 3 0,001 5	0	0,000 8 0,000 5	75 110	35,0 40,0	0	
Zand	Schoon	Los	17	19	5	200	∞	0,011 5	0	0,003 8	15	30,0	0	
		Matig	18	20	15	600	∞	0,003 8	0	0,001 3	45	32,5	0	N.v.t.
		Vast	19 20	21 22	25	1 000 1 500	∞	0,002 3 0,001 5	0	0,000 8 0,000 5	75 110	35,0 40,0	0	
	Zwak siltig, kleiig		18 19	20 21	12	450 650	∞	0,005 1 0,003 5	0	0,001 7 0,001 2	35 50	27,0 32,5	0	N.v.t.
	Sterk siltig, kleiig		18 19	20 21	8	200 400	∞	0,011 5 0,005 8	0	0,003 8 0,001 9	15 30	25,0 30,0	0	N.v.t.
Leem [e]	Zwak zandig	Slap	19	19	1	25	650	0,092 0	0,003 7	0,030 7	2	27,5 30,0	0	50
		Matig	20	20	2	45	1 300	0,051 1	0,002 0	0,017 0	3	27,5 32,5	1	100
		Vast	21 22	21 22	3	70 100	1 900 2 500	0,032 9 0,023 0	0,001 3 0,000 9	0,011 0 0,007 7	5 7	27,5 35,0	2,5 3,8	200 300
	Sterk zandig		19 20	19 20	2	45 70	1 300 2 000	0,051 1 0,032 9	0,002 0 0,001 3	0,017 0 0,011 0	3 5	27,5 35,0	0 1	50 100
Klei	Schoon	Slap	14	14	0,5	7	80	0,328 6	0,013 1	0,109 5	1	17,5	0	25
		Matig	17	17	1,0	15	160	0,153 3	0,006 1	0,051 1	2	17,5	5	50
		Vast	19 20	19 20	2,0	25 30	320 500	0,092 0 0,076 7	0,003 7 0,003 1	0,030 7 0,025 6	4 10	17,5 25,0	13 15	100 200
	Zwak zandig	Slap	15	15	0,7	10	110	0,230 0	0,009 2	0,076 7	1,5	22,5	0	40
		Matig	18	18	1,5	20	240	0,115 0	0,004 6	0,038 3	3	22,5	5	80
		Vast	20 21	20 21	2,5	30 50	400 600	0,076 7 0,046 0	0,003 1 0,001 8	0,025 6 0,015 3	5 10	22,5 27,5	13 15	120 170
	Sterk zandig	-	18 20	18 20	1,0	25 140	320 1 680	0,092 0 0,016 4	0,003 7 0,000 7	0,030 7 0,005 5	2 5	27,5 32,5	0 1	0 10
	Organisch	Slap	13	13	0,2	7,5	30	0,306 7	0,015 3	0,102 2	0,5	15,0	0 1	10
		Matig	15 16	15 16	0,5	10 15	40 60	0,230 0 0,153 3	0,011 5 0,007 7	0,076 7 0,051 1	1,0 2,0	15,0	0 1	25 30
Veen	Niet voorbelast	Slap	10 12	10 12	0,1	5 7,5	20 30	0,460 0 0,306 7	0,023 0 0,015 3	0,153 3 0,102 2	0,2 0,5	15,0	1 2,5	10 20
	Matig voorbelast	Matig	12 13	12 13	0,2	7,5 10	30 40	0,306 7 0,230 0	0,015 3 0,011 5	0,102 2 0,076 7	0,5 1,0	15,0	2,5 5	20 30
Variatiecoëfficiënt v			0,05		–	0,25					0,10		0,20	

Therefore, as can be observed, clay layers are less preferable for the construction of a quay wall, in comparison to the sandy soils. The clay soils are more vulnerable to deformation, to settlement which is a challenge for the structural integrity of the quay wall.

B. CPT data interpretation

The data available consists of 237 CPT data points across the 1444 meters of the phase B quay wall. Furthermore, there are CPT data from 2021 and from 2023. For this project the data from 2023 will be taken into account, as it is the most updated data and also goes up to almost -40m NAP in depth whereas the data from 2021 only reaches around -25m NAP. The use of 2021 data will be used only in case of exceptions or to compare the values with values of the preliminary design phase.

The soil structure is based on the soil research already available. General patterns of the soil layering are known due to the history of the Maasvlakte. This area is present due to a human-made land reclamation, where the upper layers consist mostly of reclaimed sand. Furthermore, the soundings carried out in the area show that the soil profile consists with anthropogenic sand layers with clay and silt layers that alternate through the entire depth. Moreover, these alternating clay and silt layers are not necessarily consistent over the entire length of the quay wall of phase B. Nevertheless, at depth -19m NAP to -23.5m NAP a clay layer is present over the entire length of the wall, which is attributed to the Wormer Member of the Naaldwijk Formation [10]. The thickness of this layer varies from 2.0 m in the east to 4.5 m in the middle of the longitudinal profile of the quay for Phase B. Therefore, a special attention will be given to points which have the thickest clay layer around that depth.

1. Division of sections

As previously mentioned, as there are more than 200 CPT points, and in order to properly analyze them the area will be divided into 3 main sections. When looking at how the CPT tests were performed, it can be observed that they were done following 3 main lines. This is visualized in the following Figure 13. The analysis of the CPT data will therefore be based along these 3 sections, from which the weakest point will be found for each and then the chosen weak points will be compared between them.

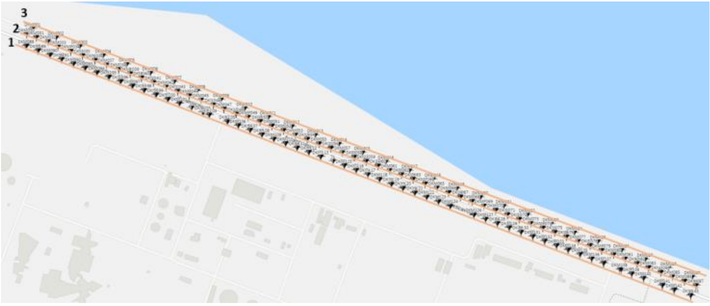

Figure 13: Division of Sections

Section 1
Based on the geometry of the quay wall the depth of interest for section 1 is mostly going to be where the anchor and the grout body of the quay wall will be placed. The way an anchor with a grout body functions is by transferring the loads from the structure into the ground, which means that the soil present surrounding the grout body needs to have a strong bearing capacity and so that the anchored structure is stable. Therefore, when checking the soil's characteristics for section 1 the main focus will be on the lower depth, from approximately -9.35m NAP to -30.36m NAP, as that is where the anchor will be placed. A special attention will be given to the placement of the grout body which is between -24m NAP and -30.36m NAP (see Figure 59 for the geometry of the quay wall).
Section 2
For section 2, the area of most interest will be the depth where the quay wall is placed as well as the tubes. Therefore the depth until -27.5m NAP is of importance, by also given special attention to the depth where the sheet pile is placed, therefore until the construction depth of -9.35m NAP.
Section 3
For section 3, the entire area will be looked at, by looking at the weak patterns and also paying attention to the clay layer present at around -20m NAP.

IX. Criteria for selection

The criteria to determine the weak points per section will be the same for each section. This selection will be based off the interpretation of the visualization of the soil layers and by the use of heatmaps that represent both the friction ratio (Rf) and the cone resistance (Qc) , all across the 1444 meters of quay wall. Then the most critical points are going to be selected and they are analyzed, until only one point is selected and evaluated as the weaker point of the section. Furthermore the numerical strength parameters Rf and Qc will also be looked at to make decisions to determine the weaker point.

1. Section 1

a) Friction ratio

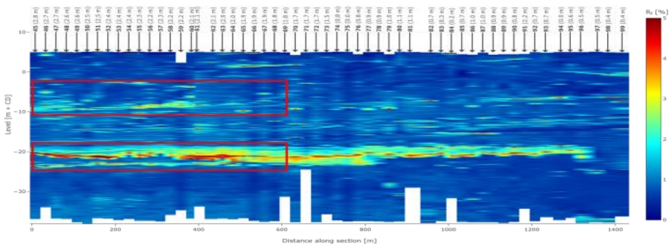

Figure 14:Friction Ratio Heatmap section 1

As previously mentioned, the objective is to identify where the soil is the weakest. As can be seen from the Rf heatmap (see Figure 14 with x axis as the distance along the section and y axis as the depth NAP), there is a consistent pattern of high Rf around the depth of -20mNAP. This pattern is also attributed to the nature of the Maasvlakte which is a reclaimed land, and results in a human-made soil layering, which at that specific depth is mostly composed of clay. Furthermore, it can be seen that the high Rf values are concentrated within the initial 600 meters and then dissipate. Therefore the first 600 meters will be looked in more detail (see Figure 15).

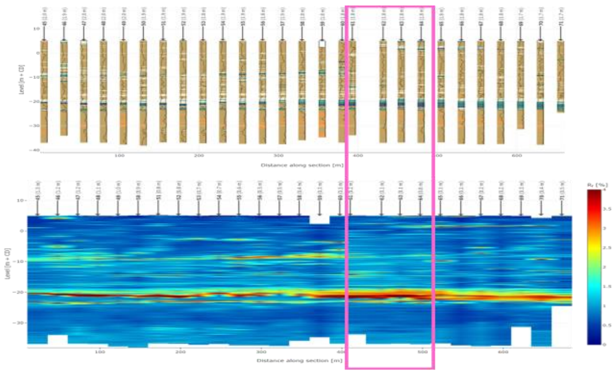

Figure 15: heatmap and soil layering (x axis: distance along section / y axis: depth NAP)

By visualizing both the heatmap and the soil layering, it can be seen that points 61,62,63 and 64 have a high Rf at the approximately depth -20mNAP, therefore they are looked in more detail as well so that each point is compared between them. In order to compare them, the visualization of the soil, the heatmap and the Rf and Qc graphs will be used to choose the weakest point between these 4. To do so, comparison between two points will be done at a time. The graphs in Figure **16**, Figure 17, and Figure 18 show the distribution of values along the depth NAP of the cone resistance on the left hand side and the distribution of values of the friction ratio on the right hand side.

61 vs 62 (see Figure 16)

By visualizing the peaks of the graph, it can be observed that based on qc, for the most part up to -25m NAP point 61 is weaker than point 62. Beyond -25m NAP point 61 is stronger than point 62 by looking at the cone resistance. However, when looking at the friction ratio for that depth, there are no big differences between the two points. Therefore, it will be concluded based on this analysis that point 61 is weaker than point 62.

61 vs 63 (see Figure 17)

When comparing points 61 and 63, it can be seen by looking at the cone resistance that at the beginning 61 is stronger than 63. Nevertheless, as the depth increases some relevant peaks can be observed for point 63 in the cone resistance graph, and in parallel some peaks are also observed for point 61 in the friction ratio graph. This suggests that 63 is stronger and 61 is weaker. Point 61 only becomes stronger around the depth -30 m NAP, however by looking at the friction ratio, the difference between both points is negligible. Therefore it is concluded that point 61 is overall weaker than point 63.

61 vs 64 (see Figure 18)

By looking at points 61 and 64, it can be observed that in the first -20m NAP 64 is stronger than 61. This can be observed by the repetitive higher peaks of point 64 in the cone resistance graph and of point 61 in the friction ratio graph. Therefore in this depth, 64 is clearly stronger than 61. Furthermore, at around -25 m NAP, 61 becomes stronger than 64 based on the peaks on the Qc graph, however when analyzing the friction ratio graph, the difference between both points is negligible. It is therefore concluded that point 61 is weaker than 64.

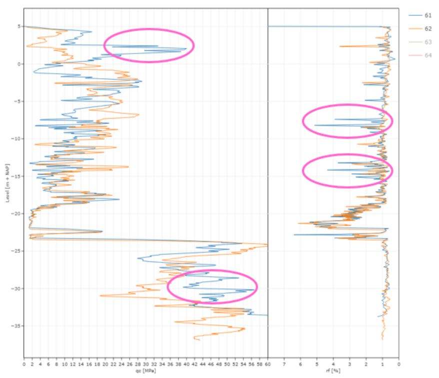

Figure 16: 61 vs 62

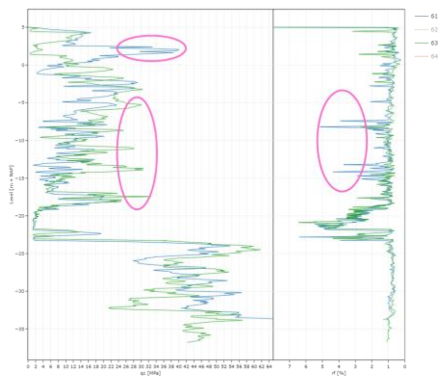

Figure 17: 61 vs 63

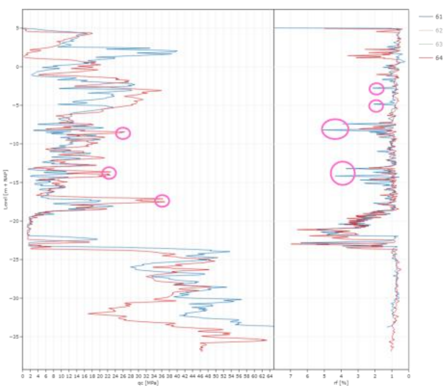

Figure 18: 61 vs 64

As can be seen from the heat map (see Figure 19), point 61 can be considered to be the point with the most inconsistencies, as it presents the more soil types along the stratigraphy especially weaker soil types.

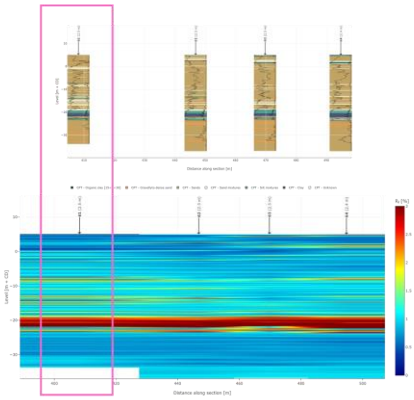

Figure 19: Rf heatmap (x axis: distance along section ; y axis: depth NAP)

b) Cone resistance

Concerning the cone resistance, the higher the value is, the stronger the soil is. In this case, there is a pattern again around the depth -20 NAP of weak soil layers. Also, these weak layers tend to dissipate to the sides as well (see Figure 20). Therefore, it can be assumed based on the heatmap, that there is a weak pattern of low qc from around 400 m to 850 m, which will be looked at more in detail as well (see Figure 21).

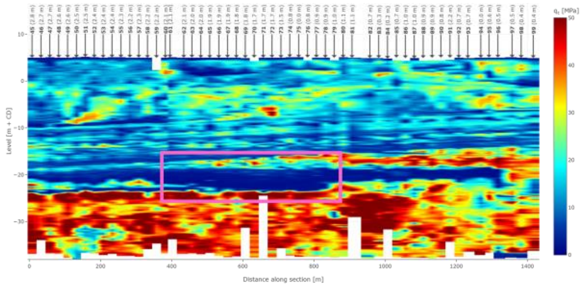

Figure 20: cone resistance heatmap

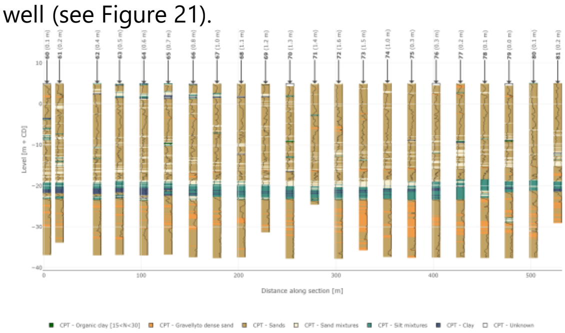

Figure 21: 400-850 m visualization

Based on the visualization, the same conclusion as with the friction ratio corroborates. The weaker layer points which have the larger thickness of clay are 61,62,63,64, from which point 61 is chosen, as seen in Figure 22.

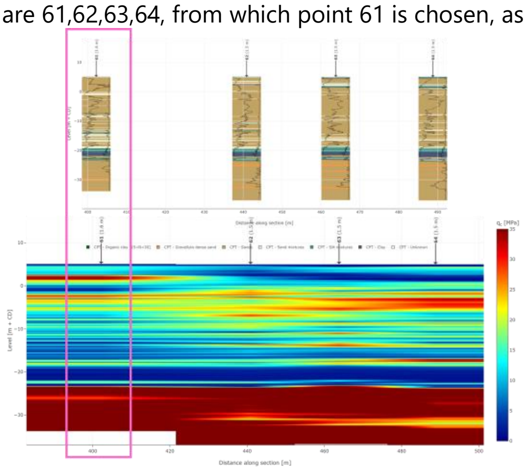

Figure 22: Qc heatmap points 61,62,63,64

2. Section 2

a) Friction ratio

Similarly as in section 1, the weak layers are around the depth -20 m NAP. From there it can be seen that there is a higher pattern in the middle and then it dissipates as well to the sides. Therefore, based on the heat map (see Figure 23) the section that will be visualized in more detail until 800 m, from points 1 to 27 (see Figure 24). Furthermore, it can already be seen that some inconsistencies around 350 meters and 600 meters are present at a depth of around +3m NAP and around -9mNAP, which needs to be carefully be analyzed. For this section, the area of interest is mostly until -9NAP which is the construction depth, therefore these inconsistencies need to be taken into account as well. Nevertheless, when looking at the values in detail especially at point 18, it can be observed that the values are disproportionate. Point 18 has a value for Rf of almost 20% which is not correct which is a high and unrealistic value. Therefore, the point 18 will be considered an error and will not be taken into account.

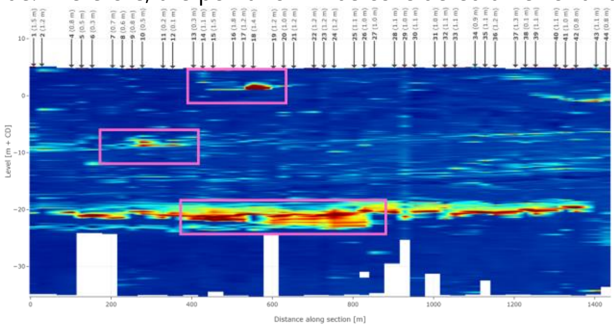

Figure 23: Friction ratio section 2 heatmap

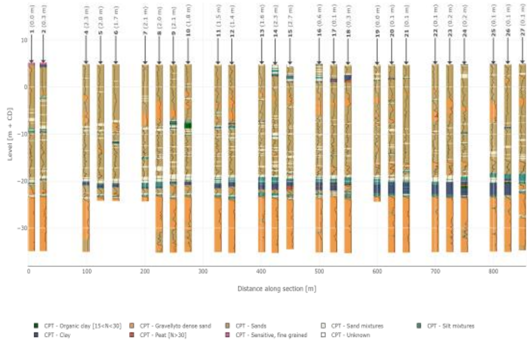

Figure 24: soil layering until 800 meters

The chosen points with the thicker layers around -20 m NAP are 19, 20, 23, 24, 25, 26. Furthermore, points 15, 16 and 17 are also chosen as they not only have peat present (which would need to be verified in more detail by the lab test), but also have weak layers at depth +3-5 NAP. Furthermore, point 10 is chosen as well as it has a layer of organic clay around -9 m NAP, which is a very unfavorable situation for this section. They are visualized in Figure 25:

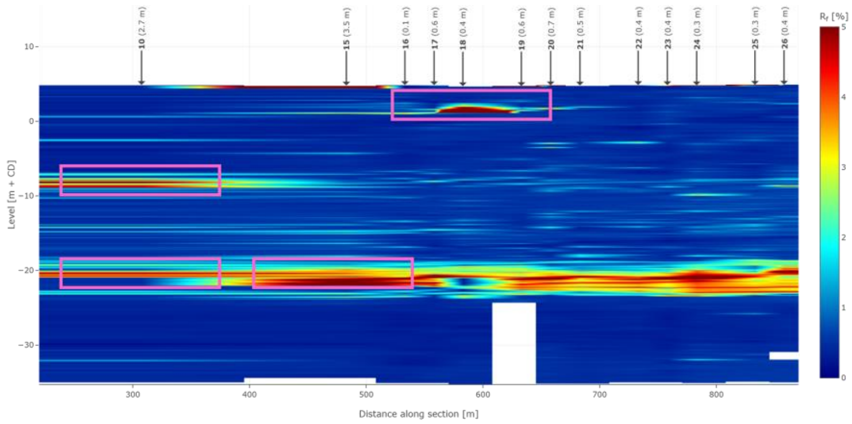

Figure 25: heatmap until 800 m

Based off the heat map of these points, it can be observed that CPT 18 has a very high Rf around depth +3mNAP, however will not be considered as it is considered an error. Nevertheless, points 16 and 17 will be considered. Moreover, point 10 has a high Rf around -9m NAP which can be very critical for section 2 and also a weak layer at -20 mNAP. Concerning the weaker layer at depth -20 mNAP, point 15 has the higher and thicker layer of high Rf.
Therefore, the chosen weaker points are 10,15, 16 and 17, based on the friction ratio and the visualization of the soil layers.

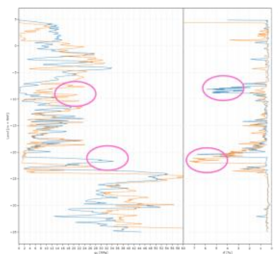

Figure 26: 10 vs 15

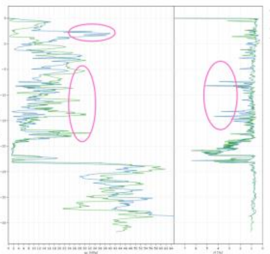

Figure 27: 10 vs 16

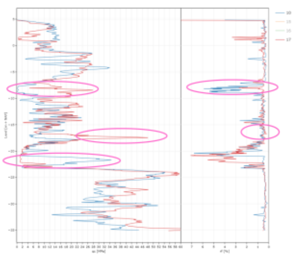

Figure 28: 10 vs 17

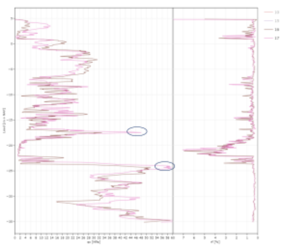

Figure 29: 16 vs 17

<u>10 vs 15 (</u>Figure 26<u>)</u>

In the comparison between 10 and 15 it was concluded that 10 is the weakest. The reason for this is that by looking at the Qc graph, in general point 15 has higher values. Furthermore, clear high peaks of point 10 in the friction ratio graph, show that at specific heights while 10 is weaker, also 15 is stronger. It can be assumed that this trend is more or less present until depth -22 m NAP, where point 10 is stronger at 15 is weaker. Nevertheless, that only happens in one peak, and after that same trend where 10 is weaker is visible again. Moreover, as previously explained as section 2 is mostly interested in the depth around - 9 m NAP (construction depth).

<u>10 vs 16 (</u>Figure 27<u>)</u>

The comparison between points 10 and 16 show that point 16 tends to present a stronger soil. This can be observed by the general higher peaks in the cone resistance, compared to point 10, and also due to the high friction ratio peaks of point 10. As previously mentioned, the area of interest for section 2 lies rather until the construction depth which is until -9.35 m NAP. In this depth section, point 10 is clearly weaker than point 16. Nevertheless, at around depth -22m NAP, there is a peak where point 10 is stronger than point 16. However, with the reasons forementioned, the decided weaker point is point 10.

<u>10 vs 17 (</u>Figure 28<u>)</u>

The comparison between point 10 and 17 was delicate because the patterns are not as clear. Furthermore, it is important to keep in mind that point 17 (DKM051) was the point chosen as the weaker one in the geotechnical design for phase B. From the graph in Figure 28, it can be observed that around depth -9 m NAP point 10 is clearly weaker and point 17 is stronger. This is observable by the high peaks of Qc for point 17 and the high peaks of Rf for point 10. Moreover, at depth approximately -17 m NAP, point 17 has a clear peak of cone resistance, however, when looking at the friction ratio, the difference between both points can be considered to be negligeable. Next, in the depth around -22 m NAP, point 17 is very weak in comparison to point 10. Therefore, in order to choose the weaker point, it had to be determined the area of interest for this section. Because if only the depth until -9.35 m NAP is considered, then point 10 is the weaker one, otherwise point 17 could be considered to be the weaker point. Therefore, based on the expert's findings and experience which suggest that point DKM051 is the weaker one, then point 17 will be chosen.

<u>16 vs 17 (</u>Figure 29<u>)</u>

Points 16 and 17 are very similar, nevertheless it can be assumed that at some depths point 17 is slightly stronger than point 16. Therefore it will be concluded that the weaker point of section 2 is point 16.

b) Cone resistance

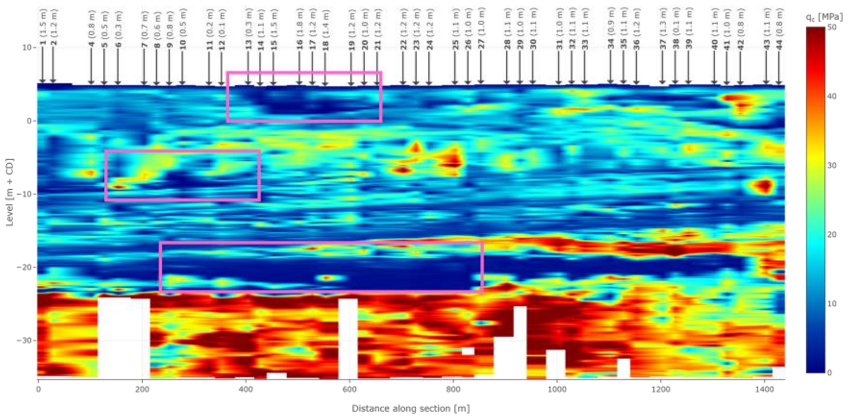

Figure 30: heatmap cone resistance section 2

Based on the visualization of the soil layers and the heatmap (see Figure 30), it will be concluded that point 16 is the weaker point due to its inconsistencies along the entire depth, due to the clay layer at the top and finally also because it has a thick layer of weak soil around depth -20mNAP.

3. Section 3

For section 3 there are no CPT points available from 2023, therefore data from 2021 will be used.

a) Friction ratio

For section 3, the thick layers of weak soil will be looked at all along the depth. A pattern of weak soil can clearly be seen around depth -20 mNAP. Going from 300 meters all the way to 1300 meters approx. (from points 007 to 027), which will be looked at in more detail (see Figure 31, Figure 32, Figure 33).

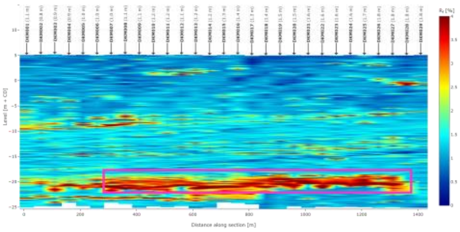
Figure 31: heatmap section 3 friction ratio

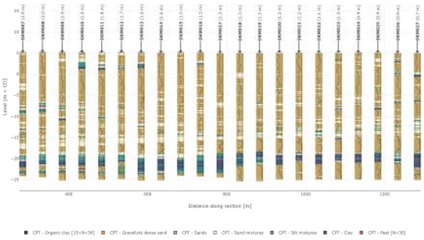
Figure 32: soil layering 300m to 1300 m

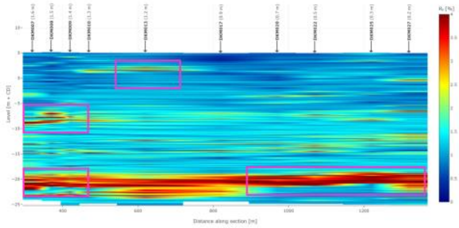
Figure 33: heatmap 300m to 1300 m

As can be visually observed, all the points have a weak layer around -20mNAP. Moreover, there are some points that also present more inconsistencies along the entire depth such as point DKM 010 which has a layer of clay and silt around 2m NAP. This is also the case of point DKM013. Some points present inconsistencies around -9m NAP such as 007,008,009, 025, 027. Also 017, 020, 022 will be looked at due its thick clay layer. The points measured here will be analyzed more closely.

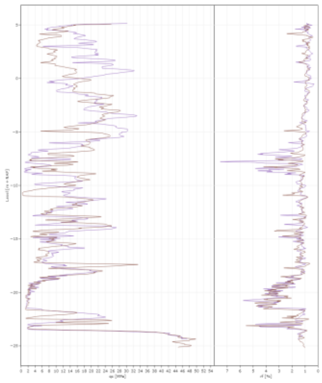
Figure 34: DKM008 vs DKM009

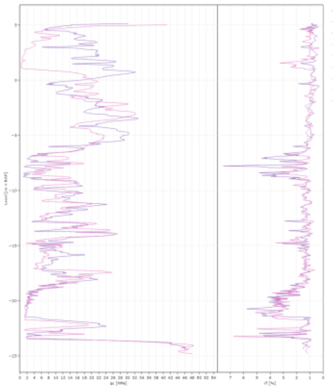
Figure 35: DKM008 vs DKM010

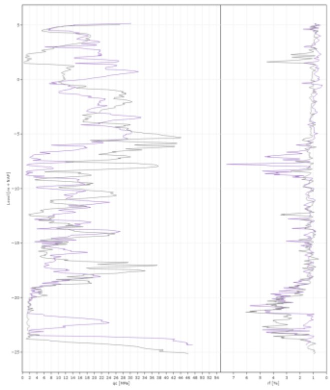
Figure 36: DKM008 vs DKM013

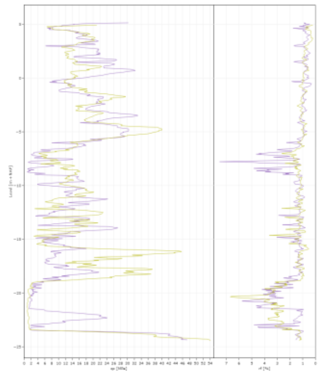
Figure 37: DKM008 vs DKM017

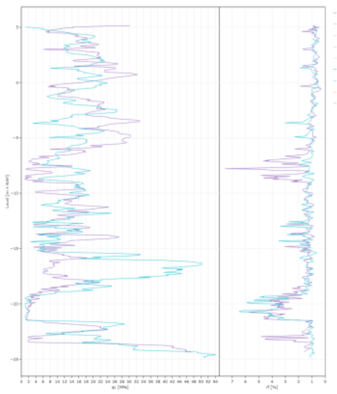
Figure 38: DKM008 vs DKM020

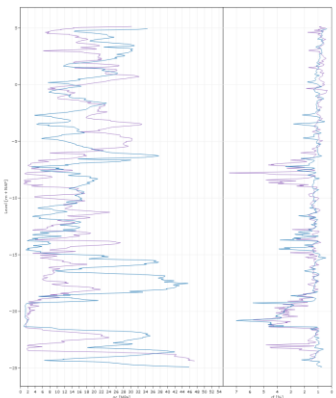
Figure 39: DKM008 vs DKM022

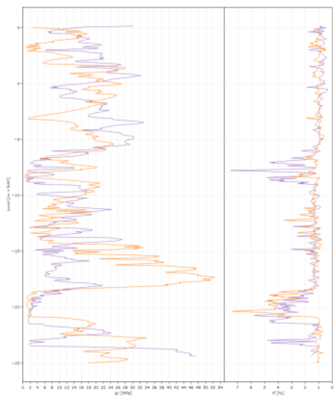
Figure 40: DKM008 vs DKM025

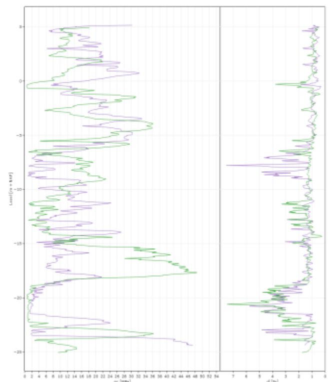
Figure 41: DKM008 vs DKM027

DKM008 vs DKM009 (Figure 34)
It can be seen that point 008 is stronger in the first meters, but then around -8-9 m NAP the point 008 is clearly weaker due to the presence of a high peak in the friction ratio graph. Nevertheless, it can be considered that both are quite weak, point 009 is chosen to be the weakest.
DKM008 vs DKM010 (Figure 35)
Same as in the previous analysis, both points are very similar and both can be considered quite weak. Nevertheless, point 008 still presents a very high peak in friction ratio, and with very low values of cone resistance at around -9m NAP. Point 008 is clearly stronger in the first meters, as point 010 presents very low values of cone resistance, however its value for friction ratio is not as high. Therefore, for these reasons point 008 is again considered weaker.
DKM008 vs DKM013 (Figure 36)
For this case, the same situation arises where in the first meters, point 008 is stronger than point 013. However, from there on, the stronger soil tends towards point 013. For example, at around depth -9m NAP, point 013 shows a

stronger tendency, by having high values of Qc and low values of Rf, whereas point 008 shows the contrary, making it the weaker soil. This tendency follows the entire depth, until one point around -22.5 m NAP where clearly point 013 is weaker and 008 stronger. Overall, it is considered that 008 is weaker than 013.

DKM008 vs DKM017 (Figure 37)

For this situation, in the first 10 meters from 5 to -5 m NAP, point 008 is stronger than point 017. However, from there on, point 008 becomes very weak, as it has very low cone resistance and very high friction ration. The strength of 017 also decreases but not as much as 008. From -15 m to -20 m NAP, point 017 is has stronger cone resistance than point 008, however the differences in friction ratio are negligeable. Both points are very similar, however overall it will be judged that 008 is weaker. Also, because when comparing 017 with 009 and 0010, 017 would be considered stronger.

DKM008 vs DKM020 (Figure 38)

For this comparison, it can be observed that even though graphs overlap at some points, the values of Qc of 020 never reach as low as the values from 008 do. Moreover, the Qc values from 008 never reach as high as the values from 020. Furthermore, around height -6 to -9m NAP, point 008 presents high values of Rf, and these values are also never reached by point 020. Therefore, point DKM 008 is considered the weakest.

DKM008 vs DKM022 (Figure 39)

All along the depth both points present a lot of inconsistencies. Therefore, judging which points was weaker was not as evident. In the depth from 0 to -5 m NAP approx., it can be observed that point 008 is stronger. From that point on, point 008 becomes very weak and its cone resistance gets very low values and its friction ratio very high values. Next, from depth -10 until -15 m NAP, point 008 seems to be stronger as it presents higher values of cone resistance, and lower friction ratio values. At depth -16 until 18 m NAP, point 022 presents higher values for the cone resistance. At depth around -20 m NAP, both points are equally weak. However, from then on, point 022 is stronger.

DKM008 vs DKM025 (Figure 40)

As in the previous cases, the first 10 meters (5 to -5) show that point 008 is stronger. Nevertheless, then point 008 is very weak from -7 to -9 meters and point 025 has very high cone resistance around -15 to -20. From -20 to -25 both are quite weak, however point 008 shows high values of Rf, making it weaker. The final decision is based on the very high peaks of Rf for 008 around -8m NAP and the very high peaks of Qc for 025 around -16m NAP, which is where the big differences take place.

DKM008 vs DKM027 (Figure 41)

The same reasons explained previously for selecting the weaker point apply here as well. Point 008 has very high peaks of Rf around -8m NAP, and point 027 has a very high cone resistance around -16 m NAP. Furthermore, the locations where point 008 is stronger, the difference is not enormous, as in depth -8 and -16. Moreover, around -20 meters point 027 has a very high values for the friction ration, however both points are very weak at that point and point 008 has almost as high values for its Rf than 027. Therefore point 008 is chosen to be the weakest.

b) Cone resistance

Based on the cone resistance heatmap (see Figure 42), the conclusion is the same: point DKM008 is the weakest point.

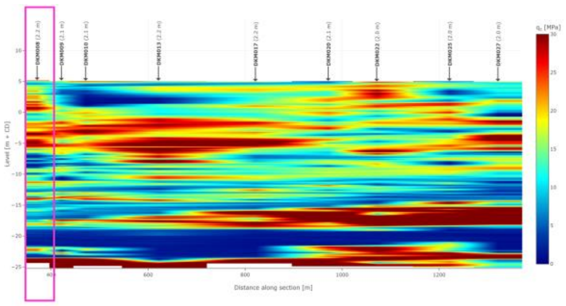

Figure 42: heatmap cone resistance

4. Comparison

Section 2 is the most important section of this project, as it is where the CPT points are closer to the quay wall. Therefore the idea is to translate the chosen weak points of section 1 and 3 onto points of section 2, that are at the same location. As can be seen on Figure 43, points are already in the same section of the quay wall's length, under a span of around 80-100 meters. Therefore, point 61 which is the selected point of section 1 will be translated to section 2 as point 13. Point DKM008 will be translated as point 12 in section 2. The idea now is to compare this transition to see if the transition can actually be assumed, or both points are very different.

Figure 43: points selected per section

61 and 13 (Figure 44)

By looking at the graphs and values from Rf and Qc, and the soil visualization, it can be observed that both points are quite similar. Some differences exist for example in the first 5 meters, where point 61 has a clear stronger cone resistance. However, in both cases, that layer corresponds to sand. Therefore it is considered that this transition can be made, and for now on point 13 will be considered as a weak point to be analyzed.

DKM008 and 12 (Figure 45)

Based on the graph, it can be observed that some points are not aligned such as in heigh -11 m NAP, where clearly point 008 has a higher cone resistance than point 12. Nevertheless, their friction ratio values are very similar therefore that difference will not be considered that important. Nevertheless, there is also a point at depth -6 m NAP where the opposite happens, 12 has a higher cone resistance than 008. And this time, also the friction ratio is importantly higher for the point 008. Therefore that is a discrepancy. Nevertheless, the pattern seems to be more or less the same for both and therefore is considered that the transition to point 12 can be done.

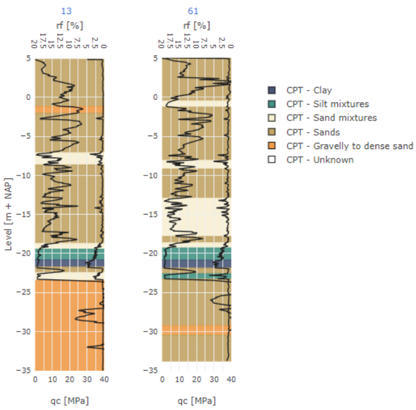

Figure 44: soil layering comparison 61 and 13

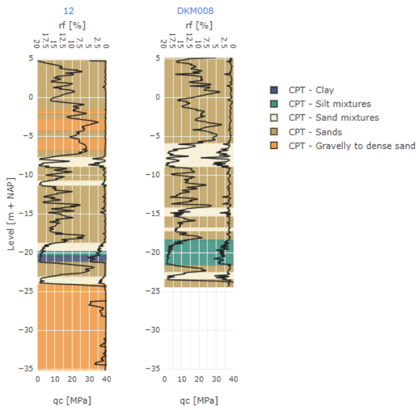

Figure 45: soil layering comparison DKM008 and 12

The main goal is to find the weaker point, and to do so the chosen points 12, 13, 16 will be compared as well as the point DKM051 which was the selected point in the geotechnical design based off the data from 2021, and from the preliminary design for phase B [27] (see section XIV.A). Also the layering of these points is visualized in Figure 46 where it can be seen that they all present a clear clay later at around depth -20mNAP, which can be unfavorable especially as it can contribute to the overturning on the wall. Furthermore, they all present inconsistencies along the stratigraphy as well.

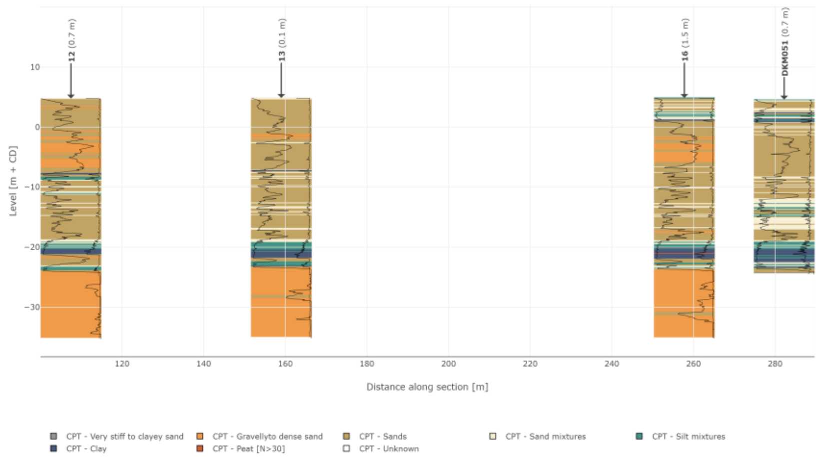

Figure 46: visualization points 12,13,16,DKM051

B. Triaxial Tests

The triaxial tests are a geotechnical laboratory analysis carried out in order to assess the shear strength and the stiffness of the soil. This test involves controlled drainage of soils and the measurement of pore water pressures. The main parameters that are obtained from these tests are the angle of friction or angle of shearing resistance (ϕ′), the cohesion (c′) , the undrained shear strength (cu), the shear stiffness (G), the compression index, the permeability constant of the soil (k). Figure 47 shows an application of the triaxial test, where triaxial compression will assess the strength at the top of a slope, and the triaxial extension will determine the strength at the base of the slope.
Moreover, the procedure of a triaxial test involves placing a cylindrical soil sample into a pressurized cell. This soil sample is then enclosed in a rubber membrane, from which the soil will be subjected to shearing, similar to real life conditions in order to observe its response and its failure. This shearing process involves axial loading, typically in compression. Figure 48 shows the setup of a triaxial test setup [19].

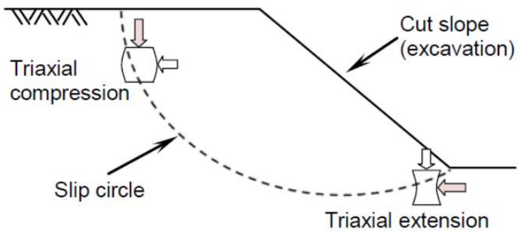

Figure 47: example of application of triaxial test [19]

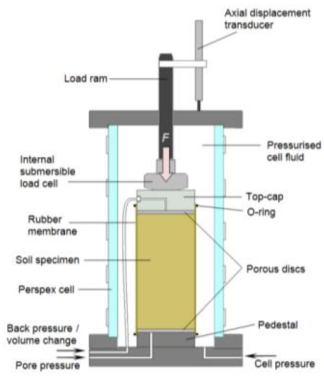

Figure 48: Set Up of a Triaxial Test [19]

The three primary triaxial tests conducted in the laboratory are:

- The Unconsolidated Undrained (UU) test: is the simplest and quickest test which assess the undrained shear strength (cu) under controlled total stresses. It is the preferred test for short-term evaluations, especially for cohesive soils.
- The Consolidated Drained (CD) test: describes long-term loading responses. It determines strength parameters (ϕ′ and c′) under effective stresses. The test takes longer for cohesive soils due to slow shear rates. For this study, this test was used.
- The Consolidated Undrained (CU) test: is the most common, which allows to determine the strength parameters (ϕ′ and c′) based on effective stresses while allowing faster shearing compared to the CD test. It is achieved by monitoring excess pore pressure changes during shearing.

Figure 49 shows the different stresses applied to the soil in a triaxial compression test. First of all, σc is the confining stress, which is induced by pressurizing the fluid on the cell that surrounds the soil. This stress is equal to the radial stress σr, or minor principal stress σ3. Next, the deviator stress, q, comes from applying axial strain (EA) to the soil, acting in the axial direction, where the axial stress (σa) acts, also referred as the major principal stress (σ1).

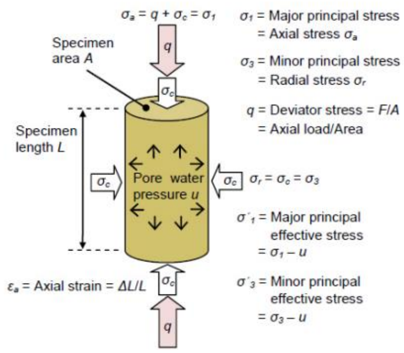

Figure 49: Specimen stress state during triaxial compression [19]

Moreover, during the shear stage, the soil's response is recorded by plotting q (deviator stress) or the effective principal stress ratio (σ′1/σ′3) against the axial strain (εa). The analysis continues until a failure is met, which can be when the deviator stresses reaches a peak, when there is a peak in the effective principal stress ration, or reaching a specific axial strain value. For this case, the failure criteria is found when the axial stress ratio reaches a value of 5%. At that value the orientation of the failure plan is estimated by finding the value for the friction angle (ϕ′).

1. Soil Boring

To analyze the soil in the laboratory, soil borings are carried out to collect soil samples. Soil boring is defined as the drilling into the ground to extract soil and other bedrock samples, in order to analyze the soil properties. Soil boring is ideal for initial soil investigations in construction projects, as it is cost-effective, and quite simple. It is also used as a verification to the CPTs to make sure the type of soil detected by the CPTs is true. Whereas the borings are more simple, the CPTs are usually preferred as they give more detailed soil investigations with bigger accuracy. The CPTs also give a continuous soil profile, whereas boring tests are done per intervals. The CPTs require more experience and expertise to analyze them, than the standard soil boring tests.

In this specific case, CPTs and borings were carried out. Multiple samples were extracted along the quay wall's length, at four CPT points: 5, 16, 28, and 40. The borings go up to -35 m NAP, and the samples are taken in ½ meter intervals, and through lab analysis, the soil density and water content at specific depths is determined more precisely, see Table 2. For the translation of the material names see Appendix XIX.A.

The idea is to get more accurate values and specific to this case, rather than using standard values which will tend to be less precise, and are taken from the table 2b from NEN 9997-1 [14] (see Table 1). Moreover, the laboratory tests were carried out by the company Van der Straaten Geotechniek B.V. [28].

2. Water Content

The water content of a soil, refers to the proportion of the water that is present in comparison to the total soil mass. It is an important parameter when analyzing the soil, as it has an influence on how the soil behaves, and therefore on its strength as well. As can be observed in the Table 2, every material has a different density and water content as well. Therefore this has an impact on the density saturated and unsaturated. The density that will be of importance will therefore be the volume weight (100% saturated).

3. Densities

As it can also be observed on the results from the triaxial tests, the clay has the highest water content which has a direct impact on its volume weight, which has a smaller value in comparison to the standard values for the Netherlands. Nevertheless, as can be observed by the standard values for clay have the same value for saturated and unsaturated densities.

4. Cone Resistance

Moreover, the cone resistance for each depth of the in situ tests is also determined for each depth for the respective boring points, based on the CPT data. This allows to get a deeper understanding of the soil, by analyzing how the soil is compacted and its strength. The borings determine the type of materials by the grain size, and the cone resistance determines its strength as well as how the soil is packed. Furthermore, the cone resistance is what will allow to separate the different tests into lose, moderate or densely packed sand from which the strength parameters (angle of friction and cohesion) will be found. The assumption is that every that samples which have a value of cone resistance below 15 are considered lose sand, between 15 and 25 are moderate sand, and above 25 are dense sand.

5. Triaxial Tests Interpretation

In order to get the most complete answer all of the data from the borings from points 5,16,28 and 40 will be analyzed. The principal stresses for each test will be found for each point for an assumed value of axial strain of 5%. The analysis is carried out by doing three tests per point, which are each obtained after an increase in pressure.

a) Division based on material description

The test to find the strength parameters is individually carried out for lose, moderate and dense sand, by performing a regression analysis, and a confidence interval of the line of best fit for all the tests that belong to each category of sand.

First, the different tests are divided into the three types of sand, based on their cone resistance value (obtained from the CPT data) and based on table 2-b of NEN 9997-1 as can be seen in Table 1. It is important to mention that triaxial tests are not performed on clay samples, which are therefore left blank in Table 2.

Next, the data that is used per analysis, are the values of S and T given by the triaxial tests, which are the center and the radius of the Mohr circle respectively, taken at a value of 5% of axial strain. For every point, at 5% EA, there are three tests that were performed, each time by increasing the pressure. Therefore, by test there are three values of S and three values of T, which are going to be part of the data set of either lose, moderate of dense sand, and will give the strength parameters (φ and c). These differences can be seen in Table 3 , and they are obtained by doing a regression analysis with a confidence interval of 95% of the line of best fit [20]. The confidence interval for a predicted y value for a given value of independent variable is calculated using equation (16), where:

$$\pm t\,(\alpha, df) S_{yx} \sqrt{\frac{1}{n} + \frac{(x_i - \bar{x})^2}{\sum_{i-1}^{n}(x_i - \bar{x})^2}} \tag{16}$$

- t = critical t statistic
- S = standard error of estimate
- xi = given value
- x̄ = average of x values
- n = number of observations

For the translation of the material names see Appendix XIX.A.

Table 2: soil borings triaxial tests

Sample	NAP	Cone Resistance Qc (MPa)	Material (based on triaxial tests)	Material description (based on Qc and CPT)
B005 A1-S6	-0.24	10.02	Zand fijn 150-200, matig	Zand Schoon Los
B005 A2-S6	-5.24	20.3	Zand fijn 105-150	Zand Schoon Matig
B005 Z8 ZA	-11.79	11.21	Zand fijn 105-150	Zand Schoon Matig
B005 Z12 ZA			Veen Vast	Klei Zwak zandig
B005 Z14 ZA	-25.79	25	Zand middelgrof 200-300	Zand Schoon Vast
B016 A1-S6	2.77	4.9	Zand fijn 105-150	Zand Schoon Los
B016 A2-S6	-3.63	29.2	Zand fijn 150-200	Zand Schoon Vast
B016 A3-S6	-11.48	19.06	Zand fijn 105-150	Zand Schoon Matig
B016 A4-S6			Klei, stijf, zwak organisch	Klei Schoon Matig
B016 A5-S6	-26.63	33.6	Zand fijn 150-200, kleiig	Zand Schoon Vast
B028 A1-S6	-2.26	21.4	Zand fijn 150-200	Zand Schoon Matig
B028 A2-S6	-12.06	13.5	Zand fijn 63-105, brokken klei	Zand schoon Matig
B028 A3-S6	-17.06	36.1	Zand fijn 150-200, brokken klei	Zand Schoon Vast
B028 A4-S6			Klei, stijf	Klei Schoon Vast

B028 A5-S6	-24.76	46.96	Zand middelgrof 200-300	Zand Schoon Vast
B040 A1-S6	2.03	2.27	Zand fijn, 150-200	Zand Schoon Los
B040 A2-S6	-4.77	19.96	Zand fijn 150-200	Zand Schoon Matig
B040 A3-S6	-11.77	2.16	Zand fijn 63-105	Zand Schoon Los
B040 A4-S6	-14.67	10.86	Zand fijn 150-200	Zand Schoon Matig
B040 A5-S6		2.27	Zand fijn 105-150	Zand Schoon Vast

Table 3: s,t values for 5%EA

ZAND SCHOON LOS	**s**	**t**
B005 A1-S6	164.8	114.5
	304.4	204.1
	483.9	333.6
B005 Z8 ZA	142.9	92.7
	291.2	191
	394	243.8
B016 A1-S6	164.8	114.5
	304.4	204.1
	483.9	333.6
B028 A2-S6	162.4	112
	366.7	266.4
	451	300.7
B040 A1-S6	152.8	102.5
	272.5	172.3
	411.3	261.1
B040 A3-S6	185.1	134.7
	273.3	173.3
	499.6	349.3
B040 A4-S6	160.5	110.3
	275	174.8
	482.2	332.1
ZAND SCHOON MATIG	s	t
B005 A2-S6	192.5	142
	342	241.7
	459.5	309.2
B016 A3-S6	180.5	129.9
	287.7	187.4
	417.1	267
B028 A1-S6	163.4	113.1
	320.3	220.1
	467.6	317.3
B040 A2-S6	139	88.8
	284.2	184
	414.7	264.5
ZAND SCHOON VAST	s	t
B005 Z14 ZA	156.2	105.9
	274.9	174.7
	409.6	259.4
B016 A2-S6	130.3	80.2
	208.2	108.2
	482.9	332.7

B016 A5-S6	140.1	89.8
	266.4	166.2
	406.7	256.7
B028 A3-S6	152	101.8
	336.1	235.8
	371	220.8
B028 A5-S6	152.9	102.6
	301.4	201.2
	432.9	282.6

As can be seen on the visualization of the results (see Figure 50) and based on the numerical values obtained for phi and c for all the types of sand (see Figure 51, Figure 52, Figure 53), it can be concluded that the results are not very accurate. There are multiple reasons for it. The first reason is that the angles of friction have very high values in comparison with the preliminary design phase B and with literature, especially for lose and moderate sand. Furthermore, it can also be observed that the values for each type of sand are very similar, even though their Qc values are clearly different. Lastly, it can be observed that there is a tendency of material strength such that : lose sand> moderate sand > dense sand. This conclusion is therefore neither reliable nor determinative. The soil company which conducted the tests obtained the same results especially for the friction angle, phi. In consequence, they were contacted to provide further elaboration on the findings.
To elaborate the analysis, it was decided to also conduct an analysis to divide the samples based on their densities and based on their relative densities to evaluate if the results were more conclusive.

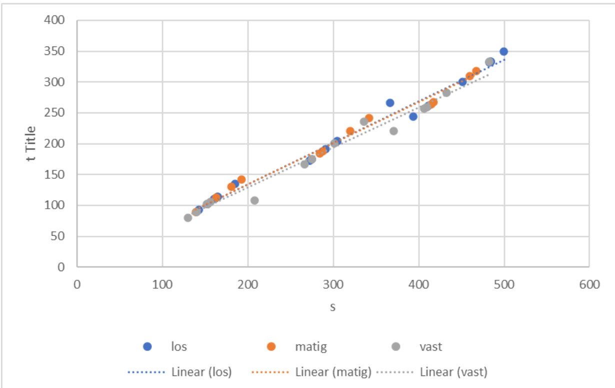

Figure 50: visualization results based on material description

	95%		trend-gemiddelde	
b	0.6585955	-	0.673678791	-
φ'	41.192847	o	42.35163463	o
a	0	kPa	0	kPa
c'	0	kPa	0	kPa

Figure 51: results lose sand

	95%		trend-gemiddelde	
b	0.6502311	-	0.668872959	-
φ'	40.559024	o	41.98013873	o
a	0	kPa	0	kPa
c'	0	kPa	0	kPa

Figure 52: results moderate sand

	95%		trend-gemiddelde	
b	0.6230086	-	0.647010458	-
φ'	38.536176	o	40.31658059	o
a	0	kPa	0	kPa
c'	0	kPa	0	kPa

Figure 53: results dense sand

b) Division based on densities

Another way of separating the material types can be done through their densities. Therefore an analysis was also carried out by separating the densities into three cases, which gave the following results (see Figure 54):

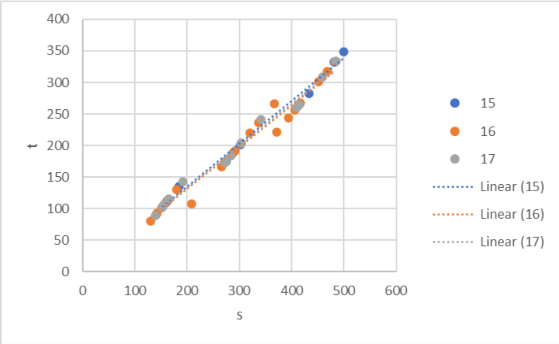

Figure 54: visualization results based on density (dry)

	95%		trend-gemiddelde	
b	0.657731	-	0.675684178	-
φ'	41.12708	o	42.50730314	o
a	0	kPa	0	kPa
c'	0	kPa	0	kPa

Figure 55: 15 < γ < 16

	95%		trend-gemiddelde	
b	0.638542	-	0.658946815	-
φ'	39.6832	o	41.21960027	o
a	0	kPa	0	kPa
c'	0	kPa	0	kPa

Figure 56: 16 < γ < 17

	95%		trend-gemiddelde	
b	0.65074	-	0.666104047	-
φ'	40.59744	o	41.76708071	o
a	0	kPa	0	kPa
c'	0	kPa	0	kPa

Figure 57: 17 < γ < 18

Once again, the results are not conclusive on their own. The main reason for this is that the analysis does not account for the full spectrum of material properties and density, therefore only knowing the density does not give any indication whether the materials are sand lose, moderate or dense. Moreover, the same pattern is observed here such that the values are very similar for all ranges of densities, which is not very logical (see Figure 55, Figure 56, Figure 57).

Therefore, to address this limitations, it is essential to conduct the analysis based on the relative densities.

c) Division based on relative density

After doing the separation of the samples based on the cone resistance, and on the densities, they are now going to be analyzed based on the relative density. The logic behind this is as based on the previous results, it seems that the soil is packed and there is no big difference in lose, moderate and dense sand. Therefore the idea is to scale them based on their relative densities. The relative density will be calculated with the following formula (see equation (17)):

$$D_r = \frac{\gamma_d - \gamma_{min}}{\gamma_{max} - \gamma_{min}} * 100\% \tag{17}$$

Where the minimum and maximum densities are taken from the soil investigation from phase A, as these values were not available on the triaxial tests of phase B. Besides, the minimum and maximum values are given for each test and sample, however an estimation will be done in this case by taking the average of the minimum and the maximum, which will be the lower and upper boundaries of the range. Therefore $\gamma\_min = 13.461$ and $\gamma\_max = 17.9$.

It is important to mention that the fact that the minimum and maximum values for gamma are taken from phase A, and not from the triaxial tests from phase B, makes the comparison unreliable. Nevertheless, it is a check to find where the samples lie when compared to phase A.

This analysis is done as for example in coarse grained soils, depending on the size, shape or gradation of the soil's grains, coarse soils can exist in two extremes states of compaction: from the loosest to the most dense. Therefore the relative density is used as an index which allows to compare the two extremes to any intermediate compaction state of the material. More specifically, what this ratio determines is the ratio of the actual decrease in the volume of voids, to the maximum possible decrease in void volume, which designates how much more can the material be compacted beyond its natural state. Based on Figure 58 the soil's compactness is determined based on the relative density.

And as can be seen on Table 4, the results of the relative density calculated are quite compacted, such that they go from medium to very dense, showing no clear distinction between lose, moderate and dense sand. The conclusion of this check is that the relative density of the samples in phase B are most likely moderate to dense in packing, compared to the samples obtained from phase A. The samples from phase B were tested with a high relatively density (so there is no loose sand in the samples). Which is probably also why the phi values are relatively high.

Table 4: relative densities

boring	Relative density	soil compactness
B040 A3-S6	54.9436796	medium
B040 A4-S6	57.19649562	medium

B005 Z8 ZA	59.44931164	medium
B016 A3-S6	66.2077597	dense
B028 A3-S6	68.46057572	dense
B016 A2-S6	75.21902378	dense
B028 A2-S6	77.4718398	dense
B005 A2-S6	81.97747184	dense
B005 Z14 ZA	81.97747184	dense
B016 A5-S6	81.97747184	dense
B028 A5-S6	81.97747184	dense
B040 A1-S6	84.23028786	dense
B040 A2-S6	84.23028786	dense
B016 A1-S6	86.48310388	very dense
B028 A1-S6	95.49436796	very dense
B005 A1-S6	100	very dense

Figure 58: soil's compactness based on relative density [1]

6. Final values for phi and c

To conclude this analysis, the results were overall considered unreliable. The first reason for this is that in almost every case, the lose material has the highest angle of friction, which in theory does not make sense. Also, in parallel the coarse material presents the lowest angle of friction which supports this inconsistency. Moreover, the second reason is that in any case the values for the angles of friction are considered to be extremely high especially for the lose material, which again supports this unreliability. Having values around 40 degrees is not what neither literature nor expert opinions support. Furthermore, the only values that could be more reliable are for the moderate and dense sand.

Following these unreliable findings, the company responsible for submitting the triaxial tests was asked about the legitimacy of the results, and their answer was that "The tests were carried out under the same packing, but with increasing consolidation stress. Loose, moderate and firm do not apply to this project". This statement therefore explains why the different samples had both very high friction angles, and no clear separation between lose, moderate and dense sand, as all the samples were put into the tri-axial tests with the same relative density.

It is also important to mention that at the moment the phi values obtained from the triaxial tests will then have to be multiplied by the (9/8) conform NEN 9997 [14], which will result in even higher results especially for lose sand. However, this rule is under revision at the moment, the discussion section XVI explains this in more detail.

Therefore, from this on the values taken for the angle of friction and for the cohesion will be taken from phase A and from preliminary phase B (see table Table 7).

7. Stiffness Parameters

As explained in section VII.F.2.a), the model used in PLAXIS is the hardening soil model. Therefore, the following stiffnesses need to be found: E_{50}^{ref} , E_{oed}^{ref} , E_{ur}^{ref}. The : E_{50}^{ref} is the secant stiffness in a standard drained triaxial test. Next, E_{oed}^{ref} is the tangent stiffness of a primary oedometer loading, and finally E_{ur}^{ref} is the unloading/ reloading stiffness (see Figure 10).

E_{50}^{ref} is determined by using the triaxial tests, and E_{oed}^{ref} , E_{ur}^{ref} are determined based on empirical correlations with the cone resistance measurements. Furthermore, the stiffness parameters for clay layers are determined on expert judgement, by using Qc. The following empirical relations are used:

Sand:

- $E_{oed}^{ref} = E_{50}^{ref}$
- $E_{ur}^{ref} = 3 \cdot E_{oed}^{ref}$

Clay:

- $E_{oed}^{ref} = 3*Qc$
- $E_{50}^{ref} = 1.5 * E_{oed}^{ref}$
- $E_{ur}^{ref} = E_{50}^{ref}$

8. Stiffness for sand

The values for the three stiffnesses for sand are based on the values found already for phase A and also used in preliminary phase B, which are taken form the triaxial tests performed in that area. It is assumed that the distances between both areas is relatively small, therefore the values can be extrapolated to phase B as well. The values of E_{50}^{ref} is given as follows for each material type, from which the rest of the stiffnesses are calculated in Table 5.

Table 5: E50ref stiffness for sand

Material Type	E_{50}^{ref}
Zand Schoon Los	20 500
Zand Schoon Matig	41 100
Zand Schoon Vast	75 500
Zand, Kleiig	15 000

9. Stiffness for clay

The values for the different material types of clay will also be compared with the already found values of phase A and of preliminary phase B. However, first a calculation with the cone resistance values is carried out to find more accurate values for this area, and also as a way of verifying the values. Moreover, the values of Qc are taken from the Table 1. The final values are found in Table 6.

Table 6: Eoedref stiffness for clay

Material Type	Qc (approx.)	E_{oed}^{ref}
Klei Zwak Zandig matig	2	6000
Klei Schoon Matig	1.5	4500
Klei Zwak Zandig Slap	1	3000

10. Power function

The power function m is a model parameter for the Hardening Soil model in PLAXIS. In accordance with CUR 2003 [6] m=0.55 is used for sand and m=0.8 for clay.

11. Poisson ratio

For the unloading-reloading Poisson ratio v_ur, the default value of PLAXIS has been used: ν_{ur}=0.2.

12. Wall friction angle

A value of 0.8 has been used for the wall friction angle R_inter, valid for combination walls. For a detailed explanation, please refer to the Quay Walls Handbook [9].

13. Final Values

Table 7 shows the final values for the strength parameters, in terms of characteristic values, so by taking the 95th percentile (see section XIII for further explanation). Furthermore, the values phi and c were calculated with Excel sheets provided by the company Witteveen+Bos for sand lose, moderate and dense, and for moderate clay, and can be found in the appendix section XIX.B.

Table 7: Final values

Material	$\gamma_{unsaturated}$ [kN/m^3]	$\gamma_{saturated}$ [kN/m^3]	c'characteristic [kN/m2]	φ'characteristic [°]	OCR	E_{50}^{ref} [kPa]	E_{oed}^{ref} [kPa]	E_{ur}^{ref} [kPa]	m [-]
Zand Schoon Los (lose sand)	17	19	0	33.7	1	20 500	20 500	61 500	0.55
Zand Schoon Matig (moderate sand)	18	20	0	39.8	1	41 100	41 100	123 300	0.55

Zand Schoon Vast (Pleistocene Zand) (dense sand)	19	21	0	38.9	1.3	75 500	75 500	226 500	0.55
Klei Zwak Zandig matig (moderate sandy clay)	18	18	3	22.5	1	6 000	4 000	18 000	0.8
Klei Schoon Matig (moderate clay)	17	17	5	26.8	1.3	4 500	3 000	14 000	0.8
Klei Zwak Zandig Slap (dense clay)	14	14	1.5	22.5	1	3 000	2 000	9 000	0.8

X. Quay Wall Design Specifications

In the following section the strength parameters regarding the combi wall and its components will be calculated. Some values are already given (see Table 8). The final results are summarized in Table 10.

A. Strength parameters

This section covers the determination of the strength parameters regarding the combined wall, the tube pipe, the anchor and the grout body. These parameters will then be injected into the PLAXIS model. The main three parameters that need to be found are the weight (w) in kg/m2, the axial stiffness EA in kN/m, and the bending stiffness EI in kNm2/m. As can be observed the different parameters are per unit length, so they will be divided by the system's width, which is calculated in section X.C.1. Furthermore, the combined wall concerning the tube pipe and the sheet pile will go from +5.5m NAP to -13.35m NAP, and from there only the tube pile will go until -27,5 NAP. (this is visualized in the cross section of the wall in Figure 59). Therefore the strength parameters are calculated for the tube only and for both the tube with the sheet pile.

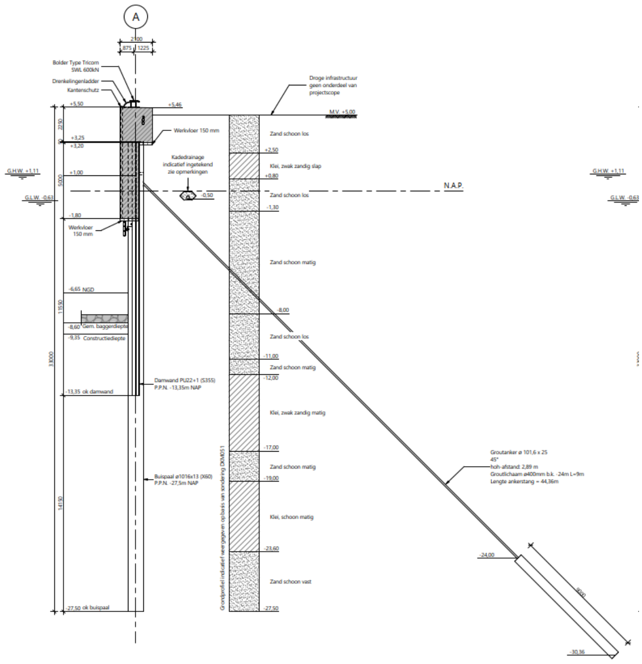

Figure 59: Cross section quay wall

B. Geometry of combined wall

As just introduced, the quay wall consists of a combined wall, which has both a tube pile and three sheet piles, that interconnect the tubes. A top view visualization can be seen in Figure 60. More specifically, the dimensions of the combi wall will be taken from the preliminary design [27]. The tubes will have a thickness of 13 mm and a diameter of 1016 mm. Moreover, the three sheet piles, are connected by interlocks. The type of sheet pile based on the preliminary design is PU 22+1. Moreover, Table 8 shows the given uncorroded geometric properties of the tube, the strength parameters of the sheet pile and other material properties of steel. Furthermore, the A and I for the tube are calculated in the following sections, whereas for the type of sheet pile they are given.

Figure 60: top view combi wall + locks sheet pile

Table 8: geometric and strength parameters

Tube	Symbol	Value
Outer diameter	Do	1016 mm
Inner diameter	Di	990 mm
Wall thickness	t	13 mm
Sheet Pile		
Type	Z/U	U
Sectional Area	A	192 cm^2/m
Moment of Inertia	I	52510 cm^4/m
Width single sheet pile element	w	600 mm
Height sheet pile element	h	450 mm
Angle web	α	62.4°
Properties of Steel		
E-modulus	E	$2.1 * 10^8$ kN/m^2
Unit Weight	γ_{steel}	7850 kg/m^3

C. Calculations for tubular pipe and combined wall

As the combined wall is made of the combination of the tube pile and the sheet pile, first the values will be given separately for both and then will be summed to get the total for which the tube and the sheet pile act together, from +5.5m NAP to -13.35m NAP. Furthermore, in PLAXIS the values should be introduced per unit length, therefore the values obtained will be then be divided by the system width.

1. System's width

The first parameter that is calculated is the system width, denoted as $x_{c.t.c}$. This parameter is calculated by summing the diameter of the tube, the width of the 3 sheet piles and the length of the locks as seen in equation (18) :

(18)

$$x_{c.t.c} = D + n.sheet\ piles * width\ sheet\ pile + length\ of\ the\ locks$$
$$= 1016 + 3 * 600 + 75 = 2891\ mm$$
$$x_{c.t.c} = 2.891\ (m)$$

2. Moment of inertia of the tubular pipe

Furthermore, the next parameter calculated is the moment of inertia of both the tube and the sheet pile. The moment of inertia of the sheet pile is given and has a value of $I_{s.p}$ = 52510 cm^4/m. The moment of inertia of the tube

I_{tube} is calculated by using the standard formula for a circle that is hollow (Figure 61) and where the inner diameter is considered (see equation (19)):

$$I_{tube} = \frac{\pi((D_o)^4 - (D_i)^4)}{64} = \frac{\pi((D_o)^4 - (D_o - 2 * t)^4)}{64} \tag{19}$$

$$I_{tube} = \frac{\pi\,(1016^4 - (1016 - 2 * 13)^4)}{64}$$

$$I_{tube} = 5.152 * 10^9\ (mm^4)$$

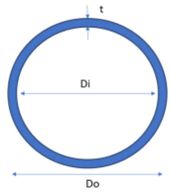

Figure 61: cross section hollow circle

a) Moment of Inertia of the tube (per unit length)

As previously calculated the moment of inertia of the tube is equal to I_{tube}= 5.152*10⁹ (mm⁴). The moment of inertia per unit length is calculated in equation (20) by dividing the moment of inertia it by the system's width.

$$I_{tube\,(u.l)} = \frac{I_{tube}}{x_{c.t.c}} = \frac{5.152 * 10^9\ mm^4}{2.891\ m} \tag{20}$$

$$I_{tube\,(u.l)} = 1.782 * 10^9\ (\frac{mm^4}{m})$$

b) Moment of Inertia of the combined wall (per unit length)

This value is obtained by summing the moment of inertia from the tube and from the sheet piles. Also the units are adapted so that the final result is given in mm^4 / m when also dividing by the system width (see equation (21)).

$$I_{c.w} = \frac{I_{tube} + I_{s.p}}{x_{c.t.c}} \tag{21}$$

$$I_{c.w} = \frac{5.152 * 10^9 + 3 * \frac{52510}{10000} * \frac{600}{1000}}{2.891}$$

$$I_{c.w} = 2.109 * 10^9\ (\frac{mm^4}{m})$$

3. Cross sectional area of the tubular pipe

The cross sectional area of the sheet pile is given based on the type of sheet pile, in this case PU 22+1, which has a value of 192 cm^2 /m [2]. The cross sectional area of the tube pile is calculated by using the equation of the area of a circle (see equation (22)):

$$A_{tube} = \pi R^2 = \pi\,(\left(\frac{D_o}{2}\right)^2 - \left(\frac{D_i}{2}\right)^2) \tag{22}$$

$$A_{tube} = \pi(\,(\frac{D_o}{2})^2 - \left(\frac{D_o - 2 * t}{2}\right)^2)$$

$$A_{tube} = \pi(\left(\frac{1016}{2}\right)^2 - \left(\frac{1016 - 2 * 13}{2}\right)^2)$$

$$A_{tube} = 4.096 * 10^4\ (mm^2)$$

a) Cross sectional area of tube (per unit length)

The cross sectional area of the tube is divided by the system's width as well, to obtain the value per unit length (see equation (23)).

$$A_{tube\,(u.l)} = \frac{A_{tube}}{x_{c.t.c}} = \frac{4.096 * 10^4\ mm^2}{2.891\ m} \tag{23}$$

$$A_{tube\,(u.l)} = 1.417 * 10^4\ (\frac{mm^2}{m})$$

b) Cross sectional area of combined wall (per unit length)

To calculate the cross sectional area of the combined wall, the sum of cross sectional area of the tube pile and of the sheet pile is calculated. Also the units are adapted, and the area is divided by the system's width, so that the final units are mm^2/m (see equation (24)).

$$A_{c.w} = \frac{A_{tube} + A_{s.p\,(total)}}{x_{c.t.c}} \tag{24}$$
$$A_{s.p\,(total)} = A_{s.p} * width * n.sheet\ piles$$
$$A_{c.w} = \frac{4.096 * 10^4 + 3 * \frac{192}{100} * \frac{600}{1000}}{2.891}$$
$$A_{c.w} = 2.612 * 10^4 \left(\frac{mm^2}{m}\right)$$

4. Weight of the tubular pipe

The weight per meter of pile and per meter of combined wall also needs to be calculated. This is done by multiplying the cross sectional area of the tube and of the combined wall, by the unit weight of their material. And as they are both made from steel, they will be multiplied by 7850 kg/m^3 , which is the unit weight of steel (see equation (25)).

$$w_{tube} = A_{tube} * \gamma_{steel} \tag{25}$$
$$w_{tube} = \frac{4.096 * 10^4}{10^6} * 7850$$
$$w_{tube} = 321.6 \left(\frac{kg}{m}\right)$$

a) *Weight of combined wall (per unit length)*

The same logic is followed to follow the weight, which is dividing the cross sectional area of the combined wall by the unit weight of steel. The units are also adapted so that the final units are kg/m^2 (see equation (26)).

$$w_{c.w} = A_{c.w} * \gamma_{steel} = \frac{2.612 * 10^4}{10^6} * 7850 \tag{26}$$
$$w_{c.w} = 205.1\left(\frac{kg}{m^2}\right)$$

5. Axial Stiffness of the tubular pipe

The axial stiffness of the tube per unit length is calculated in the following equation (27) :

$$EA_{tube} = E_{steel} * A_{tube(u.l)} = 2.1 * 10^8 * \frac{1.417 * 10^4}{10^6} \tag{27}$$
$$EA_{tube} = 2.976 * 10^6 \left(\frac{kN}{m}\right)$$

6. Axial Stiffness Combi Wall

The combi wall is made out of steel, therefore its axial stiffness per unit length is calculated in equation (28):

$$EA_{c.w} = E_{steel} * A_{c.w} = 2.1 * 10^8 * \frac{2.612 * 10^4}{10^6} \tag{28}$$
$$EA_{c.w} = 5.486 * 10^6 \left(\frac{kN}{m}\right)$$

7. Bending Stiffness Combi Wall

The bending stiffness for the combi wall is then calculated in equation (29):

$$EI_{c.w} = E_{steel} * I_{c.w} = 2.1 * 10^8 * \frac{2.109 * 10^9}{10^{12}} = 4.429 * 10^5 \left(\frac{kNm^2}{m}\right) \tag{29}$$

D. Calculations for anchor and grout body

For this quay wall, an anchor is placed in every tube, connected to a grout body which is placed into the Pleistocene sand. The strength parameters of these structures also need to be calculated, so that they can be used in the PLAXIS model. The main parameters that need to be found for the anchor are the axial stiffness EA and the spacing between each anchor. In this case as the anchors are placed per tube, the spacing between each anchor will be the system's width. Furthermore, for the grout body, the parameters that need to be found are its unit weight, its diameter and the spacing as well. Besides, the is made of steel, and the grout body is made of concrete. Table 9 shows the different parameters for the anchor and the grout body.

Table 9: given + final parameters anchor and grout body

	Symbol	**Value**
Anchor		
Outer diameter	Do	101.6 mm
Inner diameter	Di	45.6 mm
Wall thickness	t	28 mm
E modulus	E	$2.1 * 10^8$ kN/m²
Cross sectional area	A_{anchor}	$6.47 * 10^3\ \mathrm{mm}^2$
Axial stiffness	EA_{anchor}	$1.35 * 10^6\ kN$
Grout Body		
Diameter	D	400 mm
Cross sectional area	A_{grout}	$1.25 * 10^5\ \mathrm{mm}^2$
E modulus	E	$1.08 * 10^7\ \frac{kN}{m^2}$ *Assumption: The given E resembles an equivalent E-modulus, such that EA_grout = EA_steel, i.e. E = EA_steel / A_grout*
Unit weight	$\gamma_{groutbody}$	$26\ {}^{kN}/_{m^3}$

1. Cross sectional area of the anchor

The structure of an anchor is a hollow circle (see top view in Figure 61), therefore the top view cross section is found by the calculation of the area of a circle (see equation (30)).

$$\begin{aligned} A_{anchor} &= \pi R^2 = \pi\left((\frac{D_o}{2})^2 - (\frac{D_i}{2})^2\right) \\ A_{anchor} &= \pi\left((\frac{D_o}{2})^2 - (\frac{D_o - 2 * t}{2})^2\right) \\ A_{anchor} &= \pi\left((\frac{101.6}{2})^2 - (\frac{101.6 - 2 * 28}{2})^2\right) \\ A_{anchor} &= 6.47 * 10^3\ (mm^2) \end{aligned} \tag{30}$$

2. Cross sectional area of the grout body

The grout body is made of concrete and also has a cylindrical shape. Nevertheless, for the E modulus of the grout body, an assumption is made such that the E = EA_steel / A_grout.
The cross sectional area of the grout body is therefore calculated as the area of a circle (see equation (31)).

$$\begin{aligned} A_{grout} &= \pi R^2 = \pi * (\frac{D}{2})^2 \\ A_{grout} &= \pi * \left(\frac{400}{2}\right)^2 \\ A_{grout} &= 1.25 * 10^5 mm^2 = 1.25 * 10^{-1}\ m^2 \end{aligned} \tag{31}$$

Therefore E is calculated in equation (32):

$$E = \frac{EA_{anchor}}{A_{grout}} = \frac{1.35 * 10^6}{1.25 * 10^{-1}} = 1.08 * 10^7\ \frac{kN}{m^2} \tag{32}$$

3. Axial stiffness of the anchor

As the anchor is made out of steel, its E modulus has a value of $2.1*10^8$ kN/m^2. Therefore the axial stiffness is calculated in equation (33):

(33)

$$EA_{anchor} = 2.1 * 10^8 * \frac{6.47 * 10^3}{10^6}$$
$$EA_{anchor} = 1.35 * 10^6 \ (kN)$$

4. Characteristic capacity grout body

Another important parameter for the grout body is its characteristic capacity, also called in the PLAXIS model the skin resistance. This parameter indicates the actual resistance from the interaction of the grout body with the soil. This parameter is calculated in equation (34) , where the circumference of the grout body is 1257 mm, the shaft friction factor is 0.015 and the average cone resistance has a value of 20MPa, which is a regulated value

(34)

$$Tskin = \ circumference\ grout\ body * \ shaft\ friction\ factor * average\ cone\ resistance$$
$$= 377\ kN/m$$

E. Final Results

Table 10: final results strength parameters

TUBE	Symbol	Value	Unit
Moment of Inertia	I_{tube}	$5.152 * 10^9$	(mm^4)
Moment of Inertia per unit length	$I_{tube\ (u.l)}$	$1.782 * 10^9$	$(\frac{mm^4}{m})$
Cross Sectional Area	A_{tube}	$4.096 * 10^4$	(mm^2)
Cross Sectional Area per unit length	A_{tube}	$1.417 * 10^4$	$(\frac{mm^2}{m})$
Weight	w_{tube}	321.6	$(\frac{kg}{m})$
Weight per unit length	$w_{tube\ (u.l)}$	111.24	$(\frac{kg}{m^2})$
Axial Stiffness	EA_{tube}	$2.976 * \ 10^6$	$(\frac{kN}{m})$
COMBINED WALL			
Moment of Inertia per unit length	$I_{c.w}$	$2.109 * \ 10^9$	$(\frac{mm^4}{m})$
Cross sectional area per unit length	$A_{c.w}$	$2.612 * \ 10^4$	$(\frac{mm^2}{m})$
Weight per unit length	$w_{c.w}$	205.1	$(\frac{kg}{m^2})$
Axial stiffness	$EA_{c.w}$	$5.486 * \ 10^6$	$(\frac{kN}{m})$
Bending Stiffness	$EI_{c.w}$	$4.429 * \ 10^5$	$(\frac{kNm^2}{m})$
ANCHOR			
Outer diameter	Do	101.6	(mm)
Inner diameter	Di	45.6	(mm)
Wall thickness	t	28	(mm)
E modulus	E	$2.1 * 10^8$	$(\frac{kN}{m^2})$

Cross sectional area	A_{anchor}	$6.47 * 10^3$	(mm^2)
Axial stiffness	EA_{anchor}	$1.35 * 10^6$	(kN)
GROUT BODY			
Diameter	D	400	(mm)
Cross sectional area	A_{grout}	$1.25 * 10^5$	(mm^2)
E modulus	E	$1.08 * 10^7$	$(\frac{kN}{m^2})$
Capacity	$Tskin$	377	$(\frac{kN}{m})$

XI. Forces and Loads

In the design of a quay wall, as well as in the predictions of a load test, it is essential to take into account the factors that influence the wall's stability. One of these factors that also must be included in the model is the external loads. These loads are introduced and calculated in the following sections, and they need to be modeled accurately to ensure that the wall can withstand them without failure.

A. Concrete Block Load

Once the quay wall is placed into the soil, a concrete block will be placed on top of it, just above the tubular pile. There are different reasons for this. The first reason is that it will create a counter weight that also contributes to the stability of the quay wall, by ensuring its stability within the ground. Second of all, within the concrete blocks is where the bollards are installed. A bollard is a short and thick post where the ship's rope can be secured (see Figure 64). Thirdly, this concrete cover is placed to protect the quay walls from any damage, as it is important to cover the corners with compressible materials to prevent them from breaking off.
Therefore the weight of this structure is evaluated as its own self weight. The structure is made out of reinforced concrete, which has a density of 2 500 kg/m^3. Moreover, Figure 62 shows the so concrete roof and apron. Moreover, there is an extra concrete placed between the apron and the sheet piles. The total load created by that section is 49.5 kN/m, given by an expert as the due to the geometry it is difficult to calculate it by hand (see Figure 63 for top view). The self weight created by the apron and the roof are calculated as follows.

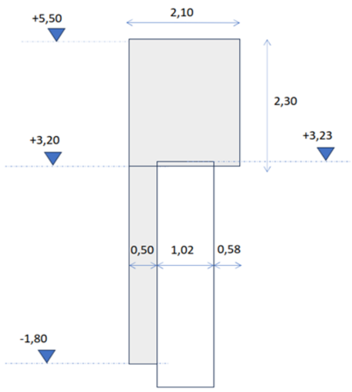

Figure 62: Concrete block on top of tubular pipe

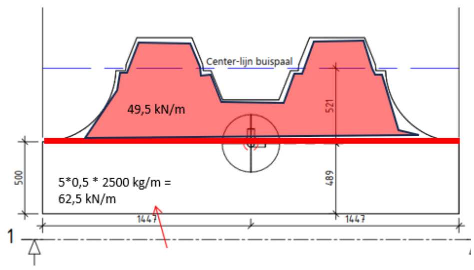

Figure 63: extra concrete between apron and sheet piles

1. Concrete roof

First the volume (per unit) is calculated for the roof, based on the dimensions of Figure 62 (see equation (35)). From this the mass is calculated by assuming a density of concrete of 2500 kg/m^3(see equation (36)). Next the load is calculated by assuming a gravitational acceleration of 10 m/s^2. The calculation is shown in equation (37) .

$$V_{roof} = b * h * t = 2.3 * 2.1 * 1 = 4.83\, m^2 \tag{35}$$

$$M_{roof} = V_{roof} * \rho = 4.83 * 2500 = 12\,075 \frac{kg}{m} \tag{36}$$

$$W_{roof} = M_{roof} * g = 12\,075 * 10 = 120\,750 \frac{N}{m} \approx 121 \frac{kN}{m} \tag{37}$$

2. Concrete apron

The same logic is followed in this case as well, see equation (38), (39) and (40).

$$V_{apron} = b * h * t = 5 * 0.5 * 1 = 2.5\, m^2 \tag{38}$$

$$M_{apron} = V_{apron} * \rho = 2.5 * 2500 = 6\,250 \frac{kg}{m} \tag{39}$$

$$W_{apron} = M_{apron} * g = 6\,250 * 10 = 62\,500 \frac{N}{m} \approx 62.5 \frac{kN}{m} \tag{40}$$

3. Total Load

The total weight is therefore the sum of the weight of the roof, of the apron and of the connection between the apron and the sheet pile, see equation (41).

$$\begin{gathered} W_{total} = W_{roof} + W_{apron} + W_{connection} \\ W_{total} = 121 + 62.5 + 49.5 \\ W_{total} = 233\, kN/m \end{gathered} \tag{41}$$

B. Bollard Load

The bollards are used for boats to tie their ropes, and are to be placed at a constant distance of around 14.5 m as can be seen in Figure 63. These bollards are designed to be able to handle significant loads, and the quay wall must also be able to resist the forces created by the mooring ropes that are attached to the bollards, to ensure the stability of the structure.

The bollard load is given as 600 kN, and in the model PLAXIS the load will be evaluated as a distributed load along 10 meters of cover. Therefore a load of 60kN/m is used. Also, it will have a moment of 24kNm/m (0.4 * 60 = 24kNm/m). The point at which the force is applied will be at a height of 40 cm, above ground level, which is the height of the bollard.

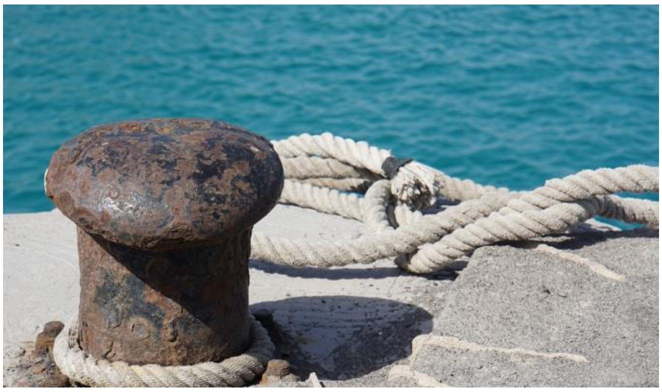

Figure 64: visualization of a bollard

C. Soil Protection Load

On the water side of the quay wall, soil protection is put in place in order to prevent erosion. Therefore a bottom protection made of rocks is placed at around -8.6 NAP (average dredging depth) and the rock layer will have a thickness of around 0.5m. This protection is applied up to 15 meters from the quay wall as can be seen in Figure 65.

In order to calculate the load in kN/m^2 for the layer of the soil protection, it will be assumed that it is made out of gravel. The soil protection that is applied has a density of 2400 kg/m3, however to apply it as a load the effective density is found. Therefore as the water has a density of 1000 kg/m3, the effective density id 2400 kg/m3 - 1000 kg/m3 which results in a density of 1400 kg/m3.
This density value is now converted to kN, which results in (see equation (42)):

$$
\begin{aligned}
Weight\ Density\ \left(\frac{kN}{m^3}\right) &= \rho \times g \\
Weight\ Density &= 1\,400\ \frac{kg}{m^3} \times 9.81\ \frac{m}{s^2} \\
Weight\ Density &= 13\,734 \frac{N}{m^3} = 13.73\ \frac{kN}{m^3}
\end{aligned} \tag{42}
$$

Based on the thickness of the layer which is assumed to be 0.52 meters (see Figure 65), the load is found by multiplying the thickness by the density just calculated (see equation (43)).

$$
\begin{aligned}
Load\ \left({}^{kN}/_{m^2}\right) &= Density\ \left(\frac{kN}{m^3}\right) \times thickness(m) \\
Load\ \left({}^{kN}/_{m^2}\right) &= 13.73\ \times 0.5 =\ 6.87\ {}^{kN}/_{m^2}\ \approx 7\ {}^{kN}/_{m^2}
\end{aligned} \tag{43}
$$

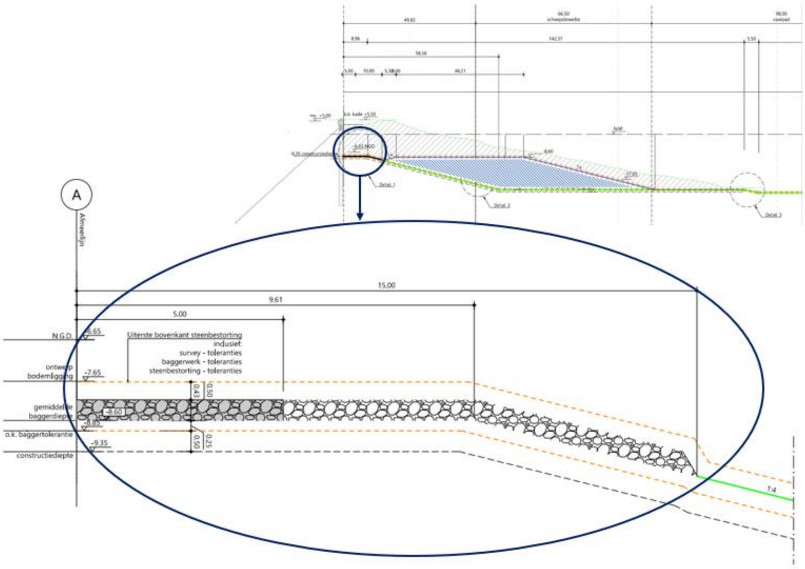

Figure 65: soil protection load

D. Site Loads

The quay construction for the Antarctikade extension has been designed for a uniform site load of 25kN/m^2 over the entire length behind the wall, for the use phase of the quay. This situation will also be tested in this model to compare it to the model made in the preliminary design, in order to verify whether the loads are within the same range, and as a way to verify this new model.
Moreover, due to logistics constraints, for the load test the load can only be applied until the road Antarcticaweg, which is found at around 10 meters behind the quay wall. The objective of the analysis of the loads is therefore to compare the forces on the wall when the load is applied over the entire length, and when it is only applied in the first 10 meters behind the wall. If the difference is considerable, then the uniform load for the load test will need to be increased in order to obtain the same maximum forces or maximum bending moments on the quay wall as in the preliminary phase. These different load situations are visualized in Figure 66 and Figure 67.

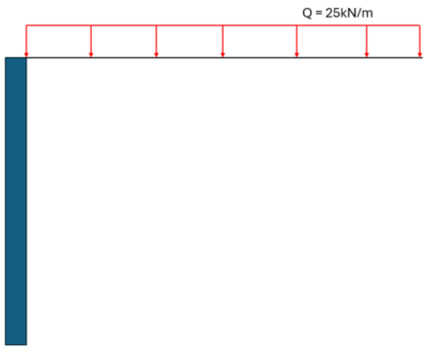

Figure 66: preliminary load situation with q = 25kN/m2

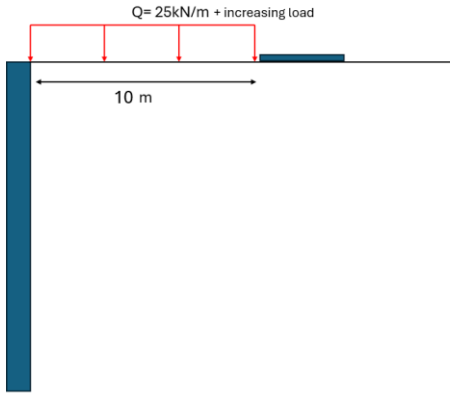

Figure 67: load test situation 1 with q = 25kN/m2

E. Ultimate Situation

In order to ensure that the structure is stable enough, some safety factors are integrated into the model, such that the assumed soil's strength is decreased, by using some partial factors. This approach accounts for variations in the soil properties over time, but also ensures that the structure will continue to be stable in unfavorable conditions. Simultaneously, the site loads are increased using the partial factors as well. This measures involves taking into account unexpected higher loads that could take place due to extreme weather conditions, heavy equipment or other unexpected events. Therefore, by integrating these factors into the modeling, the structure is tested under its ultimate conditions, where the structure needs to show its ability to resist both a decrease in the soil's strength and an increase in site loads, so that it can be concluded that the structure is safe even in extreme conditions. For each load combination, the model is run at its use phase, and at its ultimate situation, where the partial factors are put in place.

Another factor to take into account in the ultimate situation, is the soil's erosion. On the water side of the retaining structure, some soil protection concerning of rocks and gravel are put in place in order to prevent erosion, which can remove some part of the soil and therefore contribute to the failure of the retaining structure. If less soil is on the water side, and the passive pressure is decreased, then the retaining structure will be more prone to overturn, which can lead to the failure of the system. Therefore, to test the ultimate situation it is assumed that 0.5 meters are removed due to erosion, and that situation will also be tested in the ultimate phase of each load combination, together with the partial factors for the soil and for the loads. This can be seen in Figure 79 , where a section of soil is removed from the slope on the water side for the ultimate situation.

1. Partial Factors

In order to obtain the values for the safety factors, it is assumed that the earth retaining structure needs to comply with the safety class RC1 in accordance with the Eurocode 7 [14]and the PoR statement [25]. This will ensure that the structure has a high level of safety for a design life of 100 years. The partial factors used for the geotechnical parameters can be seen in Table 11 and the partial factors for the loads in Table 12, based on NEN9997-1 [14]. Lastly, a correction factor of 1.016 for class RC1 is applied as well, in accordance with CUR 166 [7] to the material factors to account for the 100 year life

Table 11: Partial factors in accordance with table A.4b and A.4c of NEN 9997-1

Parameter	Symbol partial factor	Value
angle of internal friction	$\gamma_{\phi'}$	1,15 · 1,016 = 1,1684
effective cohesion	$\gamma_{c'}$	1,15 · 1,016 = 1,1684
volumetric weight	$\gamma_{\gamma'}$	1,00
stiffness	$\gamma_{k;h}$	1,30

Table 12: Partial factors in accordance with table A.3 of NEN 9997-1

Load		Symbol	Value
permanent	unfavorable	$\gamma_{G;unfavorable}$	1,00 · 1,016 = 1,016
	favorable	$\gamma_{G;favorable}$	1,00 · 1,016 = 1,016
variable	unfavorable land load	$\gamma_{Q;unfavorable}$	1,00 · 1,016 = 1,016
	unfavorable horizontal site load*	$\gamma_{Q;favorable}$	1,30 · 0,90 · 1,016 = 1,189
	favorable	$\gamma_{Q;favorable}$	0,00 · 1,016 = 0,000

XII. Construction Phases

The construction of the quay wall, of the anchor and of the grout body, is carried out in different phases in order to ensure a progression that considers soil conditions, pressures, deformations, water levels, stiffnesses and stresses, from one phase to the next. Therefore, each phase accommodates the evolving soil conditions that are encountered as well as take into account the quay wall, the anchor, and the grout body. This also ensures that the loads are tolerated and that they are distributed properly within the system, so that it can be checked whether the stability is maintained all along.

The approach of doing it in phases allows to ensure that the construction process is safe and as a way of risk mitigation too. Each phase is adapted based on the previous phase, and to its purpose, and can be adjusted based on system's response. Therefore it mitigates structural failures as the weaknesses and critical points are analyzed during the model simulations. The phases considered in this model are presented as follows.

A. Phase 1 : Initial Phase / K0 procedure

The first phase (see Figure 68) is what the determines the initial stress state of the soil before any activity begins, by following the K0 procedure on PLAXIS. K0 is the coefficient of the earth's pressure when at rest, and this baseline measurement is essential to understand how the soil will react in following phases.

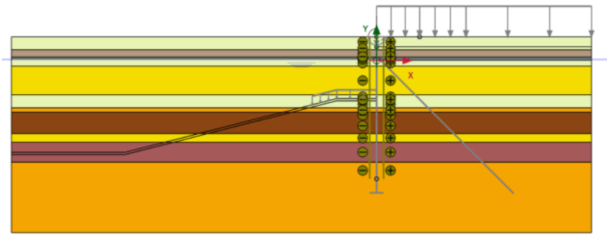

Figure 68: visualization phase 1

B. Phase 2: zero step

This phase is called the zero step, which after establishing the initial stresses, ta new equilibrium state needs to be found for the soil (does not change, therefore see Figure 68). In this phase, the idea is to find how the soil's stress distribution is distributed along the soil, under the current situations, so without any construction load yet. This will give some insights on how the soil will tend to settle or reassemble when subjected to construction loads.

C. Phase 3: installation of combi wall

As explained in previous section VII.C of this report, a combi wall consist of tubular piles and sheet piles, which need to be installed as the main structural components of the quay wall. The installment of the tubular piles will be done by vibrating the piles into the ground until the required depth, which in this case is until -27.5m NAP (see Figure 69).

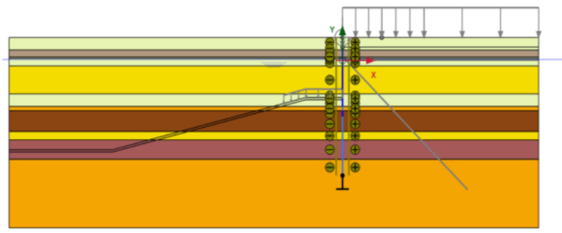

Figure 69: visualization phase 3

D. Phase 4: excavation for the anchoring

Once the tubes into place, the next step is to place the anchors (see Figure 70). For that reason, soil excavation needs to be carried out until a specific depth to allow the anchoring of the quay wall. As the anchors are placed at +1m NAP (see section X), the soil will be excavated up to +0.5 m NAP.

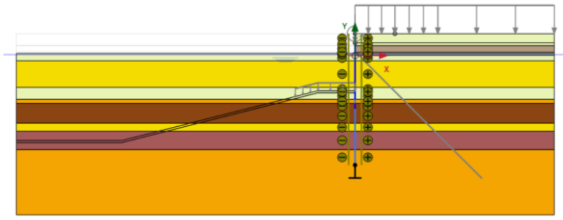

Figure 70: visualization phase 4

E. Phase 5: installment of anchor

Now that the excavation is complete, the anchors can be placed (see Figure 71). The anchors will be prestressed to 500kN per anchor. Prestressing the anchors ensures that they are under tension, and therefore improves their effectiveness. The main reason to install anchors is to provide extra support and stability to the wall to resist lateral earth pressure, as they create an extra horizontal counteracting force.

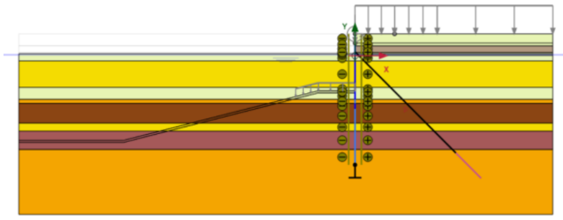

Figure 71: visualization phase 5

F. Phase 6: excavation for placing concrete structure

The next step before placing the concrete structure, is to excavate soil to a depth of +3.2m NAP in order to prepare the foundation for the concrete structure (see Figure 72). The excavation depth ensures that the placement is done properly also without compromising the wall's stability.

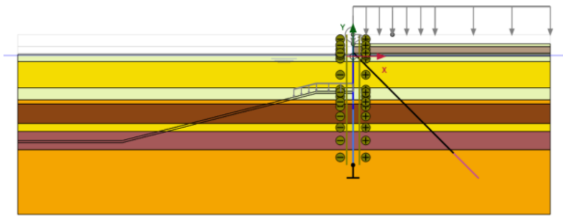

Figure 72: visualization phase 6

G. Phase 7: installment of concrete structure

Once the excavation done, the next phase is to install the concrete structure on top (see Figure 73), therefore consisting on installing the concrete apron and roof. The roof provides a protection to the quay wall as well as a finished surface, and the apron allows to distribute the loads better while adding protection against erosion as well.

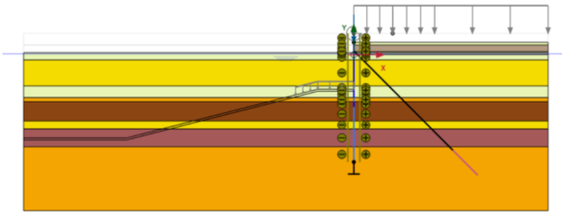

Figure 73: visualization phase 7

H. Phase 8: replenishment and construction load

Once the anchor installed, the next phase is to install the concrete structure on top (see Figure 74), therefore consisting on installing the concrete apron and roof. The roof provides a protection to the quay wall as well as a finished surface, and the apron allows to distribute the loads better while adding protection against erosion as well.

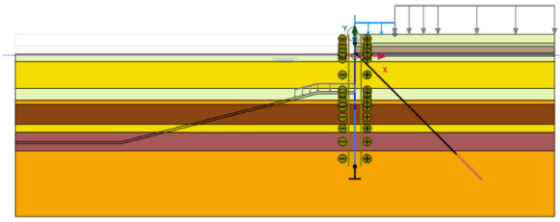

Figure 74: visualization phase 8

I. Phase 9: dredging

The next phase is dredging. This is done is order to deepen the water way in front of the quay wall, from -8.85 m NAP until -21.35 m NAP (see Figure 75). This will allow for the accommodation of bigger boats and vessels.

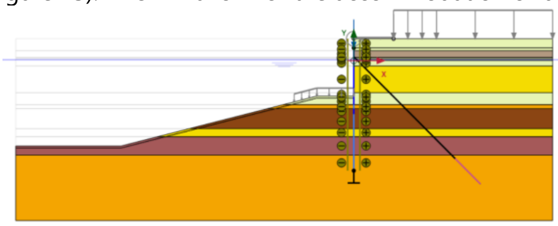

Figure 75: visualization phase 9

J. Phase 10: erosion protection

In order to prevent the soil to erode on the water side, some protection is added as explained in section XI.C (see Figure 76). The erosion protection will consist in applying rocks and gravels at the base of the quay wall. This will therefore ensure that the wall is stable during all its lifetime, as it will be protected from erosion. This will be modeled as a uniform load of 7kN/m^2, along 15 meters on the water side.

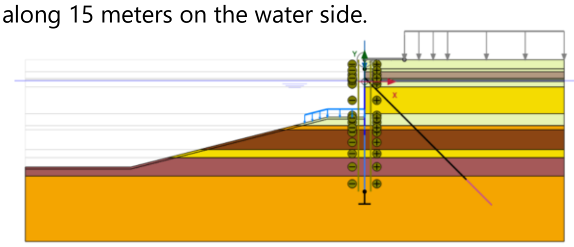

Figure 76: visualization phase 10

K. Phase 11: water level

Furthermore, the next phase is to check that the structure can withstand the expected water levels, and their associated pressures. The quay wall is designed and also tested based in a normative water level of 1/50 year frequency. Moreover, the water levels were monitored and recorded at the site during phase A, and these values are also used for this case, in phase B. The relevant water levels are:

- Water side (LAT): NAP -1.05 m (Lowest Astronomical Tide);
- GHW spring tide: NAP +1.48 m (mean high water level spring tide);

- GLW spring tide: NAP -0.80 m (mean low water level spring tide);

With these values, the goal is to determined the water level difference in spring tide, in order to calculate the groundwater on the land side, with the LAT level as reference on the water side. Therefore based on the Quay Walls Manual [9] section 6.6.5.4, the water level difference in equation (44):

$$\Delta h_{tide;spring} = 0.5 * \left(1.48 - (-0.8)\right) = 1.14\, m \tag{44}$$

Therefore, the ground water level on the land side can be determined by using the calculated water level difference. This is calculated in equation (45).

$$water\ level\ (land\ side) = LAT + \Delta h_{tide;spring} = -1.05 + 1.14 = 0.09m \tag{45}$$

The visualization of these water levels can be seen in Figure 77. Moreover, the goal of these calculations is to verify that the system can withstand the pressures from the water levels, but also the general stability also taking the soil and the different site loads into account.

Besides, another test that is conducted in the model is to use water levels which have a 1/1year frequency or less, as that provides a more realistic representation of water levels during the load test. This test is done to record the maximum loads that can be applied with water levels of more frequency, which are then considered as well during the load test to ensure that the design of the quay wall can actually handle realistic conditions perfectly, and also to have more realistic loads that can be applied during the load test so an actual outcome can be obtained from the test.

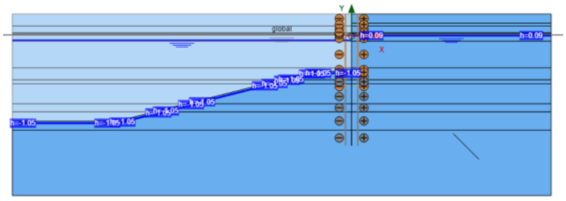

Figure 77: water levels visualization

1. Additional Tests with average water levels

Additionally, another test is conducted using average water levels instead of spring tide values in order to calculate the water difference, providing a more realistic representation of water levels. This approach helps in recording the maximum loads that can be applied to the structure. These recorded loads are then considered during the load test to ensure the quay wall's design can handle real-world conditions effectively.

L. Phase 12: load combinations

In this section of the model, different types of load combinations are tested, for which the bending moment of the wall as well as its axial force is analyzed, as well as the force of the anchor. Furthermore, for the load test only load combination 1 is taken into account. Load combination 2.1 and 2.2 are carried out only for the design of the quay wall. In this case they are still calculated to compare the values of the bending moment, the anchor force, and the displacement with the ones from preliminary design phase B, as a way to verify the model as well. This is done for both the use situation and for the ultimate situation.

1. Load Combination 1

The entire length behind the wall is subjected under a uniform load of q = 25kN/m^2. This situation represents the use phase of the quay wall, under expected loading conditions (see Figure 78). Furthermore Figure 79 shows the load combination under ultimate situation, where the soil on the slope at the water side has been removed due to erosion, and the soil parameters as well as the site loads are subjected to partial factors that increase and decrease them respectively.

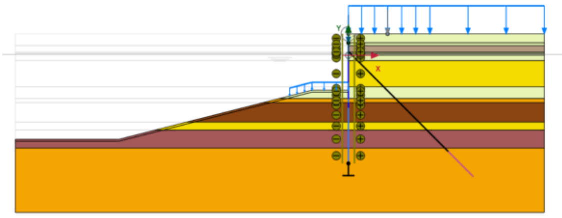

Figure 78: visualization load combination 1 (use phase)

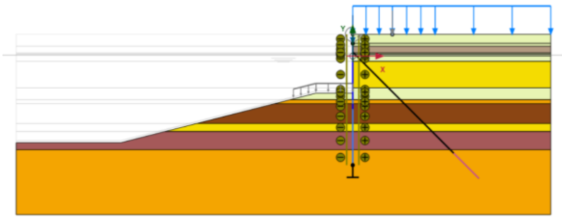

Figure 79: visualization load combination 1 (ultimate phase)

2. Load Combination 2.1

For load combination 2.1 and 2.2, the bollard load is integrated along with its moment. The uniform load still applies all along behind the wall. Nevertheless, it is assumed that both loads (uniform load and bollard load) will never take place at the same time at their full capacity. Therefore in this load combination, the uniform load is applied at its full capacity, therefore with a value of q = 25kN/m^2, but the bollard load will be applied at 0.7 of its entire magnitude, resulting in a value of 42kN/m and a moment of 16.8kNm/m. Moreover, the ultimate phase is applied in this case as well.

3. Load Combination 2.2

As previously explained for load combination 2.1, it is assumed that not all forces will act at its full magnitude at the same time. Therefore for this case the opposite situation as in load combination 2.1 happens. The uniform load will at 0.7 of its magnitude, therefore having a value of q = 25kN/m^2, and the bollard load will act with full magnitude with a force of 60kN/m and a moment of 24kNm/m. Moreover, the ultimate phase is applied in this case as well.

4. Load Combination 3:

This load combination concerns subjecting the system to a uniform load of q = 25kN/m^2 , but this time only until 10 meters behind the wall, which corresponds approximately to the distance from the quay wall until the road Antarcticaweg (see Figure 80). This situation represents as well the use phase of the quay wall, but with constrained load applications due to the site physical limitations. The results from this analysis will be compared to the results from the preliminary load situation, and if the difference is significant then the uniform load will be increased to match the same forces on the wall as in the preliminary situation. Therefore, the load on top will be increased until the system reaches the maximum bending moment, maximum axial force or anchor force calculated in the load combination 1. The values from the preliminary design from phase B will be used in this case such that :

- Max Bending moment (sheet pile wall) = 990kNm/m (decisive from load combination 1)
- Max Anchor force =2410kN per anchor (decisive from load combination 2.1)
- Max horizontal displacement in the combination wall ux= 97mm (decisive from load combination 2.1)

Therefore the goal is to increase the load until one of these aforementioned values is reached. Furthermore, the values for the moments and the forces will be taken based on the ultimate situation, whereas the displacement only on the use phase. Moreover, it is important to note that this load combination is the most important for this research, as it is what takes into account the physical boundary limitations of the site. Also, the uniform load on top will be increased to the maximum, and then that load will be tested with different parameters such as the average soil strength parameter and/or the average water levels (see sections XIII and XIV.D).

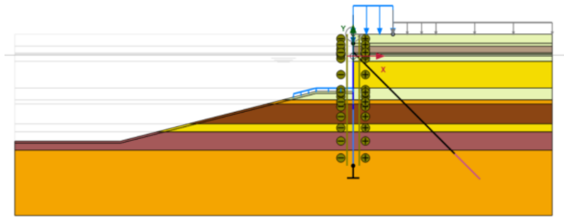

Figure 80: visualization load combination 3

XIII. Average strength parameters

The soil strength parameters that were obtained from the triaxial tests can be interpreted using different statistical measures, which impacts the actual value of the parameter. On the first place, the strength parameters were obtained by using the 95th percentile (see section IX.B) also called characteristic values. Statistically speaking, this means that the parameters chosen are such that only 5% of soil values are weaker than this value. Therefore, 95% of the cases for the soil strength are considered. This approach is therefore more conservative, as it ensures that the model is safe in almost all the possible variations of the data, therefore suggesting that the structure can withstand more load without deforming, which increases the safety factor and reduces the risk of failure. Nevertheless, by using the characteristic values, it can result in an overdesign and in higher costs.

However, in practice during the actual load test, the load values obtained with the soil parameters from this approach, might result in very little observable deformations or other outcomes, as the soil will be modeled to be weaker than it actually is.

Therefore, to achieve more realistic results, in this section the average value for the soil parameters will be used instead. The average value represents the central tendency of the data, and therefore represents the most typical value. This means that 50% of soil values can be weaker than the average value. Furthermore, the average value will lead to higher values, which can lead to more deformation in case there is a situation where the loads exceed the average strength which also will reduce the safety factors. Nevertheless, these values are used to get a more accurate representation of the soil under typical conditions. During the actual load test, it is then expected to observe more deformations, or other outcomes. This is also because the loads that are calculated in the model, will be more realistic to actual field conditions, which results in more accurate and realistic results. Moreover, if the design was to be done with these values, it would be designed for a lower load-bearing capacity, which can be potentially riskier but also result in lower costs.

The average values are therefore taken from the analysis of the triaxial tests from phase A (as explained in section IX.B), and are also multiplied by the factor 9/8. Therefore the new values are shown in Table 13.

Table 13: average strength parameters

Material	Average value phi [deg]	Average value phi *(9/8) [deg]	Average cohesion c
Zand Schoon Los	30.8	34.69	0
Zand Schoon Matig	36.1	40.65	0
Zand Schoon Vast	34.6	35.7	0
Klei Schoon Matig	23.7	26.7	28.2
Klei Zwak Zandig Matig	26.9		7.44
Klei Zwak Zandig Slap	26.9		0

As there is no triaxial tests for the Weak Clay Sandy Moderate (Klei Zwak Zandig Matig), nor for the Weak Clay Sandy (Klei Zwak Zandig Slap), the respective strength parameters are calculated by statistical formulas, and by using the values from Table 1. The formula used to find the average value in shown in equation (46), where the characteristic value is taken from the Table 1, and the variation coefficient is 0.1 for phi and 0.2 for c (also from Table 1). Also the value 1.64 is the factor that corresponds to the 95th percentile in a normal distribution. Furthermore, the coefficient 9/8 is not applied in this case.

$$average\ value = \frac{characteristic\ value}{1 - v * 1.64} \tag{46}$$

<u>Klei Zwak Zandig Matig:</u>

$$average\ value\ phi = \frac{22.5}{1 - 0.1 * 1.64} = 26.9\ deg \qquad average\ value\ c = \frac{5}{1 - 0.2 * 1.64} = 7.44$$

Klei Zwak Zandig Slap:

$$average\ value\ phi = \frac{22.5}{1 - 0.1 * 1.64} = 26.9\ deg \qquad average\ value\ c = \frac{0}{1 - 0.2 * 1.64} = 0$$

XIV. Analysis of results

A. Weakest Point

As introduced in section VIII, one of the goals of this study is to identify the location of the weaker point within the quay wall's length, in order to perform the test at that location. Based on the soil analysis carried out also in section VIII, the selection was complex and requires careful evaluation. Therefore, the first analysis carried out was to integrate the different soil layers from points 12, 13, 16, 17 and DKM051 which were the points chosen as weakest in previous analysis. The point that for which the wall will experience the highest bending moment or highest force, will be considered the weakest, as this indicates that the wall is subjected to higher deformations or stress which suggests therefore that the soil is providing less support and behaving weak. The load combinations tested are 1, 2.1 and 2.2 (see section XII.L for specifics). Also, the higher values are highlighted in bold (see Table 14).

Table 14: results load combinations 1 and 2

	Load Combinations	M (maximum) [kNm/m]		N [kN/m]		u_x [mm]	F_{anker} [kN]	F_{anker} [kN]
		use phase	ultimate	use phase	ultimate	use phase	use phase	ultimate
Point 12	1.	545.6	696.9	875.1	959	61.98	1323.9	1558.5
	2.1	530.7	741.9	894.2	1009	63.93	1433.3	1769.9
	2.2	507.2	652.3	877.8	971.5	61.72	1441.17	1716.1
Point 13	1.	528.6	734.7	867.1	974.2	61.21	1275.95	1646.4
	2.1	498.6	670.9	897.4	996.2	62.84	1416.43	1780
	2.2	459.9	619	876.9	975.9	59.19	1417.95	1766.15
Point 16	1.	424.2	636.4	841	975.1	48.41	1294.2	1702.5
	2.1	357	512.1	886	1006	62.38	1483.32	1877.6
	2.2	418.8	530.8	872.1	997.1	66.93	1485.2	1873
Point 17	1.	390.4	501.6	833.9	890	44.37	1160.8	1421.2
	2.1	305.3	431.2	877.2	942.8	55.98	1354.96	1644.22
	2.2	410.5	497.3	860.8	924.8	70.21	1364.4	1634.6
DKM 051	1.	620.4	**936.7**	951.5	1110	92.12	1741	2216.5
	2.1	586.8	932.2	981.2	**1161**	**94.21**	1895.98	**2418.38**
	2.2	539.2	832.2	956.4	1110	88.37	1848.45	2316.29

Therefore as can it can clearly be observed by the results in Table 14, the weakest point is DKM051 (same as in the preliminary design phase). Therefore the rest of the load combinations will be tested only with the soil layering of that point. It is also important to mention that even though point 17 and point DKM051 are only some meters apart, the difference within the soil layers can be big, especially because they are within a tidal area. Furthermore, DKM051 is especially weaker as it has a high clay layer at around -13m NAP (see Figure 82), which has a big impact on the bending moment of the structure. Also, by visually comparing both point 17 and DKM051 it can already be seen that DKM051 presents weaker tendencies, due to a more inconsistent soil, but also because especially at depth -13m NAP point 17 presents sand. This analysis proves that the location where the load test should be performed is around the location of point DKM051 (see Figure 81). This information is very important for this study as it answers one of the main research questions.

Figure 81: location near DKM051

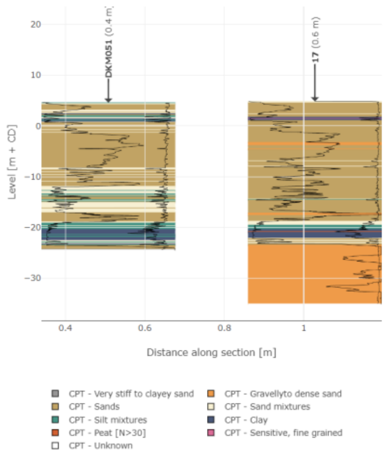

Figure 82: comparison point 17 and point DKM051

B. Unity Check

Moreover, even though the value of the bending moment seems to reach the maximum bending moment calculated during the preliminary design, a unity check is performed as it is a crucial step in ensuring that the structural components can tolerate the loads without failing. In this case, as a combi wall is made out of tubular piles and a sheet pile, tubes are especially susceptible to buckling when subjected to loads. Therefore a unity check is done based on the CUR211 [9] to compare the applied loads and the moments to the maximum limits, to make sure that the loads do not exceed the capacity of the structure.

Furthermore, as the tubes in this case will be filled with sand (tubes are hollow, and they are placed within a sand layer, therefore the sand will go into the tubes), the check is essential to account for
other factors that might influence the stability, as the presence of sand tends to increase the tube's structural performance, as it increases its stiffness, which prevents ovalization and therefore reduces the risk of buckling.

Therefore, the combined bending and normal forces are analyzed with the following formula (equation (47)):

$$\left(\frac{M_{Sd}}{M_{Rd}}\right) + \left(\frac{N_{Sd}}{N_{Rd}}\right)^{1.7} \leq 1 \tag{47}$$

Where:

- $M_{Sd}: bending\ moment$
- $M_{Rd}: design\ resistance\ bending\ moment$
- $N_{Sd}: design\ normal\ force$
- $N_{Rd}: design\ resistance\ force$

The calculation of the design resistance normal force, the additional stiffness created by the sand and other related factors, lie outside of the scope of this study.

C. Results load combination 3 with soil values from 95th percentile

For load combination 3, first a uniform load of q = 25kN/m^2 was put in the model, from which the results can be found in Table 15. It can be concluded that the value of the load can be safely increased as neither of the values reach the failure limits. Therefore the value is increased until approximately q = 27kN/m^2, where the sheet pile wall is the first component to fail by having a moment of around 990kNm/m (see Table 16). Therefore in this situation for the load test, the load can only be increased 2kN/m^2 until the sheet pile reaches its structural capacity and fails, which is a critical information for the load test.

Table 15: results load combination 3 q=25kPa

Q=25kN/m^2	Use phase	Ultimate
M [kNm/m]	643.0	961.2
N [kN/m]	951.8	1081
ux [mm]	94.39	
Fanchor [kN]	1744.764	2152.077

Table 16: results load combination 3, q=27kPa

Q=27kPa	Use phase	Ultimate
M [kNm/m]	650.4	987.6
N [kN/m]	960.9	1096
ux [mm]	95.52	
Fanchor [kN]	1768.79	2195.72

A unit check was carried out for the load of Q=27kPa, and a result of 0.95 was obtained. Therefore there is still a safety margin, which allows for the load to be increased, even though the maximum bending moment reached the value from the preliminary design (M=990kNm/m). Therefore, the load was increased 4kPa more to a value of q=31kPa, which has a unit check of 0.99. The results can be found in Table 17.

Table 17: results Q=31kPa

Q=31kPa	Use phase	Ultimate
M [kNm/m]	666.3	1022
N [kN/m]	979.3	1121
ux [mm]	98.02	
Fanchor [kN]	1818.03	2267.16

Moreover, as this is the maximum load that can be applied in the conditions where the strength parameters for the soil are from the 95th percentile and the water levels are based on the spring tides, also by taking into account the unity check, this load will be applied to other conditions for soil strength and parameters, to evaluate the structure's response in other conditions. Moreover, the forces and moments are checked based on the ultimate phase, and the displacements are going to be based on the use phase. It is also important to recall that the in the use phase the characteristic values were used, whereas in the ultimate phase, the values are lower, due to the application of partial factors.

To conclude this section, an important research question is answered by stating that the maximum load that can be applied for the load test will have a value of 31kPa. Figure 83, Figure 84 and Figure 85 show the horizontal deformation distribution in its use state, the moment distribution and the normal force distribution in its ultimate state. The next sections are going to serve as a sensitivity analysis to figure out the different deformations that the wall experiences when subjected to different water levels (spring tide and average), and with different values for the soil parameters (characteristic or average values).

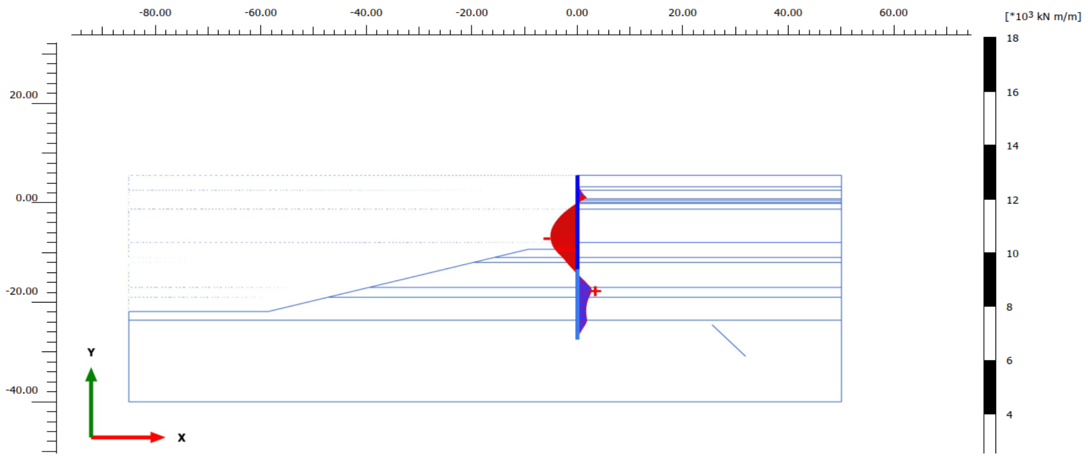

Figure 83: bending moment q=31kPa ultimate state

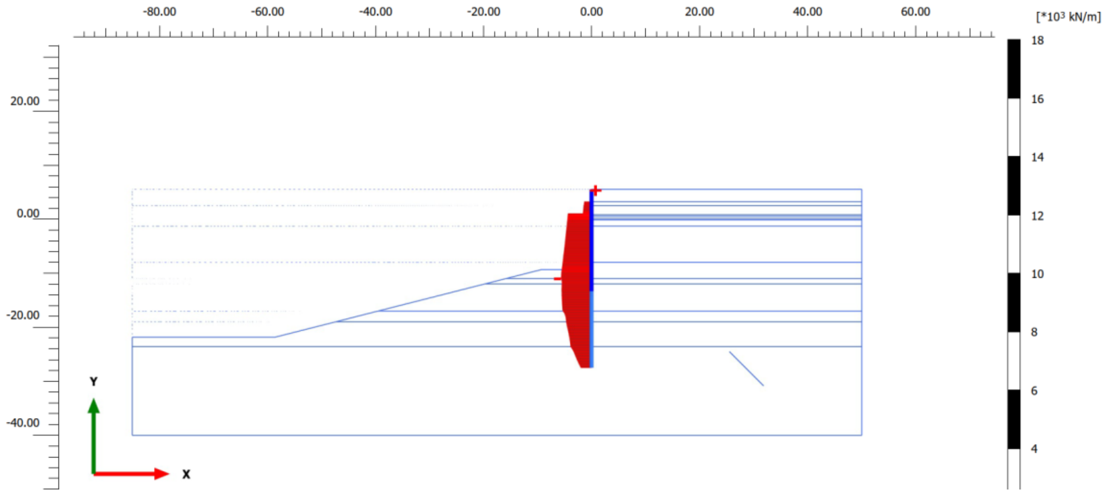

Figure 84: normal force q=31kPa ultimate state

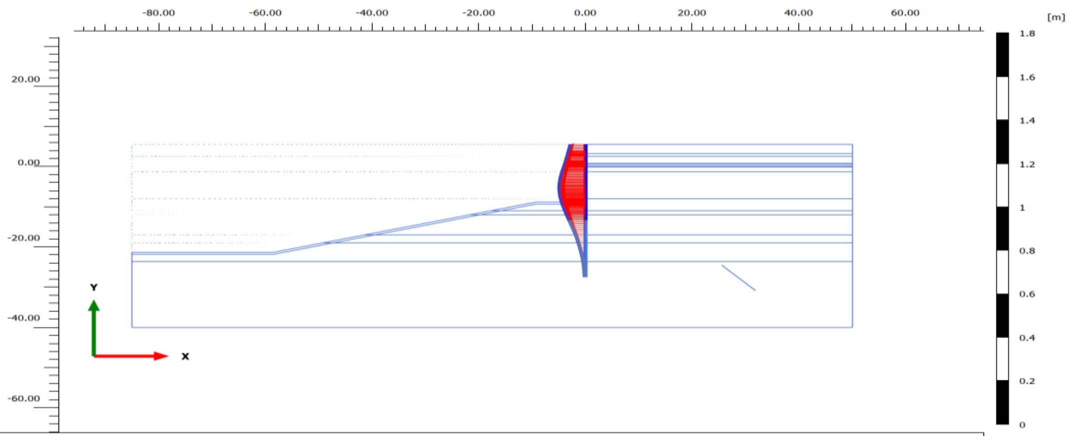

Total displacements u_x (scaled up 50.0 times)

Maximum value = $-2.946*10^{-3}$ m (Element 29 at Node 15828)

Minimum value = -0.09802 m (Element 14 at Node 16845)

Figure 85: horizontal deformation, q=31kPa, use state

D. Results water level average

Previously, the water level on the ground side was obtained by calculating the water difference, based on the spring tide. Nevertheless, in this case, to obtain a water level that is likely to be present during the load test, the average difference in water levels must be found. The recorded water levels are from the Tennessee harbor (see Figure 86 and Table 18), also present in the Maasvlakte. The average difference is found the same way the tidal height difference was found: by subtracting the mean low water level average (GLW) from the groundwater level average (GHW), and dividing by two. The result obtained will then be added to the LAT from the water side (-1.05m NAP). This is shown in equation (48):

$$\Delta h, average = 0.5 * (GHW - GLW) = 0.5 * \left(1.32 - (-0.48)\right) = 0.5 * 1.8 = 0.9\ m \tag{48}$$

Therefore, the new water level on the ground side is calculated in equation (49):

$$water\ level\ (ground\ side) = -1.05 + 0.9 = -0.15m \tag{49}$$

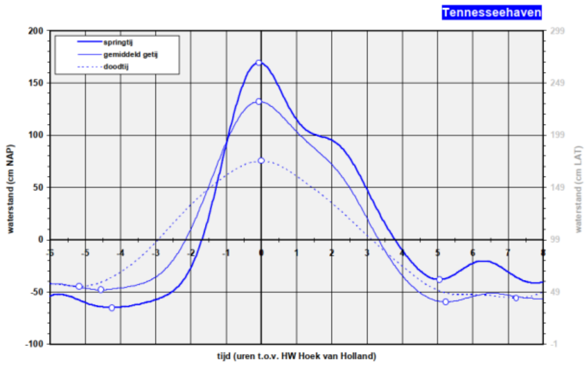

Geen wind	doodtij	gem. getij	springtij	
HW	75 / 174	132 / 231	169 / 268	(cm NAP/LAT)
Tijdverschuiving HW *	nvt	- 0:04	- 0:04	(uu:mm)
LW (laatste LW voor HW)	-45 / 54	-48 / 51	-65 / 34	(cm NAP/LAT)
Tijdverschuiving LW *	+ 0:09	+ 0:11	- 0:04	(uu:mm)
Tijdsduur NAP-nuldoorgang --> HW **	2:55	2:04	1:37	(uu:mm)
Tijdsduur HW --> NAP-nuldoorgang **	3:08	3:24	3:52	(uu:mm)

Figure 86: water levels Tennessee harbor

Table 18: water levels Tennessee harbor

Situatie	Waterstand [m NAP]
gemiddeld laag water (GLW) springtij	-0,65
gemiddeld laag water (GLW)	-0,48
gemiddelde hoog en laag water	+0,42
gemiddeld hoog water (GHW)	+1,32
gemiddeld hoog water (GHW) springtij	+1,69

As explained in section XIV.C, the load of Q=31kPa is tested with the new water level. The soil strength parameters stay as the characteristics values from the 95th percentile. The new results can be seen in Table 19. By applying the average water levels, the water difference between the land side and the ground side is smaller than with the spring tidal water levels. Therefore, having a smaller difference in water levels result in having lower hydrostatic pressure acting on the quay wall, which reduces the bending moments that the structure might experience. Also, the overall stress on the quay wall structure is reduced as well, which results in higher stability. Moreover, the risk of experiencing overturning is reduced as well, as this failure happens when the moments that are created by the

external forces are higher than the resisting moments of the structure and its anchor. And when the water level difference is smaller, then in consequence the external moments are also lower.
Furthermore a unity check was also performed in this situation, and the result was 0.93.This indicates that the safety margin is also higher and therefore the structure will be able to resist more forces or unexpected situations without failure.
Lastly, the main goal of these analyses is mostly to compare the different displacements in the use phase, as it is the main factor that will be measured during the actual load test. Therefore, it can be seen that by using the average water levels, the displacement decreased from 98.02 mm to 94.4 mm, which is a decrease of approximately 3.69%.

Table 19: average water level, q = 31kPa

ground water = -0.15m NAP / q=31kPa	Use phase	Ultimate
M [kNm/m]	640.7	980.1
N [kN/m]	970.8	1105
ux [mm]	94.4	
Fanchor [kN]	1772.858	2197.243

E. Results average soil strength parameters

The load combination 3 was first tested with more conservative soil strength parameters based on the 95th percentile values, and it was found that the load could be increased until q = 31kN/m^2. Nevertheless, in this case it will be tested with the average soil strength parameters to obtain more realistic results. This was done as the average values represent typical situations, which reduces safety factors and therefore can better reflect the soil's behavior. Also for this case, there is not going to be an ultimate situation, as the goal of the analysis is isolate the actual soil condition by removing all sort of safety factors and partial factors that would reduce the soil's strength. In this case, the water level difference is kept as the water level calculated based on the spring tide situation (see in results in Table 20).
Therefore, by using the average parameters for the soil and the spring tide water levels, the model showed that the system can handle higher loads before reaching the limit state. And this can be explained as the soil has a higher support capability without the safety factors. To be more precise, in the average conditions (use phase), all of the values are lower than in the case where the 95th percentile values were used. The deformation is also decreased a lot, going from 98.02 mm in the case of the characteristic values for the soil, down to 74.90 mm in this case, which results in a decrease of approximately 23.59%.
Moreover, it can also be concluded that the average soil parameters have more impact in decreasing the wall's deformation when subjected to a load of Q=31kPa, in comparison to the average water levels.

Table 20: results average soil parameters, spring tide water level, q=31kPa

ground water = 0.09m NAP / q=31kPa	Average conditions
M [kNm/m]	549.5
N [kN/m]	922.3
ux [mm]	74.90
Fanchor [kN]	1602.813

F. Results average water level and average soil strength parameters

This would be the situation the most similar to reality, as for both the average water levels and the average soil parameters are used. Furthermore, the main parameter in this case is the displacement, as during the actual load test, the displacement is going to be recorded and therefore gives indication of what is happening. Furthermore, there is no ultimate situation in this case either for the same reasons explained in section XIV.E. The results can be seen in Table 21. Once again, the results are lower than the results obtained in Table 17. And the displacement is reduced as well, going from 98.02m to 71.86 mm, which results in a decrease of approximately 26.68%.

Table 21: average water level, average soil parameters, q = 31kPa

ground water = -0.15m NAP / q=31kPa	Average conditions

M [kNm/m]	523.3
N [kN/m]	914.9
ux [mm]	71.86
Fanchor [kN]	1562.216

G. Conclusion deformation results

In the first place is compared the impact of the soil's strength, therefore a comparison is done between using the characteristic values for the soil (95^{th} percentile values) and the average soil parameters. Both have a spring tide conditions for the water level. The comparison shows that there is a decrease in range in deformation from 98.02 mm to 74.9 mm. Therefore this reduction shows that the average values for the soil are more representative and the soil is stronger, however the safety margin is of course reduced. The average values may not take into account unexpected situations or variations, for example due to extreme weather events that can lead to higher deformations. Therefore, even if the average values for the soil provide a decrease in the deformation, the quay wall can not be modeled with these values, as even if it could perform better in usual conditions, if at some point there are high stresses, the structure could exceed its safety limits and fail. On the contrary, the 95^{th} percentile values cover these unexpected situations, as they are representing values that are only exceed 5% of the time, and rakes into account unexpected events. Nonetheless, as the average soil conditions provide more accurate predictions during typical conditions, it is an important information to know during the actual load test, where typical conditions will be present.

The same logic applies when using the average water levels in comparison to the spring tide water levels. When using average water levels, there are different deformations as well in both situations of average and 95^{th} percentile values for the soil. The deformations range from 98.02 mm to 94.4 mm (95^{th} percentile values for soil) and from 74.9 to 71.86mm (average values for soil). However to take into account potential higher levels, the spring tide water levels should be used, and to be more realistic during the load test then the average values should be used, following the same logic as for the soil. See summary of results in Table 22.

Table 22: final results deformation

Situation	Deformation: Ux, Q=31kPa	Use phase (mm)
1	95^{th} percentile values for soil + spring tide water difference	98.02
2	Average values for soil + spring tide water difference	74.9
3	95^{th} percentile values for soil + average water difference	94.4
4	Average values for soil + average water difference	71.86

XV. Influence of road

Moreover, another important factor to consider is the influence of the road on the deformation of the wall. Therefore, a indicative load of 15kPa is applied along 10 meters, which is the length of the road, along with the load for the load test of 31kPa. The goal of this analysis is to find out whether this additional load can be considered negligible due to its impact on the wall or not. This is done for the 4 situations mentioned in Table 22. Furthermore, Figure 87, shows the visual representation of applying both the load test load and the load due to the road, just behind. The new deformation results as well as the increase in deformation can be seen in Table 23.

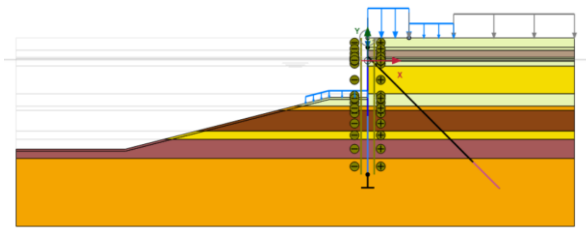

Figure 87: Road load

Table 23: Deformation results due to road influence

Situation	Deformation: Ux, Q=31kPa + Q=15kPa (road influence)	Use phase (mm)	increase w.r.t situation with no road influence (%)
1	95th percentile values for soil + spring tide water difference	101.3	3.345%
2	Average values for soil + spring tide water difference	77.22	3.097%
3	95th percentile values for soil + average water difference	97.64	3.432%
4	Average values for soil + average water difference	74.04	3.032%

As can be seen from the results obtained for the horizontal deformations, there is an increase for every situation. Moreover, it can be concluded that the road load makes the deformation of the wall to increase. However, by looking at the results it will be considered to be the impact on the wall's deformation to be negligible, as all situations experience an increase of around 3%. Furthermore, as previously mentioned, the unity check for Q=31kPa under situation 1 was of 0.99, therefore with the increase of the load it is expected that this value also increases, due to increase in forces and displacements, and therefore suggesting that the road would have an impact into the stability of the quay wall.

To dive deeper into the research, in order to reduce that increase in deformation, the road load will now be applied on only one lane, and the second lane is considered to be closed. Furthermore, the lane situated further away from the quay wall was the one to remain open (see Figure 88 for visualization). Therefore the load is applied on 5 meters. This can be a temporary measure while the load test is carried out, and the lane can be assumed to remain closed or the road could also be redirected temporarily. Table 24 shows the results for the deformation with only the further away lane open.

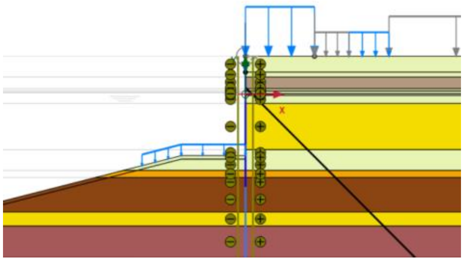

Figure 88: Only second lane open

Table 24: Results deformation only 1 lane

Situation	Deformation: Ux, Q=31kPa + Q=15kPa (road influence)	Use phase (mm)	increase w.r.t situation with no road influence (%)
1	95th percentile values for soil + spring tide water difference	99.18	1.183%
2	Average values for soil + spring tide water difference	75.64	0.988%
3	95th percentile values for soil + average water difference	95.41	1.07%
4	Average values for soil + average water difference	72.51	0.904%

To conclude on the impact of the road, the following three scenarios are visualized in Figure 89:

- No road considered
- 2 lanes of the road considered (load applied along 10 meters)

- 1 lane of the road considered (load applied along 5 meters)

It can be seen that the road has an impact on the deformation of the wall, as it creates more horizontal deformation. On top of that, when considering the road with the 2 lanes open, it has a bigger effect than only considering 1 lane. Therefore, it is concluded that for the load test it would be appropriate to consider only the road with one lane only, and close the second lane temporarily while the test is performed. Nevertheless, when comparing both situations with the road, with the situation with no road, the respective percentage increases are of around 3% and 1%, which in both cases could also be considered as negligeable.

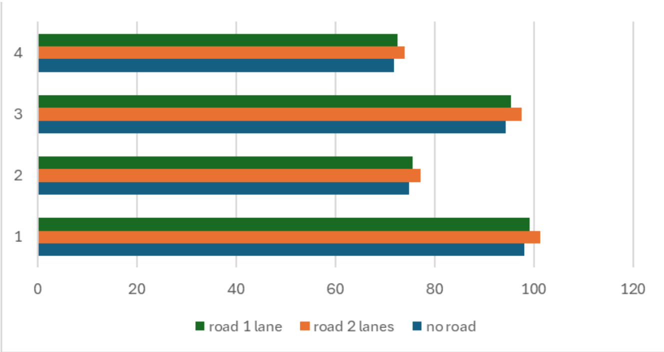

Figure 89: comparison deformations

Lastly, in further research if the road was considered to have an important impact into the stability of the wall, it is suggested that the road is rerouted during the load test intervention. Figure 90 shows an initial suggestion for the rerouting, however no study was carried out and this is not concluded to be feasible.

Figure 90: rerouting of Antarcticaweg

XVI. Discussion

In this discussion section, are introduced a brief proposition on how the actual load test is going to look like, a discussion on the results from the triaxial tests, the role of sensors in the monitoring of the quay wall during the load test is introduced, followed by a discussion on the geotechnical insights gained form this study, and the main lessons learned.

First of all, in order to actually carry out the load test it is important to do it after the dredging work, before the quay wall is put into use and before other infrastructure such as gates and pavements are put in place. Furthermore, in order to apply the load on top of the soil, in this case a load of 31kPa, dry sand will be placed on top to exert that load. This dry sand has a density of 18kN/m3, which in this case will result in a height of sand of 1.72 meters so that the 31kPa are exerted. Another way to exert the load can be with the use of concrete blocks. To be more precise, the area has physical boundary conditions due to the presence of the road, therefore this can only be done in the first 10 meters behind the wall. Also, in order to guarantee that the sand stays in place some barriers need to be place as well. Regarding the process of this, the soil needs to be placed in layers, with some days in between so it also has time to settle. Based on the load test from phase A, it can be approximated that in total the process will take around 1 month, however if the Port of Rotterdam allows it is recommended to leave the option to do it an entire year.

Next, concerning the triaxial tests, as explained in the report the use of the results carried out for phase B could not be used in this study, due to the lack of distinction in densities of the different soil types when carrying out the tests. Therefore, it can be stated that the values that were obtained could hypothetically be used for the dense sand and also the moderate, however this would need to be checked very carefully. It is recommended that further research is carried out in phase B to obtain more accurate results for the soil properties of that area. Moreover, it is also important to mention that in this research the ratio (9/8) from the Eurocode 7 was applied, however this ratio is at the moment under discussion to be removed, as it results in high inaccuracies and overestimations of the soil parameters.

Moreover, this quay wall is equipped with sensors both during the construction phase and the use phase. Sensors have an essential role when monitoring the structural response and performance o the quay walls, as they provide real-time data for several parameters, which are crucial for the resilience of the wall. For example, this is the case of deformation. Sensors are placed sometimes in the interlocks of the sheet pile wall, so that they can measure the displacements along the quay wall. These serve for the monitoring of the load test, but also in every day use, as they assess immediately the external forces on the wall. Furthermore, the sensors allow the monitoring of load distributions, which allows for the optimization of the design, the maintenance and the reinforcement if needed of the wall. Also, they can also evaluate potential erosion risks by measuring the pressures from the soil and the water. And concerning maintenance, they can also track corrosion levels, which gives insights to set maintenance strategies in order to prolongate the life of the wall. Moreover, the sensors can give real-time data, which can then be monitored directly by the Port of Rotterdam, and which in turn can provide action if needed. Also, they measurements of the sensors can serve to optimize the design of the quay wall, validate it and also reduce the knowledge gap in this field. Lastly, the also measure the anchor force and strain along the anchor.

Furthermore, the Port of Rotterdam has also developed the world’s first smart bollard (see Figure 91). This bollard is similar to a standard bollard, but it is able to measure the loads of the mooring lines on the bollard. These real time measurements can be integrated into the port control systems. This way, the port can monitor vessel operations in real time, which results in safe berthing operations, by avoiding unsafe situations and allows to apply mitigation measures if needed. Before the smart bollards, the designs had to be based on maximum forces and could not be optimized due to the lack of measured data. Therefore with smart bollards better insights on mooring loads can be collected, especially important with bigger vessels [16].

Figure 91: smart bollard

Furthermore, the first insight gained from this study concerning geotechnical parameters, is the importance of aligning soil analysis and investigations, with the parameter determination. This is an inflection point of the study which determines the entire study and how the wall will behave, as the soil and its parameters will reflect the stress situations, and also determine possible failure mechanisms. Therefore, it is crucial to carry out soil investigation through accurate methodologies in order to anticipate the rest of the construction phases; soil investigation being the pillar of the project.

Also, especially the case in this study, due to inaccurate data information for the soil analysis, the data from phase A of the soil investigation was interpolated for phase B. This can therefore lead to risks, as clay or silt layers can be underestimated which can lead to piles being placed deeper than predicted, which can then lead to high costs in terms of mitigating measures but also in terms of engineering errors. Therefore it is important for this case, as there was an interpolation of results, to make sure that the interpolation could actually be done, and secondly accurate monitoring during the construction needs to take place to avoid any potential errors.

XVII. Conclusion

To conclude, this study has covered the structural complexities and performance of the quay walls, with main case study the quay walls of the Yangtzecanal phase B of the Port of Rotterdam, at the Prinses Amaliahaven.

The first aim of this study was to identify the optimal location and method to conduct the load test for phase B of the quay wall. This involved carrying out a soil investigation, which addressed the complexities of soils characteristics, soil layering, CPT interpretations, triaxial tests interpretations and more. As phase B is still in the design phase, this research aimed to identify the optimal location for the load test so that the complications that happened in the installment in phase A are not reproduced. The criteria that was used to select the weakest point was first to analyze CPT data and compare visually the heatmaps of the friction ratio and the friction angle of every point, as well as its values, and also by selecting the CPT points with the thicker clay layers and inconsistencies along their stratigraphy. Furthermore, the locations of the clay layers played an important role, especially when situated around the water bottom on the passive side, as it would contribute more to the failure of the wall, especially due to overturning. From this, several points were considered to be decisive, from which point DKM051 was when injecting its layering into the model, the wall behaved the weakest, hence being the weakest point along the entire quay wall. Therefore the load test should be carried at the location of the quay wall near DKM051.

Furthermore, this research also aimed to delve into the structural dynamics of the combi quay walls, by identifying the different loads acting and where they were acting on. The goal was to obtain an accurate representation and insights on the tolerance limit of the quay wall, when subjected to different load combinations and soil strengths. This information is essential for the planning of the load test on site. Moreover, this was carried out through modeling with PLAXIS, which enabled to identify key factors that impact the quay wall's response to loads, such as the soil characteristics, the different water levels, the strength parameters and also the influence of a road nearby. The main outcome is that the construction design is based on the preliminary design where a uniform load of 25kPa behind the wall is used as reference, and when applying the boundary conditions, from this was that the maximum load that could be applied before the failure of the wall, along 10 meters behind the wall is 31kPa. This took into account a unity check as well as the failure of the different elements of the wall.
With this result, a sensitivity analysis was performed in order to obtain insights into the different horizontal deformation that the wall could experience. Therefore, four scenarios were introduced with a combination of average soil values, characteristic soil values, spring tide water levels and average water levels. With these scenarios a range of deformations could be obtained, which ranged between 71.86 mm to 98.02 mm without considering the road.
As another goal of the study was also to evaluate the impact of the infrastructure nearby. Therefore, the same 4 scenarios were also tested with the integration of a load for the 2 lanes of the road of 15kPa, which had an impact on the deformation on the wall, presenting a new range for the deformation going from 74.04 mm to 101.3 mm. Also, the 4 combinations were also tested with only 1 lane of the road which resulted in a range of 72.51 mm to 99.18mm. Therefore, if the two extremes are selected, the most complete range of deformation the wall can be predicted to be experience is from 71.86 mm to 101.3 mm.

Besides, this thesis has contributed to the study of quay walls, more specifically to the quay walls in the Port of Rotterdam, with its analysis and for its design, as it has taken into account data from the site. This study can therefore contribute to the elaboration of the project to widen the Yangtze canal or for further projects in the area.

Finally, it can be concluded that this thesis study has achieved its ultimate research objective, by determining the optimal location to conduct the load test on phase B. It has provided insights on the wall's stability and to identify factors that affect the load testing results, such as the average conditions for the soil parameters and the water levels. Therefore, overall this study contributes to the improved design of the quay wall, which enhances the resilience of the infrastructure from the Port of Rotterdam, which in turn promotes the economic prosperity of the Netherlands.

XVIII. References

1. Apriyono, A., Yanto, Y., Santoso, P. B., & Sumiyanto, S. (2018, March). Soil classification based on cone penetration test (CPT) data in Western Central Java. In *AIP Conference Proceedings* (Vol. 1941, No. 1). AIP Publishing.
2. ArcelorMittal - Steel Sheet Piles. (2020, April 1). *PU 22+1 - ArcelorMittal - Steel Sheet Piles*. https://sheetpiling.arcelormittal.com/products/pu-22_plus1/
3. ÇELİK, S. (2017). Comparison of Mohr-Coulomb and Hardening Soil Models' Numerical Estimation of Ground Surface Settlement Caused by Tunneling. *Journal of the Institute of Science & Technology/Fen Bilimleri Estitüsü Dergisi*, *7*(4).
4. *Combi-Walls – Soletanche Bachy Canada*. (2019). https://www.sb-canada.com/techniques/shoring/combi-walls/
5. Combi-Walls: A combination of steel tubular piles and sheet piles. (n.d.). https://www.soetaert.be/en/techniques/combi-walls
6. CUR (2003). 'Bepaling geotechnische parameters', ISBN 90-3760-3424, referentienummer 2003-7, d.d. oktober 2003
7. CUR (2012). 'CUR 166 - Damwandconstructies 6^e druk, deel 1', ISBN 90-3760-063-8, d.d. juli 2012;
8. De Gijt, J. G. (2010). A History of Quay Walls: Techniques, types, costs and future.
9. SBRCURnet publication 211E (2014). Handbook Quay Walls - Second edition. ISBN 978-1-138-00023-0;
10. Deltares. (2017). Geological Desk Study: Hollandse Kust (noord) Wind Farm Zone (No. 11200513-002-BGS-0001).
11. Editor Engineeringtoolbox. (2023, September 8). *Dirt and mud - densities*. https://www.engineeringtoolbox.com/dirt-mud-densities-d_1727.html
12. HTG. (2015). Recommendations of the Committee for Waterfront Structures Harbours and Waterways: EAU 2012. John Wiley & Sons.
13. Matrix Software. (n.d.). *Cone resistance (qc) and friction (fs) values*. Matrix Knowledge Base. https://knowledge-base.matrix-software.com/help/matrix-tools/geotechnics/cone-penetration-test-diagram/cone-resistance-and-friction-values
14. NEN 9997-1+C2:2017. Eurocode 7: Geotechnisch ontwerp - Deel 1: Algemene regels;
15. Plaxis, B. V., Vermeer, C., & Team, P. (1998). Plaxis. *Benchmarking*, *1*, 5.
16. *Port of Rotterdam – Smart Bollard – World Port Sustainability Program*. (n.d.). https://sustainableworldports.org/project/port-of-rotterdam-smart-bollard
17. *Quay wall construction Amaliahaven*. (n.d.). Port of Rotterdam. https://www.portofrotterdam.com/en/building-port/ongoing-projects/quay-wall-construction-amaliahaven
18. *Quay walls for the future*. (n.d.). TU Delft. https://www.tudelft.nl/citg/over-faculteit/afdelingen/hydraulic-engineering/sections/hydraulic-structures-and-flood-risk/research/quay-walls-for-the-future
19. Rees, S. (2013). Part one: introduction to triaxial testing. *Published on the GDS website www. gdsinstruments. com*, *1*, 1-4.
20. *Regression analysis - Confidence interval of the line of best fit*. (n.d.). https://people.stfx.ca/bliengme/exceltips/regressionanalysisconfidence2.htm
21. *Ronez - Aggregate*. (n.d.). Ronez. https://www.ronez.com/products/aggregate
22. *STABAU - Founded on Steel : Combined tubular sheet pile walls*. (n.d.). https://www.stabau.net/special-solutions/combined-tubular-sheet-pile-walls/
23. *The port that will take you ahead*. (n.d.). Port of Rotterdam. https://www.portofrotterdam.com/en/why-rotterdam/port-will-take-you-ahead
24. Van Gelder, P. H. A. J. M. (2001). Statistical methods for the risk-based design of civil structures.
25. Witteveen+Bos (2022). 'Verbreding Yangtzekanaal -MV - Programma van Eisen Start Ontwerptraject', ref. 131828/22-010.637, definitief 1.0 , d.d. 15 juli 2022;
26. Witteveen+Bos (2022). 'MV-Verbreding Yangtzekanaal- Definitief Ontwerp onderbouw kademuur fase A', ref. 131828/11-017.208, definitief, d.d 6 december 2022;
27. Witteveen+Bos (2023). 'MV-Verbreding Yangtzekanaal- Voorlopig Ontwerp Fase B - onderbouw kademuur', ref. 137146/23-015.966, definitief, d.d 20 oktober 2023;
28. Rapport Geotechnisch Bodemonderzoek Maasvlakte Yangtzekanaal V1 23.06-013

XIX. Appendix

A. Translation

Zand Schoon Los = Sand Clean Loose
Zand Schoon Matig = Sand Clean Moderate
Zand Schoon Vast = Sand Clean Dense
Klei Zwak Zandig = Clay Weak Sandy
Klei Schoon Matig = Clay Clean Moderate
Zand Fijn = Sand Fine
Veen Vast = Peat Solid
Klei, stijf, zwak organisch = Clay, stiff, weakly organic
Kleiig = Clayey
Brokken Klei = Chunks of Clay
Stijf = Stiff

B. Soil Investigation

1. Loose Sand

Uitgangspunten

Type verzameling	**lokaal**	-
1-α	**0**	-
Aantal proeven	**15**	-
cohesie = 0 dwingen	**nee**	-

Proefresultaten

Nr	s'	t'	σ'1	σ'3	p'	q'
[-]	[kPa]	[kPa]	[kPa]	[kPa]	[kPa]	[kPa]
1	220	120	340	100	180	240
2	427	227	654	200	351	454
3	628	328	956	300	519	656
4	236	135	371	101	191	270
5	432	232	664	200	355	464
6	638	338	976	300	525	676
7	219	119	338	100	179	238
8	419	217	636	202	347	434
9	606	304	910	302	505	608
10	218	118	336	100	179	236
11	413	213	626	200	342	426
12	592	291	883	301	495	582
13	208	108	316	100	172	216
14	390	190	580	200	327	380
15	568	268	836	300	479	536

Bepaling statistische waarden

Helling	0.49	-
Snijpunt	11.9	kPa
Aantal proeven	15	-
Standaard afwijking	9.8	kPa
Gemiddeld x	414	kPa
SSX	377527	
t(a,df)	1.77	

Bepaling t'95% --> gekromde lijn

nr	s'	t'trend	t95%
[-]	[kPa]	[kPa]	[kPa]
0	0	12	-1
1	32	27	16
2	64	43	32
3	96	59	49
4	128	74	65
5	160	90	81
6	191	105	98
7	223	121	114
8	255	136	130
9	287	152	146
10	319	167	162
11	351	183	178
12	383	199	194
13	415	214	210
14	447	230	225
15	479	245	240
16	510	261	256
17	542	276	271
18	574	292	285
19	606	307	300
20	638	323	315

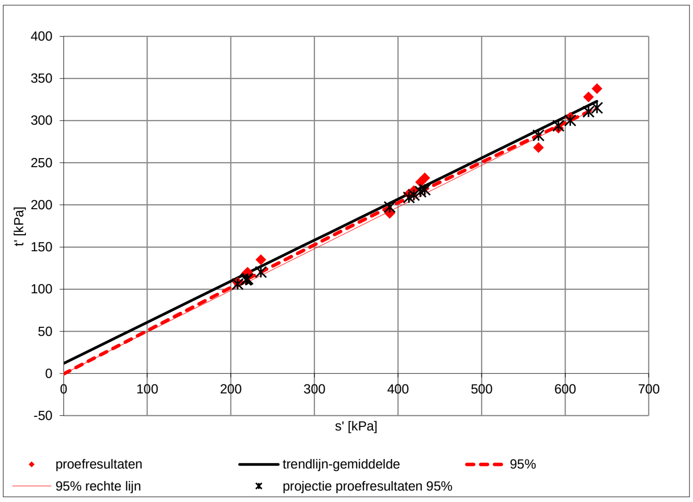

Resultaten cohesie en interne wrijvingshoek bepaling

	95%	Trend gemiddelde	
b	0.50	0.51	-
φ'	30.0	30.8	o
a	0.0	0.0	kPa
c'	0.0	0.0	kPa

2. Moderate Sand

Uitgangspunten

Type verzameling	**lokaal**	-
1-α	**0**	-
Aantal proeven	**9**	-
cohesie = 0 dwingen	**nee**	-

Proefresultaten

Nr	s'	t'	σ'1	σ'3	p'	q'
[-]	[kPa]	[kPa]	[kPa]	[kPa]	[kPa]	[kPa]
1	268	168	436	100	212	336
2	487	287	774	200	391	574
3	738	438	1176	300	592	876
4	262	162	424	100	208	324
5	498	297	795	201	399	594
6	736	435	1171	301	591	870
7	236	136	372	100	191	272
8	463	263	726	200	375	526
9	719	419	1138	300	579	838

Bepaling statistische waarden

Helling	0.58	-
Snijpunt	5.0	kPa
Aantal proeven	9	-
Standaard afwijking	6.3	kPa
Gemiddeld x	490	kPa
SSX	341046	
t(a,df)	1.89	

Bepaling t'95% --> gekromde lijn

nr	s'	t'trend	t95%
[-]	[kPa]	[kPa]	[kPa]
0	0	5	-6
1	37	26	16
2	74	48	38
3	111	69	61
4	148	91	83
5	185	112	105
6	221	134	127
7	258	155	149
8	295	176	171
9	332	198	193
10	369	219	215
11	406	241	236
12	443	262	258
13	480	284	280
14	517	305	301
15	554	327	322
16	590	348	343
17	627	369	364
18	664	391	385
19	701	412	406
20	738	434	427

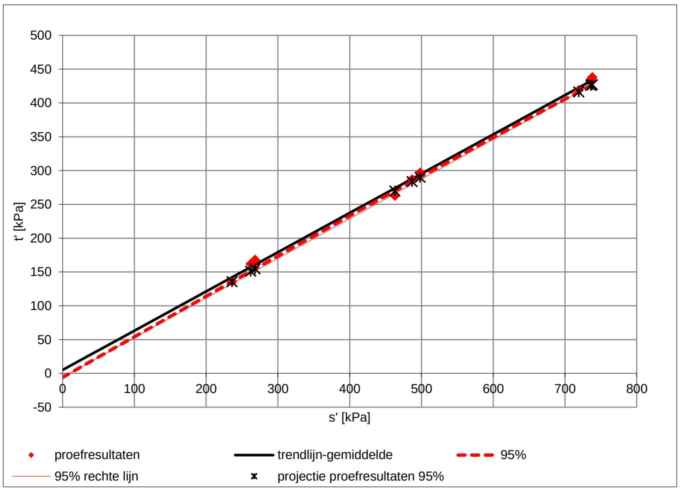

Resultaten cohesie en interne wrijvingshoek bepaling

	95%	Trend gemiddelde	
b	0.58	0.59	-
φ'	35.4	36.1	o
a	0.0	0.0	kPa
c'	0.0	0.0	kPa

3. Dense Sand

Uitgangspunten

Type verzameling	**lokaal**	-
1-α	**0**	-
Aantal proeven	**12**	-
cohesie = 0 dwingen	**nee**	-

Proefresultaten

Nr	s'	t'	σ'1	σ'3	p'	q'
[-]	[kPa]	[kPa]	[kPa]	[kPa]	[kPa]	[kPa]
1	675	415	1090	260	537	829
2	959	568	1527	390	769	1137
3	1621	970	2591	650	1297	1941
4	648	373	1020	275	523	745
5	1051	636	1687	415	839	1272
6	1636	946	2581	690	1321	1891
7	634	379	1012	255	508	757
8	993	613	1606	380	789	1226
9	1481	846	2328	635	1199	1692
10	672	401	1073	270	538	802
11	928	523	1451	405	754	1046
12	1499	823	2322	675	1224	1647

Bepaling statistische waarden

Helling	0.56	-
Snijpunt	24.5	kPa
Aantal proeven	12	-
Standaard afwijking	23.5	kPa
Gemiddeld x	1066	kPa
SSX	1698378	
t(a,df)	1.81	

Bepaling t'95% --> gekromde lijn

nr	s'	t'trend	t95%
[-]	[kPa]	[kPa]	[kPa]
0	0	25	-12
1	82	71	36
2	164	117	85
3	245	163	133
4	327	209	181
5	409	255	230
6	491	301	278
7	572	347	326
8	654	393	374
9	736	439	422
10	818	485	470
11	900	531	517
12	981	577	564
13	1063	623	610
14	1145	669	656
15	1227	715	701
16	1309	761	746
17	1390	807	790
18	1472	853	835
19	1554	899	879
20	1636	945	922

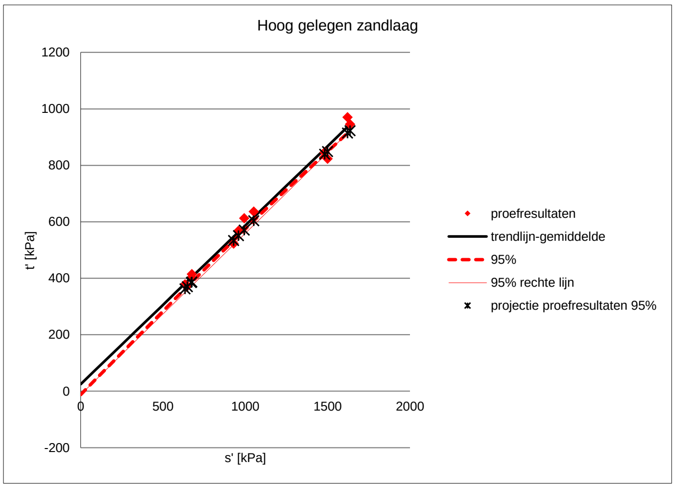

Resultaten cohesie en interne wrijvingshoek bepaling

	95%	Trend gemiddelde	
b	0.57	0.58	-
φ'	34.6	35.7	o
a	0.0	0.0	kPa
c'	0.0	0.0	kPa

4. Moderate Clay

Uitgangspunten

Type verzameling	**lokaal**	-
1-α	**0**	-
Aantal proeven	**23**	-
cohesie = 0 dwingen	**nee**	-

Proefresultaten

Nr	s'	t'	σ'1	σ'3	p'	q'
[-]	[kPa]	[kPa]	[kPa]	[kPa]	[kPa]	[kPa]
1	218	146	364	72	169	292
2	299	162	461	137	245	324
3	466	198	664	268	400	396
4	220	95	315	125	188	191
5	316	142	458	174	269	284
6	481	261	742	220	394	522
7	202	108	310	94	166	216
8	319	148	467	171	270	296
9	496	231	727	265	419	462
10	215	99	314	117	182	197
11	327	151	478	176	277	302
12	519	199	718	320	453	398
13	88	49	137	40	72	97
14	180	90	270	90	150	179
15	333	166	499	167	278	332
16	92	61	154	31	72	123
17						
18						
19						
20						
21						
22						

Bepaling statistische waarden

Helling	0.40	-
Snijpunt	25.8	kPa
Aantal proeven	23	-
Standaard afwijking	18.3	kPa
Gemiddeld x	266	kPa
SSX	381173	
t(a,df)	1.72	

Bepaling t'95% --> gekromde lijn

nr	s'	t'trend	t95%
[-]	[kPa]	[kPa]	[kPa]
0	0	26	11
1	26	36	22
2	52	47	34
3	78	57	45
4	104	68	57
5	130	78	68
6	156	88	80
7	182	99	91
8	208	109	102
9	234	120	113
10	260	130	124
11	285	141	134
12	311	151	144
13	337	162	154
14	363	172	164
15	389	182	173
16	415	193	183
17	441	203	192
18	467	214	202
19	493	224	211
20	519	235	220

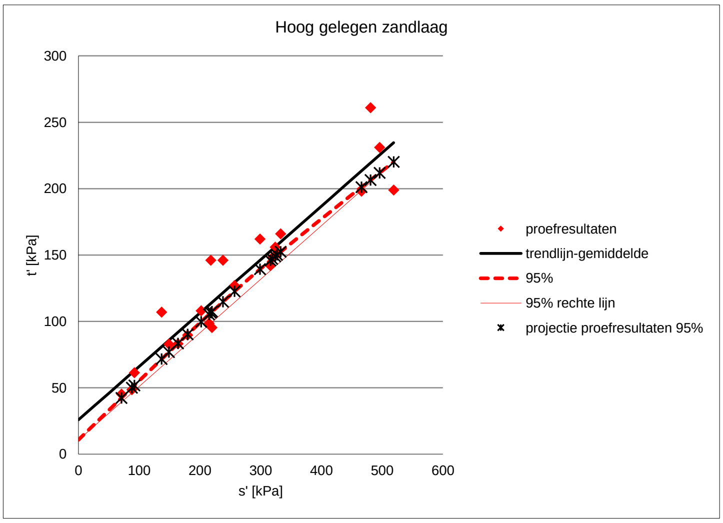

Resultaten cohesie en interne wrijvingshoek bepaling

	95%	Trend gemiddelde	
b	0.40	0.40	-
φ'	23.8	23.7	o
a	10.7	25.8	kPa
c'	11.7	28.2	kPa